

# Minimizing Social and Economic Impacts of Increased Post-Fire Debris-Flow Occurrence, Including Climate Change Effects

---

## Final Report to the Joint Fire Science Program

JFSP Contract 12-2-01-35

### Principal Investigators:

Steffen Rebennack, Colorado School of Mines (PI)

Paul Santi, Colorado School of Mines (Co-PI)

Daniel Kaffine, University of Colorado Boulder (Co-PI)

Dennis Staley, U.S. Geological Survey (Co-PI)

September 30, 2015



Colorado School of Mines



United States Geological Survey



Joint Fire Science Program

---

## FINAL REPORT

### Project Title:

# Minimizing Social and Economic Impacts of Increased Post-Fire Debris-Flow Occurrence, Including Climate Change Effects

### JFSP Contract 12-2-01-35

**Principal Investigator(s):** Steffen Rebennack<sup>1</sup>, Paul Santi<sup>2</sup>, Daniel Kaffine<sup>3</sup>, Dennis Staley<sup>4</sup>

**Researcher(s):** Kevin M. McCoy<sup>2</sup>, Vitaliy Krasko<sup>1</sup>, Timo Lohmann<sup>1</sup>, Ian Donovan<sup>2</sup>, Hayden Brown<sup>2</sup>

**Affiliations:** <sup>1</sup>Colorado School of Mines, Division of Economics and Business  
<sup>2</sup>Colorado School of Mines, Department of Geology and Geological Engineering  
<sup>3</sup>University of Colorado Boulder, Department of Economics  
<sup>4</sup>U.S. Geological Survey, Landslide Hazards Program

**Addresses:** <sup>1,2</sup> 1500 Illinois St, Golden, CO 80401  
<sup>3</sup> Economics Building Room 212, 256 UCB, Boulder, CO 80309-0256  
<sup>4</sup> Box 25046, DFC, MS 966, Denver CO 80225

**Telephone/Facsimile Number(s):** <sup>1</sup>(303)273-3925 (Rebennack)  
<sup>2</sup>(303)273-3108 (Santi)  
<sup>3</sup>(303)492-6652 (Kaffine)  
<sup>4</sup>(303) 271-8568 (Staley)

**E-mail:** <sup>1</sup>srebenna@mines.edu, <sup>2</sup>psanti@mines.edu, <sup>3</sup>daniel.kaffine@colorado.edu,  
<sup>4</sup>dstaley@usgs.gov

**Point of Contact:** Steffen Rebennack, Colorado School of Mines, Division of Economics and Business, 1500 Illinois Street, Golden, CO 80401, (303)273-3925, srebenna@mines.edu

**Federal Cooperator:** Dennis Staley, U.S. Geological Survey, Box 25046, DFC, MS 966, Denver CO 80225, dstaley@usgs.gov, (303)273-8604

# Table of Contents

Executive Summary	v
Deliverables	vi
1.0 Introduction	1
2.0 Background	3
2.1 Quantifying Damages from Post-Fire Debris Flows	3
2.1.1 Post-Fire Debris-Flow Hazard and Risk	3
2.1.2 Probability and Volume Modeling and Model Inputs	4
2.1.3 Runout Models	5
2.1.4 Quantifying Effectiveness and cost of Selected Mitigation Methods	6
2.1.5 Model Uncertainty and Alternative Methods	6
2.2 Optimization Framework and Natural-Hazards Management	7
2.3 Expected Changes in Post-Wildfire Debris Flows with Climate Change	8
3.0 Methods	15
3.1 Quantifying Economic-Costs of Post-Fire Debris Flows	15
3.1.1 Estimation of Debris-Flow Probability and Volume	15
3.1.2 Modeling Debris-Flow Runout	15
3.1.3 Identifying Features Intersected by Debris-Flow Runout	16
3.1.4 Estimating Damage Costs	19
3.1.5 Damage Curves	21
3.1.6 Economic Risk	22
3.1.7 Estimating Cost and Effectiveness of Post-Fire Debris-Flow Mitigation	
Methods	22
3.2 Optimization Modeling	26
3.3 Description of Three Sites for Case Study	27
3.4 Evaluating Increases in Debris-Flow Occurrence with Climate Change	30
3.4.1 Data acquisition, post-wildfire debris flows	30
3.4.2 Database analysis	30
3.4.3 Analysis of better-documented post-wildfire debris flows	30
3.4.4 Analysis of post-wildfire debris-flow probabilities	31
4.0 Results	33
4.1 Results of Debris-Flow Damage and Optimization Modeling at 3 Case Study Sites	33
4.1.1 Damage Estimates	33
4.1.2 Optimization Modeling	37
4.1.3 Limitations	40
4.2 Evaluating Increases in Debris-Flow Occurrence with Climate Change	41
5.0 Conclusions	44

Appendix A Basin Characteristics for 3 Case Study Sites

Appendix B Climate Change Study - Debris-Flow Dataset DS1

Appendix C Calculated Debris-Flow Probability and Volume for 2-year and 10-year Rainfall Scenarios at 3 Case Study Sites

Appendix D Publications and Presentations

# List of Figures

Figure 1. Increase of wildfires on USFS land over 1,000 acres and avg. annual spring temperature .....	8
Figure 3. Example of features intersected by modeled debris-flow runout in GIS .....	17
Figure 4. Key parameters for calculating volume of sediment trapped per unit width behind a straw wattle, log erosion barrier, or check dam .....	24
Figure 5. Location of modeling study sites in the western United States.....	28
Figure 6. Damage as function of volume in three basins from Site 1.....	34
Figure 7. Expected debris flow damage in Jesusita fire case study without mitigation .....	35
Figure 8. Expected debris-flow damage in Track fire case study without mitigation .....	35
Figure 9. Expected debris-flow damage in Medano fire case study without mitigation, direct trail damage .....	36
Figure 10. Expected debris flow damage in Medano fire case study without mitigation, lost trail access .....	36
Figure 11. Expected debris-flow damage in Jesusita fire case study with mitigation .....	38
Figure 12. Expected debris-flow damage in Track fire case study with mitigation .....	38
Figure 13. Expected debris-flow damage in Medano fire case study with mitigation, trail clean up.....	39
Figure 14. Expected damages with one mitigation strategy, Jesusita fire, 10-year storm.....	40

# List of Tables

Table 1. Unit values for features intersected by debris-flow runout in ArcGIS .....	20
Table 2. Cost and Effectiveness Assumptions for Mitigation Strategies.....	23
Table 3. DS2, A subset of data focusing on well-documented post-wildfire debris flow areas..	32
Table 4. Site features and estimated damages (2012 USD) from 2-yr and 10-yr recurrence storm scenarios.....	37
Table 5. Budget where marginal reduction in damage is equal to marginal cost of mitigation. .	39
Table A - 1 – Site 1 Basin Characteristics	A-1
Table A - 2 – Site 2 Basin Characteristics	A-4
Table A - 3 – Site 3 Basin Characteristics	A-6
Table B - 1 – Climate Change Study Dataset DS1	B-1
Table C - 1 – Site 1 Calculated probability and volume for 1-hr, 2-yr recurrence storm	C-1
Table C - 2 – Site 1 Calculated probability and volume for 1-hr, 10-yr recurrence storm	C-2
Table C - 3 – Site 2 Calculated probability and volume for 1-hr, 2-yr recurrence storm	C-3
Table C - 4 – Site 2 Calculated probability and volume for 1-hr, 10-yr recurrence storm	C-5
Table C - 5 – Site 3 Calculated probability and volume for 1-hr, 2-yr recurrence storm	C-7
Table C - 6 – Site 3 Calculated probability and volume for 1-hr, 10-yr recurrence storm	C-9

# Executive Summary

**Overview:** In this study we developed methods to comprehensively analyze the economic risk of post-wildfire debris flows and proof of concept models to optimally allocate resources towards various mitigation options. These methods utilize previously existing post-fire hazard assessment calculations, debris-flow runout models, and easily obtainable GIS feature data to model the expected debris flow damages in individual drainage basins following a fire.

The process is modular; a variety of probability, volume, and runout models can be used depending on data availability, project needs, and skills of the analyst. The output of this model can guide allocation of emergency management funds and selection of cost-optimized debris-flow management strategies for entire burned areas.

These methods can be employed rapidly following a fire and have the potential to transform the way hazard managers approach debris-flow mitigation decisions following wildfires. Preliminary case study results suggest that this process can identify the drainage basins posing the greatest economic risk and the mitigation strategies with the highest marginal benefit and lowest marginal cost.

**Results:** The results of this study have led to the following conclusions:

- 1) The best mitigation strategies are highly site specific, including runout characteristics as well as economic risk exposures.
- 2) For the sites with high potential economic risks, mitigation strategies are available which both are effective in reducing the risks and in being economically viable (compared to the exposed risks).
- 3) For debris basins to become economically efficient, additional positive effects beyond post-wildfire debris flow mitigation, need to be taken into account due to their relative high cost compared to the other mitigation strategies available.
- 4) The proposed natural hazard-management framework passed the stage of a “proof-of-concept” study. We see great potential for an actual employment and hope for further developments in that context.

**Deliverables:** The results of this study have been presented to consultants, and academic experts in the fields of geologic sciences, natural-hazards management, and operations research at a several annual meetings and specialty conferences. The methods developed during this study for evaluating impacts of post-fire debris flows and evaluating optimal post-fire debris-flow mitigation response, results of a case-study of the process applied to three sites in the western United States, and discussion of the influence of climate change on post-fire debris-flow occurrence will be submitted for publication as one conference-proceeding paper and two peer-reviewed journal articles. Technical aspects of this research have been disseminated as 6 presentations at professional society meetings, three PhD theses, two MS theses and technical papers.

# Deliverables

<b>Proposed</b>	<b>Accomplished / Status</b>
Annual progress reports	Annual progress reports completed
Peer-reviewed journal article quantifying economic costs of debris flows	This topic was covered in a conference-proceeding paper published by the American Society of Civil Engineers (McCoy et al. 2014)
Peer-reviewed journal article linking climate change forcings to debris-flow occurrence	This topic is covered in a peer-reviewed journal article submitted to the journal Environmental and Engineering geoscience (currently in second round of review) (Brunkal and Santi in review)
Peer-reviewed journal article providing general framework of optimal natural hazard management	A journal article summarizing the general framework for optimal natural hazard management and case studies from 3 sites in the western United States (McCoy et al. in preparation) is currently in preparation for submittal to the peer-reviewed journal Natural Hazards. We anticipate submitting the paper for review by November, 2015.
Peer-reviewed journal article of optimal natural hazard management case study	
Final report to JFSP at completion of project	Attached
New items (not initially proposed) being pursued, partly attributable to JFSP funding	<ul style="list-style-type: none"> <li>• Analysis of influence of uncertainty in model inputs on expected debris-flow damage</li> <li>• Article submitted to Landslides journal on probabilistic debris-flow volume modeling</li> <li>• Working paper describing an urban real estate model that incorporates endogenous natural hazard risk, models the unique spatial aspects of the urban-wildland interface, and analyzes the response of households to changes in natural hazard risk</li> <li>• Working paper that extends the general framework of optimal natural hazard management to consider a stochastic storm uncertainty and incorporates elements of the emergency supply pre-positioning problem</li> </ul>

Debris flows are often one of the most hazardous consequences of wildfires in the wildland-urban interface. Damages include destroyed houses and buildings, blocked and washed out roads, loss of land access, degradation of habitat and water quality, as well as loss of human life, as evidenced by recent flows following wildfires in Arizona (2010) and California (2003). As global climate change results in longer fire seasons, with more frequent and larger fires (Westerling et al. 2006), debris flows and floods in burned areas will increase in frequency (Cannon and De Graff 2009). As debris-flow impacts continue to increase in the future, better quantitative tools need to be developed to assist land managers in making decisions to optimize resources and best protect elements and people at risk. A linkage between natural hazards and social science models has never previously been developed for post-fire debris flows, and this feedback and decision making framework can serve as a template for other natural hazards such as wildfire damage, erosion, floods, or landslides. The purposes of the studies described in this report were to: establish a baseline natural hazard risk from debris flow in recently burned areas, develop a general framework of optimal natural hazard management, demonstrate the application of this optimal natural hazard management framework in a case study of three sites, and quantify the link between climate change and post-fire debris-flow risk.

The interdisciplinary nature of this project, combining natural science and social science perspectives, is in and of itself an advance in scientific knowledge of natural hazard management. The rigorous modeling framework that was developed provides management tools that go beyond qualitative recommendations and can be tailored to specific geologic, climatic and economic conditions. From an optimal management perspective, the literature on management of natural hazard risk is thin. While the natural science literature provides much insight into risk assessment of natural hazards, most studies simply note that risk assessment can inform a vaguely defined risk management process (e.g., Chen et al. 2003; Dai et al. 2002). For example, in the context of landslides, Dai et al. (2002) provide an overview of risk assessment and management. They note that government agencies need to make decisions on allocations of funds for managing risk, in this case towards options such as planning, prevention of events, control of events, acceptance and/or monitoring. However, they provide little rigorous guidance into how decision makers should allocate their scarce resources beyond a recommendation of cost-benefit analysis. Likewise, the debris-flow literature is limited to risk studies that calculate the probability and volumes of events (e.g., Cannon et al. 2010b; Lin et al. 2006), that suggest general approaches to including vulnerability and economics (Fuchs et al. 2008), or that have limited impacts analysis but no feedback or optimization related to the natural science model (Archetti and Lamberti 2003). The interdisciplinary approach in this proposed project extends this literature by providing quantitative recommendations for natural hazard management decisions based on state-of-the-art natural and social science methods.

Additional scientific contributions arise from the natural science component. First, an extensive economic analysis of potential impacts from post-wildfire debris flows has not been published. This will be an important extension of data already available on costs and effectiveness of

erosion control and debris-flow prevention efforts. Second, the expected changes in debris-flow frequency, magnitude, and impacts resulting from climate change have not been quantified, although the linkage has been proposed (e.g., Cannon and De Graff 2009).

In the context of coupled natural-human systems, the economics literature provides many examples of optimal policy and management studies that integrate ecological and economic systems (e.g., Clark 1990; Costello and Kaffine 2010) or climate and economic systems (Nordhaus 1992). Studies such as Settle et al. (2002) and Finnoff and Tschirhart (2008) emphasize the importance of accounting for feedbacks between natural systems and economic decisions in policy-making. While there do exist a few studies with similar features to the project, for example the climate change management literature with its focus on adaptation versus mitigation (Wilbanks et al. 2003), to our knowledge this project represents the first attempt to develop a coupled natural-human model of natural hazards that yields optimal decision rules for natural hazard management.

The issues of post-fire debris-flow hazard management in a changing climate in were investigated through three key tasks. First, an optimal resource management model was developed, that incorporates both natural science and social science perspectives, for use in a novel decision-making framework for natural-hazard management. Second, the decision-making framework was applied to case studies at three sites in the western United States with varying intensity of development in the wildland-urban interface; a range of debris-flow mitigation and erosion-control best-management-practices were evaluated with the decision-making framework to minimize the anticipated damages from post-fire debris flows while utilizing a minimal budget for a range of hydrologic basins at each site. Finally, a review of wildfire-related debris-flow histories was performed; climate model predictions of wildfire-increases and rainfall-changes were combined with data from the review to quantitatively analyze increases of expected debris-flow occurrence in a changing climate.

As the current literature provides only qualitative guidance for natural hazard risk management, the proposed quantitative optimal natural-hazard-management framework constitutes a significant advance of existing knowledge. Additionally, the evaluation of anticipated changes to post-fire debris-flow hazard will provide an important basis for understanding how climate change will affect community protection in the increasingly populated wildland-urban interface in the western United States. The methods and key results of each of the three key tasks are summarized in the following sections. The work described in this report supports ongoing efforts to develop more quantitative approaches to natural-hazard risk management through the use of integrated natural and social models.

## 2.0

# Background

The following subsections provide a general overview of the issues addressed by the studies discussed in this report. Section 2.1 provides background about quantifying costs related to post-fire debris-flows. Section 2.2 provides background on optimization modeling and optimal natural-hazard management framework, and Section 2.3 provides background related to expected increases in post-fire debris flows with changing climate. Much of the discussion provided in the following sections was previously published in McCoy et al. (2014), McCoy et al. (in preparation), and/or Brunkal and Santi (in review).

### 2.1 Quantifying Damages from Post-Fire Debris Flows

The discussion provided in Section 2.1 and associated subsections will be published in McCoy et al. (in preparation).

Estimated damages and associated risks from expected post-fire debris flows are used as inputs to the natural-hazards management framework. The estimation process involves three steps 1) estimating probability, volume, and runout of a potential post-fire debris flow, 2) identifying and valuing the elements at-risk, and 3) calculating economic risk. Additionally, the optimal hazard-management framework requires estimates of cost and effectiveness for commonly-used debris-flow management techniques and erosion-control best-management practices. Because there are several distinct fields involved with this process, background information about each aspect is divided into subsections below.

#### 2.1.1 Post-Fire Debris-Flow Hazard and Risk

Methods for rapidly performing post-fire debris-flow hazard assessments have been developed over the past decade and are now commonly performed following wildfires in the western United States (e.g., Cannon et al. 2010a; Tillery et al. 2011). However, the scope of these hazard assessments is often limited to estimating probability and volume of potential debris flows; few assessments include modeling of debris-flow runouts and when they do, the analysis is usually limited to production of hazard zone maps. While these hazard assessments are an important component of post-fire debris-flow hazard management, they alone do not provide enough information to select appropriate treatment technologies. In addition to understanding the debris-flow hazard (i.e. probability and volume), practitioners need to consider the effectiveness and cost of treatment, as well as the nature of downstream values-at-risk in order to select the appropriate treatment technology (Napper 2006).

Methods for estimating cost (Napper 2006) and effectiveness of treatment (Napper 2006; Robichaud et al. 2010) have been prepared by the United States Forest Service using results from historical project data. However, identifying and assessing downstream values-at-risk is a more complicated task. Calkin et al. (2007) describes a framework for assessing post-fire values-at-

risk developed by the Forest Service. This framework is based on a combination of mass based sediment yield calculations described by Robichaud et al. (2007) and professional judgment. In this framework, calculations are based on probability of occurrence of a given mass-based magnitude of soil erosion instead of potential debris-flow runout. The framework indicates that debris-flow hazards may exist and that associated values-at-risk should be considered, but it does not specify how to identify features affected by debris flows or how to assign values to them. Therefore, additional work is needed to develop simple, rapid, and consistent methods for identifying and assigning values to elements-at-risk from post-fire debris flows.

### **2.1.2 Probability and Volume Modeling and Model Inputs**

The following discussion was previously published in McCoy et al. (2014).

Methods of estimating probability and volume for post-fire debris flows in southern California and the intermountain western United States have been described by Rupert et al. (2008), Gartner et al. (2008), and Cannon et al. (2010b). These methods are generally based on regression of local geologic, hydrologic, and burn severity characteristics of specific burned basins. The use of a given set of probability and volume equations is generally limited to the region for which a particular model was derived. Cannon et al. (2010b) describe several models for probability based on data from 388 burned basins, for use in the intermountain western United States. Cannon et al. (2010b) and Gartner et al. (2008) describe a single model for volume based on data from 53 burned basins in Colorado, Utah, and California, that is applicable to both the intermountain west and southern California. Models may be revised or superseded as additional data is obtained (e.g., USGS 2014). Additionally, new models may be developed to more effectively model unique site conditions.

Rainfall data related to debris-flow generation is developed from several sources. Cannon et al. (2008) described rainfall conditions that led to post-fire debris flows in southwestern Colorado and southern California. Staley et al. (2013a) discuss recently revised methods for estimating intensity/duration thresholds in southern California. Rainfall intensity and depth recurrence interval data can be downloaded from the National Oceanic and Atmospheric Administration (NOAA) online precipitation frequency data server (NOAA 2013). Single precipitation intensity/depth values for a specific recurrence interval storm may be selected for a region, or a GIS grid of expected intensity distribution may be downloaded for more precise estimation.

Burn severity data are either generated from satellite imagery, or by Burned Area Emergency Response (BAER) personnel on the ground (Parsons et al. 2010). Satellite burn severity data are readily available online. The BAER imagery support data download site (Forest Service 2013) now provides soil burn severity data following fires. Users should be aware that older data or preliminary data from this website, such as the burned area reflectance classification (BARC) that was available prior to 2012, reflect vegetation burn severity and not necessarily soil burn severity. Soil burn severity data include both the loss of vegetation, and impacts to soil characteristics (e.g., reduced infiltration rates of burned soils). Additionally, because preliminary data are usually collected shortly after a fire, they may capture transient features such as clouds or residual smoke that affect the digital image interpretation. Field verification of BARC imagery is used to address these issues. As discussed by Parsons et al. (2010), satellite burn

severity data must be field verified and edited to generate soil burn severity data (which may be more useful for debris-flow calculations). This process may result in changes to the reported burn severity classifications. Field verification may be performed by BAER teams. Parsons et al. (2010) provides a description of field methods to map burn severity on the ground, and to ground truth BARC data immediately following a fire.

An alternative source of burn severity data is the Monitoring Trends in Burn Severity (MTBS) website (MTBS 2014). Similar to the preliminary BARC data, MTBS data reflects vegetation burn severity, not soil burn severity. MTBS data is typically collected approximately 1-year following a fire in order to observe the site near the maximum vegetation growth season (MTBS 2014; Parsons et al. 2010). Because these data are collected on a less critical time scale, image quality and interpretation is often better than that used for the BARC data. Drawbacks of these data for debris-flow hazard and risk assessments are that the data do not reflect soil impacts (e.g., reduced infiltration rates), and the data are usually not available for at least a year following the fire.

Several models for predicting probability and volume have been developed by various investigators. A particular regression model may have been derived using a specific type of burn severity data (i.e. BARC, soil burn severity, or MTBS). Experience running models with different data sources suggests that while differences between these different sources may be subtle in some cases, they can be dramatic in others. It is therefore important to know the source of the burn severity data used for analysis, and what data were used to derive the specific model that will be used to predict probability and volume. For emergency debris-flow hazard analysis, soil burn severity data obtained from the responsible local or federal agency or field verification of the downloaded BARC data are usually the best option, but in some cases preliminary BARC data must be used. For longer-term studies, MTBS data may be more appropriate if those data were used to derive the model. In some cases, it is not clear which burn severity data source was used to derive the model, or that data source may not be available. If this is the case, the user should be aware that there could be unquantified error in the probability and volume calculations.

### **2.1.3 Runout Models**

The following discussion was previously published in McCoy et al. (2014).

Rickenmann (2005) discusses a broad range of methods for evaluating landslide runout, some of which may be useful for post-fire debris-flow modeling. One relatively simple model to evaluate debris-flow runout is the GIS based computer program LAHARZ (Iverson et al. 1998; Schilling 1998). The program utilizes a pair of semi-empirical relationships between planimetric and cross-sectional areas inundated by a lahar or debris flow to model the expected runout and footprint of the flow in a GIS.

The LAHARZ program was initially developed by the USGS to model lahars in volcanic terrain. It has subsequently been modified to model non-volcanic debris flows and rock avalanches (Griswold and Iverson 2008), and post-fire flows (Bernard 2007). Magirl et al. (2010) describe use of the program to analyze large debris flows in Arizona and Witt et al. (2012) describe use of

the program for hazard assessment in North Carolina. Berti and Simoni (2007) describe development of a computer code that is conceptually similar to LAHARZ, but features more control in unconfined channel reaches and the ability to batch model a range of planimetric and cross-sectional areas to account for uncertainty in the inundation area regression models.

Alternative methods that are sometimes used for modeling debris-flow runouts include Flow-R and FLO-2D (Horton et al. 2013; Jakob et al. 2013, respectively). These programs have the ability to model more complex flow relationships than the simple space-filling model of LAHARZ. However, caution should be exercised when using more complex flow models. As Magirl et al. (2010) point out, some of the key parameters necessary to operate more complex flow models may be difficult to estimate, and may vary over space and time during a debris flow, especially under post-fire conditions where debris flows often form from channel erosion and may not have a predictable explicit source location. Further, calibration of input parameters for these models may require levels of time and effort that conflict with the need for rapid hazard assessment after a fire.

#### **2.1.4 Quantifying Effectiveness and cost of Selected Mitigation Methods**

The following discussion will be published in McCoy et al. (in preparation).

Significant previous work has been done to estimate costs and effectiveness of post-fire erosion control and debris-flow management techniques (e.g., deWolfe 2006; deWolfe and Santi 2009; deWolfe et al. 2008; Napper 2006; Prochaska et al. 2008; Robichaud et al. 2010). The post-fire debris-flow risk model described in this proposal provides unique curves of damage and risk as functions of debris-flow volume for each basin as input to the optimization model. However, it is also necessary to identify mitigation methods, estimate the cost per unit application, and to frame the effectiveness as either a unit reduction in debris-flow volume, or a unit reduction in probability of occurrence in order to complete the optimization process. Some refinement of the information presented by Robichaud et al. (2010) and Napper (2006) is necessary to meet this need.

#### **2.1.5 Model Uncertainty and Alternative Methods**

The following discussion was previously published in McCoy et al. (2014).

The methods of calculating probability and volume of post-fire debris flows discussed in Section 3.1 have been widely used by the United States Geological Survey (USGS) to evaluate post-fire debris-flow hazards. Cannon et al. (2010b) and Gartner et al. (2008) indicate that their volume model is valid to within an order of magnitude of the predicted debris-flow volume. These methods are most commonly used to evaluate hazards to within an order of magnitude by calculating probability and volume for a specific rainfall scenario, generalizing expected volumes and probabilities into relative hazard classes, and identifying the relative hazard along a portion of a mountain front through combined probability and volume classes. Examples of this process can be seen in (Cannon et al. 2010a) and (Tillery et al. 2011). One reason for this generalized approach is the uncertainty inherent in the models, especially modeled volumes.

An alternative to modeling any single value is to calculate multiple volume estimates within reasonable bounds using either the standard error of the regression model at a selected confidence interval as was done in the case study described herein, or by using a single order of magnitude as a bound for the range as described by Magirl et al. (2010). For extremely large storms, or unfavorable basin conditions, modeled volumes may exceed reasonable expectations. Reasonable upper bounds can be selected from historically observed post-fire debris-flow activity using a database such as that compiled by Santi and Morandi (2013). Using a database, a range of reasonably expected volumes can be calculated for a given scenario.

Even though a range of likely volumes can be predicted, a limitation of many existing volume models is an inability to predict probability of a specific volume occurring. As Lee and Jones (2004) discuss, probability of a given volume or runout occurring is a necessary input for a true landslide risk assessment. Donovan (2014) recently developed a probabilistic method for estimating volume along channel lengths. Donovan (2014) indicates that the probabilistic model also provides improved accuracy over the previously discussed volume models. This model may prove useful for future post-fire debris-flow risk calculations; however, the model was not used for the work described in this report because it was developed after the case study analysis was completed.

## **2.2 Optimization Framework and Natural-Hazards Management**

The discussion provided in Section 2.2 will be published in McCoy et al. (in preparation).

From a computational perspective, the case study analysis comprises a novel application of existing optimization techniques to the natural hazard management problem. There has been a body of related research conducted from the perspective of insurers, who try to optimize their position in the market when insuring natural hazards (e.g., Amendola et al. 2000). However, to our best knowledge, there is no previous technical literature on the application of optimization techniques to minimize total expected damages from post-wildfire debris flows by optimally allocating resources for mitigation.

Following a wildfire, the land manager is responsible for a number of drainage basins with risk of post-wildfire debris flows. Each basin has a probability of debris flow occurrence and an estimated debris flow volume based on its physical characteristics. The relationship between debris flow volume and economic damage is also unique to each basin depending on how many structures it has and their spatial layout in relation to the runout path. The manager also has multiple options for mitigation strategies that may decrease debris flow probability, volume, or both.

In order to minimize the expected damages from post-wildfire debris flows, the land manager must decide which drainage basins to mitigate, which mitigation strategies to use, and the magnitude of each mitigation effort while keeping costs below the specified budget. This problem can be classified as a mixed integer nonlinear program. It has a nonconvex objective function, but the nonconvexity and nonlinearity can be moved to the constraints through standard reformulations to aid in solving the problem to global optimality.

### 2.3 Expected Changes in Post-Wildfire Debris Flows with Climate Change

The discussion provided in Section 2.3 and associated subsections will be published in Brunkal and Santi (in review).

The connection between climate change in the last half of the twentieth century and the length of the wildfire season has been addressed by multiple authors in the published literature, most notably Westerling et al. (2006). They note that wildfire activity increased suddenly and markedly in the mid-1980's, with higher large-wildfire frequency, longer fire durations, and longer wildfire seasons, strongly associated with increased spring and summer temperatures, as seen in the graph in Figure 1.

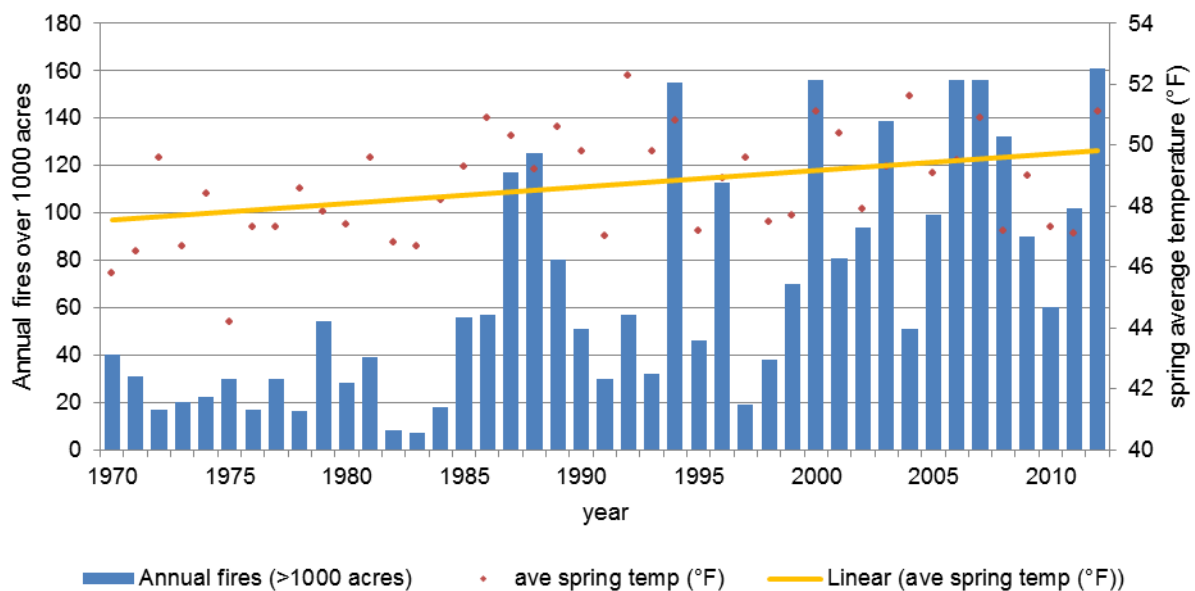


**Figure 1.** Increase of wildfires on USFS land over 1,000 acres and avg. annual spring temperature for the western U.S. The relationship between increasing wildfire numbers and increasing temperature in the western U.S. is shown. Reproduced from Westerling et al., 2006, and ClimateCentral.org (Brunkal and Santi in review).

A review of published literature reveals that the connection between increases in wildfire, both frequency and size, and climate change is not a new one. The climate, drought and fire connection was becoming emphasized after the devastating fires in Yellowstone National Park in 1988 (Balling et al. 1992; Meyer et al. 1992; Millspaugh et al. 2000). In 1994, an article in the *Journal of Climate* concluded that, in a modeled scenario of 2 times atmospheric CO<sub>2</sub>, lightning-caused wildfires would increase by 44%, area burned would increase by 78%, and all western states would see an increase in lightning-caused wildfires (Price and Rind 1994). Grissino-Mayer et al. (2004) conclude that fire severity, frequency and extent are expected to change dramatically in the coming decades in response to changing climatic conditions. Littell et al. (2009) state that the total area burned by wildfire, in any given year, is directly related to climate through the influence on fuels production and drying of vegetation. They conclude that the area burned by wildfire, despite the influence of fire suppression, exclusion, and fuel treatment, is

substantially controlled by climate. Their conclusion that weather and climate are the most important factors influencing fire activity is also supported by Flannigan et al. (2000) and Morgan (2008). The assertion that future warmer temperatures will increase burned area and contribute to an earlier start to a longer wildfire season is strongly supported in the scientific literature.

Landscapes burned by wildfire are especially prone to producing large run-off events including floods, hyperconcentrated flows and debris flows (e.g., Cannon et al. 2003; Giraud and McDonald 2007; Moody et al. 2008; Scott 1971; Wells 1987). Within the first few years after a fire, intense precipitation (typically brief summer convective storms or cells of high intensity rainfall in winter storms) produces runoff from bare, burned slopes, with progressive sediment bulking on slopes and in channels (Meyer et al. 2001). These post-wildfire debris-flow events also threaten communities and infrastructure at the wildland-urban interface. For example, the 2009 Station Fire in Southern California burned 160,000 acres, 58 homes were lost in the fire and 73 homes were lost to subsequent debris flows that were initiated by a winter rain storm (Burns et al. 2011).

Climate-change models show an increase in temperatures that will lead to more wildfires, but they also show a significant change in the precipitation patterns that are known to initiate post-wildfire debris flows. Regional scale climate models predict that the change in the precipitation patterns across North America will deliver rainfall in more intense storms. Changes in precipitation have already been documented across North America in the 20th century. Data shows that since 1910 precipitation has increased by about 10%, and this change is reflected primarily in the heavy and extreme daily precipitation events (Karl and Knight 1998). Models presented by Meehl et al. (2000) predict that precipitation extremes will increase, resulting in a decrease in the return period for 20- year extreme precipitation events almost everywhere. Heavy rainfall events have become more frequent over the past 50 years, even in locations where the mean precipitation has decreased or is unchanged (Chen and Knutson 2008). These findings are significant for debris flow initiation, as Cannon et al. (2008) show that post-wildfire debris flows require only short recurrence interval storms to propagate.

In this preliminary investigation into the effects of climate change on post-wildfire debris flow numbers, we examined the published literature for analysis of current climate change models, and the predicted changes to wildfire and precipitation occurrences in the western U.S. Climate change models are improving in their resolution and accuracy with increasing data inputs and with better definition of boundary conditions. Two main model types exist, General Circulation Models (GCM) and Regional Climate Models (RCM); these are used for different modeling scenarios, and are available from sources such as the National Center for Atmospheric Research (<http://ncar.ucar.edu/>) and the Hadley Centre for Climate Science (<http://www.metoffice.gov.uk/publicsector/climate-programme>).

A GCM is a numerical model representing the physical processes in the atmosphere, ocean, cryosphere and land surface. GCMs are the most advanced tools currently available for simulating the response of the global climate system to increasing greenhouse gas concentrations (<http://www.ipcc-data.org/>). Coupled atmosphere-ocean global climate models (AOGCMs) are the modeling tools traditionally used for generating climate change projections and scenarios.

AOGCMs depict the climate on a coarse resolution of 250-600 km, so many physical processes that occur on a smaller scale cannot be modeled unless used in conjunction with nested regional models. These nested models have the potential to provide geographically and physically consistent estimates of regional climate change that are required in impact analysis.

RCMs provide a higher spatial/temporal resolution and are often a better representation of some weather extremes than GCMs. What is commonly referred to as nested regional climate modeling technique consists of using output from global model simulations to provide initial conditions and time-dependent lateral meteorological boundary conditions to drive high-resolution RCM simulations for selected time periods of the global model run. Sea surface temperature (SST), sea ice, greenhouse gas (GHG) and aerosol forcing, as well as initial soil conditions, are also provided by the driving AOGCM (Mearns et al. 2003). These regional climate simulations can be applied to the prediction of fire conditions and regional precipitation patterns.

Another technique for obtaining regional predictions is statistic or dynamic downscaling; this provides high spatial resolution information in non-uniform regional climate models (Mearns et al. 2003). There is a potential with this technique to address a diverse range of variables. One of the primary advantages of these techniques is that they are computationally inexpensive, and thus can be easily applied to output from different GCM experiments. Another advantage is that they can be used to provide specific local information (e.g., points, catchments), which in many climate-change impact studies is the most applicable outcome. The applications of downscaling techniques vary widely with respect to regions, spatial and temporal scales, type of predictors and predictands, and climate statistics, and there are disadvantages such as assuming consistency of empirical relationships in the future (Mearns et al. 2003). Fowler et al. (2007), Maraun et al. (2010), Chen and Knutson (2008) are a few examples of publications that provide a thorough review and assessment of different downscaling techniques and their application to hydrological modeling. These studies address ultimately how model data inputs and results can be best used to enable stakeholders, managers and other end users of the climate models to make informed robust decisions on adaptation and mitigation strategies.

There is an extensive library in the published literature on climate model types, the use and effectiveness of climate models, and their general applicability. It is not the purpose of this paper to review all methods, benefits and limitations of global and regional scale climate models. The selected models used to assess potential future scenarios for post-wildfire debris flows and the methods applied are discussed in Section 3.3.

### **Climate and fire models**

Fire frequency, severity and burned area extent have been shown to be increasing in the last half of the 20th and first decade of the 21st century. Climate Central (<http://www.climatecentral.org/>) has compiled and made available to the general public the results of historical data analysis for temperature and fire area, as well as numbers of large wildfires in the western U.S. The 2012 summary of western wildfires by Climate Central provides a review of the length of wildfire season and the climatic factors affecting it, including increasing temperatures and the resulting earlier spring snowmelt. Climate models consistently predict that the Western U.S. will get

hotter and drier, and with this the fire season will get longer and the amount of area burned each year will increase.

Flannigan et al. (2000) use two transient GCMs (the Hadley Centre and the Canadian GCM) to estimate fire season severity in the middle of the century for North America. Fire Season Severity Rating (SSR) is an index to examine changes in fire severity recognizing that the fire regime at any given location is the result of complex interactions between fuel, topography, ignitions and weather. The SSR is a component of the Canadian forest fire weather index, and is essentially the seasonal mean of the daily estimate of the control difficulty of a potential fire, in generalized fuel types. The fire severity assessment is a proxy measurement of the potential intensity of a fire. The fuels moisture models form the core of the fire weather index, with consideration of multiple other fire-related factors. Both of the GCMs used by Flannigan et al. (2000) suggest an increase in SSR of 10-50% across much of North America by 2060. They research conclude that the fire season will start earlier in the year and extend longer into autumn, resulting in universal increases in area burned and fire intensity/severity.

Brown et al. (2004) employ a high-temporal resolution meteorological output from the Parallel Climate Model (PCM) to assess changes in wildland fire danger across the western U.S. due to climatic changes in the 21st century. The authors compare the base period (1975- 1996) to predicted outputs from the GCM using the USDA/USFS National Fire danger rating system (NFDRS), which focuses on the Energy Release Component (ERC), an indicator of fire severity (amount and extent of fire) and fire business (decisions, economies, treatments). Changes in relative humidity, especially drying over much of the West, are projected to increase the number of days of high fire danger in comparison to the base period. The research presented shows that the climate models used can be applied to future fire danger evaluation, and that nearly the entire western U.S. is projected to experience increases, by as much as two weeks, in the number of days that the threshold for large expensive fires is exceeded.

Fried et al. (2004) present research using GCM output to estimate the impact of climate change on wildland fire in Northern California. The Changed Climate Fire Modeling System (CCFMS) models potential fire behavior based on weather, fuel conditions, and slope for the historical weather and the climate change scenario. This model bridges the differences in the spatial and temporal scales of climate model output and historical fire data to model fire behavior, fire suppression, and outcomes of individual fires. Conclusions indicate that warmer and windier conditions corresponding to a 2xCO<sub>2</sub> scenario produce fires that burned more intensely and spread faster in most locations. Changes in area burned were on average increased by 5000 hectares. The best-case forecast from this study is a 50% increase in area burned and an over 100% increase in fire escape frequency. Representative fires were modeled to arrive at precise estimates of the frequency of escapes and other statistics that cannot be estimated by modeling average fire characteristics. For the northern California region, it was shown that there is an expected 34% increase in area burned from fires in grass and brush, and a 65% increase in area of oak woodland burned under climate change conditions in the near future (Fried et al. 2004).

### **Climate and Precipitation Models**

Far more abundant in the published literature are studies that seek to model the changes in precipitation and the hydrologic cycle with changing climate. Water resource availability,

drought, and changes in rainfall and snow accumulation are important considerations for the western U.S., these factors affect wildfire scenarios as well as post-wildfire runoff and erosion, including debris flows. Changes to precipitation patterns have been documented for the past decades, and are expected to change in the coming decades with an increase in atmospheric CO<sub>2</sub>. Trenberth et al. (2003) substantiate that the incidence of heavy rainfall has steadily increased at the expense of moderate rainfall events throughout the 20th century, and on the basis of evaporation and temperature relationships, they conclude that all weather systems, from individual clouds and thunderstorms to extratropical cyclones, are likely to produce correspondingly enhanced precipitation rates with increased atmospheric CO<sub>2</sub>. Meehl et al. (2000) find that early models that show global increase in precipitation are supported with consistent results from newer models; precipitation extremes increase more than the mean, resulting in a decrease in return period for 20-year extreme precipitation events almost everywhere (e.g. to 10 years over North America).

Leung et al. (2004) use a regional scale climate model to assess the impacts of climate change on the western U.S. In their research they use The Penn State/NCAR Mesoscale Model (MM5) to downscale the original NCAR/DOE Parallel Climate Model (PCM). This strategy yields ensemble regional climate simulations at 40km spatial resolution for the western U.S. Results from this model show an average warming of 1-2.5 Celsius, and an increase in cold season extreme daily precipitation by 5-15 mm/day (15-20%) along the Cascades and Sierra. The overall warming in the west will result in increased rainfall at the expense of snowfall. The conditions caused by warmer temperatures, such as less snow for spring runoff, reduced soil moisture in the summer, and more intense precipitation are all common model outputs for the western U.S.

Dynamic downscaling presented by Kim (2005) is used as a means to predict the effects of climate change on extreme hydrologic events in the western U.S. To obtain regional scale climate change signals, Kim (2005) uses two GCMs downscaled using a RCM employed for dynamic downscaling. This model was found to show good agreement in hindcast without significant biases on the projected climate change signals. The conclusions of this model evaluation suggest that heavy precipitation events are likely to increase under increased CO<sub>2</sub> climate conditions, most notably in the mountainous regions along the Pacific Ocean and the Sierra Nevada, and the largest increases in heavy and extreme precipitation occur during the fall and winter. The important relationship demonstrated is that both the number of wet days and the mean intensity of each event will increase, causing the precipitation-intensity frequency distributions to shift toward higher values.

Models used for flood risk and streamflow timing in the western U.S. are presented by Hamlet and Lettenmaier (2007) and Hidalgo et al. (2009), respectively. These papers explore the differences in observed shifts in the delivery and timing of precipitation, and the model predictions for changes across the western U.S. Both studies show that climate change and variability will affect drainage basins by increasing rain events, decreasing snow pack, and increasing flood risk over much of the West. They also note that evolving flood risks will impact design standards, flood-inundation mapping, and water planning and will also result in substantial changes to sediment transport and channel formation processes.

Nearing (2001) takes a soil conservation approach to the changing delivery of precipitation with an evaluation of rainfall erosivity using climate models. The research presented uses two coupled Atmospheric-Ocean Global Climate Models (UK Hadley Center and the Canadian Centre for Climate Modeling and Analysis) as the basis for change in rainfall delivery and the Revised Universal Soil Loss Equation to calculate potential soil erosion rates. Conclusions from this research show that warmer atmospheric temperatures will lead to a more vigorous hydrologic cycle including more extreme rainfall events.

The published literature provides many types of models and predictive methodologies for precipitation under climate change conditions both globally (e.g., Allan and Soden 2008; Kharin et al. 2007; Meehl et al. 2000; Trenberth et al. 2003) and regionally (e.g., Chen and Knutson 2008; Kim 2005). The majority of the model outputs show an increase in precipitation that is delivered as higher intensity rainstorms. This has been a measured trend across the western U.S. in the past decades and is expected to keep trending to more extreme cases with increased atmospheric CO<sub>2</sub>.

### **Debris flow initiation in burned areas**

The relationship between wildfires and debris flows is well established (Cannon 2001; Cannon and Gartner 2005; Cannon et al. 2010b; Shakesby and Doerr 2006; Spittler 1995), and the reasons that debris flows are common in burned basins are also well described in the literature (Shakesby and Doerr 2006; Wells 1987; Wondzell and King 2003). Areas that have been burned by wildfire are susceptible to debris-flow initiation because of several factors, including decreased rainfall interception by vegetation, decreased soil infiltration capacity and stability, and the potential for hydrophobic layers at shallow depths that promote run-off and rilling (Ebel and Moody 2013; Moody et al. 2008). Post-wildfire debris flows are most common in the first two-years after a fire (Cannon et al. 2003) and are usually triggered by short duration, high-intensity rainfall.

Post-wildfire debris flows often occur with little antecedent moisture and generally have no identifiable initiation source, such as a distinct landslide scar (Cannon et al. 2008). Short-duration, high intensity convective storms with recurrence intervals of two years or less have been shown to create a debris-flow response from burned basins in the Western U.S. Frontal storms are also shown to trigger debris flows with low-intensity, longer -duration rainfall, still with a recurrence interval of less than two years (Cannon et al. 2008). The threshold rainfall conditions for floods and debris flows from burned areas are lowest in the first two years following the fire and then increase as fire recovery begins (Gartner et al. 2004). In southern California as little as 7 mm of rainfall in 30 minutes has triggered debris flows, and any storm that has intensities greater than about 10 mm per hour is a risk of producing a debris flow (USGS fact sheet 2005-3106). Debris flows were produced from 25 recently burned watersheds in Colorado in response to 13 short-duration, high intensity convective storms and after as little as 6 to 10 minutes of storm rainfall (Cannon et al. 2008). Cannon (2001) shows that of 95 post-wildfire areas studied, 37 drainages produced debris flows, and of those 23 were considered the more destructive type that transport materials up to and including boulders. These destructive types of erosional responses from burned areas are the focus of this study because of the potential impacts with an increase in number of events.

The emergency assessment of the debris-flow hazards from drainage basins burned by wildfires has been refined and used in many instances by the U.S. Geological Survey (Cannon et al. 2010a; Skinner 2013; Staley 2013; Staley 2014; Staley et al. 2013b) and BAER (Burned Area Emergency Response) teams (DeGraff et al. 2007). Empirical models, that can be used to calculate the probability of debris-flow production from individual drainage basins in response to given storms, have been developed from data from burned areas in the intermountain west; (Cannon et al. 2010b) describes the development of a logistical regression multivariate statistical model for estimating debris flow probability. The analyses consider and evaluate a set of independent variables that potentially characterize runoff processes in burned basins including: basin gradient, basin aspect, burn severity distribution within the basin, soil properties, and storm rainfall conditions. Cannon et al. (2010b) identified 5 statistically significant multivariate models that incorporate the variables most strongly correlated with debris-flow occurrence. The percentage of the basin burned at a combination of high and moderate severity and the average storm intensity were significant in every model. The 5 models provide varying results for specific locations so application of the correct model to the correct area is important for the most applicable results. These probability models can be applied to assess the changes likely in debris-flow probability due to climate change and the increase in area burned at high severity and rainfall intensities.

## 3.0

## Methods

The following subsections describe methods to complete the tasks described in Section 1.0. The method descriptions in these sections were previously published in McCoy et al. (in preparation), and Brunkal and Santi (in review). Section 3.1 describes methods for evaluating post-fire debris-flow hazard, Section 3.2 describes methods for optimization modeling, Section 3.3 describes the three case study sites, and Section 3.4 describes methods for evaluating increases in debris-flow occurrence with climate change.

### 3.1 Quantifying Economic-Costs of Post-Fire Debris Flows

This section summarizes methods for evaluating debris flow hazards and associated costs following fires at three sites in the western United States. The method descriptions in Section 3.1 and associated sub-sections were previously published in McCoy et al. (in preparation) and McCoy et al. (2014).

#### 3.1.1 Estimation of Debris-Flow Probability and Volume

Probability ( $p$ ) and Volume ( $v$ ) were estimated following equations described by Cannon et al. (2010b). The maximum volume of post-fire debris flows can be significantly less than other forms of debris flow and volumes predicted using the empirical regression models described above may exceed reasonable values when compared to historical observations. This is especially true for cases of high-intensity low-recurrence interval storms, or where site conditions lead to large upper bounds of uncertainty in modeled debris-flow volume. In order to manage this artifact of the empirical models, we limit the upper bound for reasonably expected post-fire debris-flow volume to 500,000 cubic meters ( $m^3$ ) based on records of post-fire debris-flow activity compiled by Santi and Morandi (2013). As discussed by McCoy et al. (2014), there are various methods available to account for uncertainty in the predicted volume; however, the use of these methods significantly complicates the optimization process. For the modeling discussed in this report, it is assumed that the probability of debris-flow occurrence given occurrence of a storm will apply to the modeled volume - i.e. if a debris flow occurs, it will be of the volume modeled, constrained by the previously stated upper bound.

#### 3.1.2 Modeling Debris-Flow Runout

Debris-flow runout for each scenario was modeled in ArcGIS (version 10.0, ESRI 2010) using the LAHARZ program (Iverson et al. 1998; Schilling 1998). The program was initially developed by the USGS to model lahars in volcanic terrain, and has been subsequently calibrated for non-volcanic debris flows and rock avalanches by Griswold and Iverson (2008), and for post-fire debris flows by Bernard (2007).

Selecting an appropriate location for onset of deposition for post-fire debris flows can be difficult. Bernard (2007) briefly discussed some of the difficulties in locating the onset of deposition for post-fire debris flows; the author mentioned that recent debris flows visible on aerial imagery could be used to identify the location, but did not provide any positive guidance for how to model the onset point for areas that have not recently experienced debris flows. Brock (2007) compared various methods of locating the point of onset of deposition for debris flows in unburned areas with observations from burned areas following two fires that occurred in 2003; she noted that none of methods for debris flows in unburned areas provided adequate results for the burned basins. Brock (2007) did develop a method for locating the point of onset of deposition for post-fire debris flows in southern California, but the method was specifically calibrated to two mountain ranges and does not cover any of the areas used in this study. Furthermore, the method was developed using a 2-meter (m) resolution digital elevation model (DEM); Brock (2007) indicated that the method would not work using a 10-m DEM, which was the best resolution available for the sites discussed in this paper.

Because of the lack of consistent methodology available for locating the point of onset of deposition, debris-flow deposition was assumed to begin at the pour-point used to define the basin for the sites discussed in this paper. This point was either located directly above a feature of interest, or coincided with the edge of the burned area, a noticeable change in slope, or both. Debris-flow runouts were modeled for a range of plausible volumes to generate curves of damage vs. debris-flow volume from each basin as discussed in the following sections.

### **3.1.3 Identifying Features Intersected by Debris-Flow Runout**

The discussion in this section and associated subsections was previously published in McCoy et al. (2014) and/or McCoy et al. (in preparation).

Features (residences, roads, streams, and trails) intersected by the modeled debris-flow runout were identified in ArcGIS. Figure 3 shows an example of features intersected by modeled debris-flow runouts representing the modeled value, and +/- 95% confidence bounds (McCoy et al. 2014). The following subsections briefly summarize the process of identifying intersected features in GIS. Data sources and procedures for identifying features directly intersected by potential debris-flow runouts from individual basins were described in detail by McCoy et al. (2014).

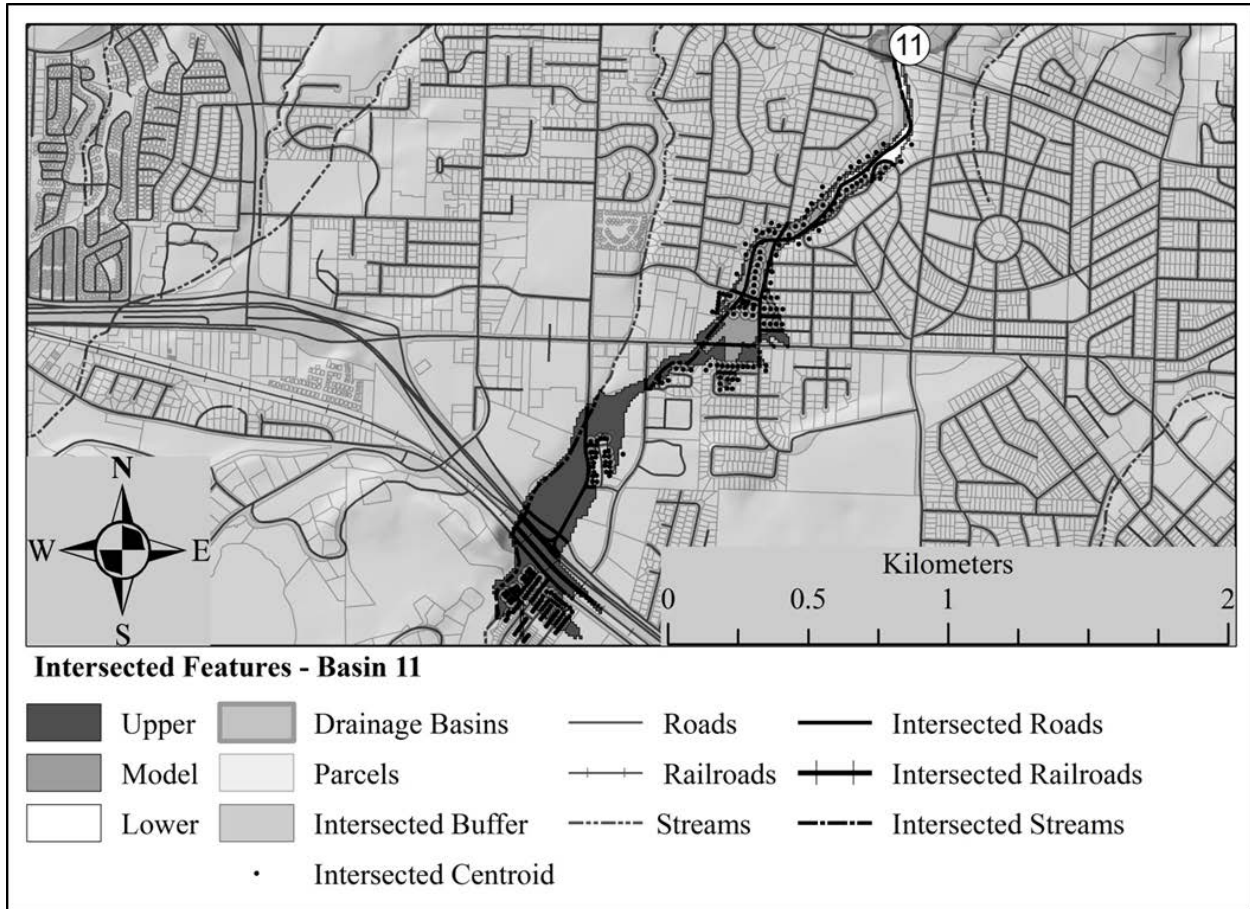


**Figure 2.** Example of features intersected by modeled debris-flow runout in GIS (McCoy et al. 2014).

### Point Features

Point features (residences and campsites) were located using a variety of publicly available data sources. Vulnerability of residences was estimated as 30% of median home value as described below. Vulnerability of campsites was assumed to be 1 (i.e. complete loss-of-access was assumed if the campsite buffer was intersected). Exposure of all point features was assumed to be 1.

Where available, assessor’s parcel maps were used to locate residences in ArcGIS. The centroid of each parcel was automatically located in ArcGIS using spatial analyst tools, and a 20-m-diameter circular buffer was created around the parcel centroid or digitized point to approximate the extent of the structure. Where parcel maps were not available, residences were located on aerial imagery. A point was placed over the approximate center of structures near potential debris-flow runout areas, switching between imagery in ArcGIS and Google Street View to limit the catalogued structures to those that were most likely residences. A 10-m-diameter circular buffer was created around the point. The smaller diameter buffer was based on improved spatial control on the location of the structure using the aerial imagery. Where applicable, campsites were identified to support evaluation of cost associated with lost access. Campsites were located in ArcGIS as points using a shapefile provided by the National Park Service (A. Valdez, personal

communication). A 40 m-radius circular buffer was placed around each point to represent the generalized area of the campsites.

The intersect tool was used in ArcGIS to identify structure or campsite buffers that were intersected by the runout footprint. A point feature was considered damaged if the modeled runout intersected any part the buffer. The dissolve tool was used to clean up extracted buffers so that no point feature was counted more than once per modeled runout. McCoy et al. (2014) provide an example of the process, including a schematic showing intersected features. The lack of easily obtainable statistics related to economic impacts to homeowners from post-fire debris flows makes it difficult to assess vulnerability of residences. Vulnerability of residences was estimated by multiplying the median home value by 0.30 (30%) based on expert opinion. Because of the limited data available, this assumption cannot be readily validated. We chose to use a coefficient of median home value to represent vulnerability of residences to debris-flow impact because modeling debris-flow depth and impact energy, cataloguing home construction type, and estimating explicit damages would require more complex runout models and survey time than the methods described in this paper. Alternative methods could provide more precise and accurate estimates of damages, but would be difficult to implement in an emergency management situation.

### **Linear Features**

Major linear features (roads, railroads, and streams) were located using TIGER/Line<sup>®</sup> shapefiles (Census 2012). Additional local linear features (4x4 trails and hiking trails) were digitized in ArcGIS from aerial photos or from georeferenced national park maps available online. Vulnerability and exposure of all linear features was assumed to be 1 - i.e. the full unit value of damage will be counted for all intersected lengths.

The ArcGIS intersect tool was used to identify linear features intersected by the runout footprint. Lengths of linear features from each category (roads, railroads, streams, 4x4 trails) that fell within the footprint of a given modeled debris-flow runout were summed and multiplied by unit values to evaluate damage. The process was described in more detail by McCoy et al. (2014). Hiking and 4x4 trails are evaluated using two different methods for comparison purposes. The direct damage method assumes that the damaged trails will be cleaned up shortly following the debris flows, and defines trail damage as the cost of sediment removal for the impacted area. The lost access method assumes that trails will remain inaccessible and defines their damage as the lost recreational value of all trails beyond the impacted part. Lost access to trails was evaluated using ArcGIS network analyst tools. The linear features were digitized into ArcGIS as described above. Each feature was given flow-directionality, assuming the goal of users was to traverse from one region to another. A geometric network was built assuming “source” and “sink” nodes for the “upstream” and “downstream” ends of the network, respectively. A range of debris-flow runout scenarios for varying debris-flow volume issuing from each basin was checked for intersection with the feature. The ArcGIS intersect tool was used to locate the points of intersection; the “downstream” point was then manually located for each debris-flow runout scenario that resulted in an intersection with that linear feature. Linear features were split at the point of intersection, and the length of feature “upstream” of the intersection was identified and multiplied by the unit access value to quantify value of lost access.

## Lakes and Reservoirs

Potential impacts to lakes and reservoirs were identified manually in ArcGIS. Lakes and reservoirs were identified from aerial images, from boundaries drawn on National Park Service Maps, or from large scale features identified using the “fill” tool in ArcGIS; boundaries of the features were digitized for further analysis. Vulnerability and exposure of all lakes and reservoirs was assumed to be 1.

Damage cost estimates differ between small and large reservoirs. Therefore, features were qualitatively classified as either “small” or “large”; however, a rigorous definition was not developed to divide these two categories. A range of debris-flow runout scenarios for varying debris-flow volume was modeled for each basin that emptied toward a lake or reservoir. For each basin, scenarios were checked to identify the minimum debris-flow volume required for the modeled runout to reach the boundary of the lake or reservoir. This volume was subtracted from the subsequent larger debris-flow volumes to arrive at a modeled “impact volume” to the water body. Due to potential complexity in modeling complete-reservoir-filling scenarios, volumes that exceeded estimated lake or reservoir volumes (for small water bodies) were ignored.

### 3.1.4 Estimating Damage Costs

The following paragraphs describe methods for quantifying direct damage and lost access to hiking and 4x4 trails and impacts to reservoirs from loss of volume from post-fire debris flows.

Table 1 shows estimated unit values for features intersected by debris-flow runout footprints in ArcGIS. The “site” column in Table 1 refers to the three case study sites. Unit costs presented in Table 1 were estimated based on various publicly available sources published over a range of years; costs were adjusted to 2012 United States Dollars (USD) using the Consumer Price Index (CPI) (BLS 2013) for consistency during method development. In practice all dollar figures mentioned in this study should be inflation adjusted to a common year so that their marginal costs and benefits may be equated during optimization. The following paragraphs describe the bases for these values.

As previously described by McCoy et al. (2014), values of residential structures at Site 1 were estimated by census block group using median home values from a pre-existing map based on the 2010 United States census. The map was accessed from ArcGIS Online through ArcGIS (ArcMap, ESRI 2010) on February 27, 2013. Polygons of census block group were digitized in ArcGIS using the map boundaries and median home values were manually assigned to the new polygons based on the values shown on the map. The median home value of each census block polygon was applied to parcel centroids falling within the polygon. Values of residential structures at Site 3 were estimated by identifying a residential structure within or near a debris-flow runout using aerial imagery in ArcGIS, manually locating Zestimate<sup>®</sup> values from Zillow.com for a range of nearby residences, averaging the results, and applying the average to the structure. Damage from a modeled debris flow was estimated as 30% of the median home value for each structure intersected by a modeled debris-flow runout; the sum of the damages from all structures intersected by a single modeled debris-flow runout was calculated to estimate total damage to residences from each scenario.

**Table 1.** Unit values for features intersected by debris-flow runout in ArcGIS (McCoy et al. in preparation)

Feature	Site	Unit	Unit Cost	Reference
Residences – direct damage (repair)	1,3	unit	varies	ArcGIS Online Zillow
Roads – direct damage (sediment removal)	1,3	linear meter	\$81.86	(Means 1999a)
Highways – direct damage (sediment removal)	3	linear meter	\$109.75	(Means 1999a)
Railroad – direct damage (track repair and sediment removal)	1,3	linear meter	\$143.38	(Means 1999a)
Stream – direct damage (restoration)	1,2,3	linear meter	\$3.28	(Holmes et al. 2004)
4 x 4 trail – direct damage (sediment removal)	2	linear meter	\$32.76	(Means 1999a)
4 x 4 trail – lost access	2	linear meter	\$1.58	(Deisenroth et al. 2009)
Hiking trail – direct damage (sediment removal)	2	linear meter	\$8.19	(Means 1999a)
Hiking trail – lost access	2	linear meter	\$3.39	(Bowker et al. 2007)
Camp site – lost access	2	unit	\$7,007	(National Park Service 1995)
Small reservoir – direct damage (sediment removal)	1,3	cubic meter	\$4.25	(Crowder 1987)
Large reservoir – direct damage (sediment control design and sediment removal)	3	cubic meter	\$1.42	(Crowder 1987)

As described by (McCoy et al. 2014), direct damage to infrastructure (roads and railroads) was quantified per unit length based on construction cost guides (e.g., Means 1999a; Means 1999b) and some assumptions of feature width and debris-flow deposit depth. Road damage was estimated as \$81.86/m assuming \$8.19/m<sup>3</sup> for soil removal, a 10-m-wide roadway, and a 1-m-thick deposit. Damage to highways (at Site 3) was estimated as \$109.75/m assuming \$8.19/m<sup>3</sup> for soil removal, a 13.4-m-wide roadway in each traffic direction, and a 1-m-thick deposit. Railroad damage was estimated as \$143.38/m, assuming \$61.52/m of track repair + \$81.86/m of soil removal (based on a 10-m-wide track bed, and a 1-m-thick deposit). 4x4-trail-damage was estimated as \$32.76/m assuming \$8.19/m<sup>3</sup> for soil removal, a 4-m-wide roadway, and a 1-m-thick deposit. Hiking trail damage was estimated as \$8.19/m, assuming \$8.19/m<sup>3</sup> for soil removal, a 1-m-wide trail, and a 1-m-thick deposit. Soil removal costs are derived from Means (1999a) assuming bulk excavation of clayey soils with a scraper, assuming 450 m haul distance; this cost is not significantly different from the cost using a front-end loader with a 1 m<sup>3</sup> bucket. Railroad track repair costs are derived from Means (1999a) assuming resurfacing and realigning additional track with crushed stone ballast. Costs assume local disposal of excavated materials and do not include costs for loading trucks, transporting excavated soils, or disposal. Costs for mobilization of equipment, or local variability in unit costs are also not included. The depth of inundation was estimated based on an assumption that on a flat open surface (e.g. a road) the deposit from an average post-fire debris flow would generally not exceed 1-m. More detailed

estimates are not available from the model because LAHARZ does not provide an estimate of deposit thickness. Direct damage to streams was estimated at \$3.28/m based on the value of lost ecosystem services following based on values presented by Holmes et al. (2004).

Value of lost access for hiking and 4x4 trails was estimated following methods outlined by Bowker et al. (2007) and Deisenroth et al. (2009). Value of lost access to hiking trails was estimated at \$3.39/m, using an estimated value of \$1/mile per trip based on values presented by Bowker et al. (2007), and assuming approximately 2% of visitors to Great Sand Dunes National Park and Preserve hike into high country. This assumes 33 trips per day for 7 days a week for 26 weeks of the year. Lost access to 4x4 trails was valued at \$1.58/m assuming an average value to users of \$7/mi per trip based on values presented by Deisenroth et al. (2009), and assuming an average of 2 trips per day for 26 weeks. Lost access to campsites was valued at \$7,007 per campsite per year, assuming an average cost of \$38.50/day for use based on values presented by National Park Service (1995), and assuming full usage 7 days/week for 26 weeks.

Value of lost reservoir capacity due to sedimentation from debris flows was estimated based on values presented by Crowder (1987). Crowder (1987) indicates that sedimentation to reservoirs can be controlled by building extra capacity, preventing sediment from settling in the reservoir, dredging to remove sediment, and replacing lost capacity with new construction. When converted to 2012 USD, the estimated unit cost of removing sediment by dredging (Crowder 1987) is approximately \$4.25/m<sup>3</sup>. However, Crowder (1987) states that dredging is only feasible in small lakes and reservoirs - although he does not provide a quantitative distinction for small vs. large reservoirs - suggesting that dredging may cost 3 to 8 times more than building replacement capacity, not including cost for disposal of dredge spoils. Crowder (1987) additionally states that broadly calculating economic damages from dredge costs alone would lead to overestimates of damage and suggests instead using combined costs from dredging, inclusion of sediment storage volume into new reservoirs, and construction of replacement storage. Because of the relatively high cost of dredging, the unit cost for sedimentation decreases dramatically using the combined costs of dredging, in-reservoir sediment storage capacity, and new dam construction, to approximately \$1.42/m<sup>3</sup> in 2012 USD based on the estimates provided by (Crowder 1987). For this study, two classes of reservoir were qualitatively selected, small reservoirs and large reservoirs; no attempt was made to develop quantitative criteria for distinguishing between the two classes. The dredging-only costs were applied to small reservoirs. The combined costs of dredging, in-reservoir storage, and new capacity were applied to large reservoirs.

### **3.1.5 Damage Curves**

To support optimization modeling and analysis of multiple debris-flow scenarios, we model a range of plausible debris-flow volumes and associated runouts for each basin. The quantity of intersected features is summed for each single runout model, and multiplied by the appropriate unit value. The resulting damages from each feature are then summed to estimate the total damage cost associated with a debris flow of given volume issuing from a given basin. The process is repeated for the range of debris-flow scenarios; the resulting data points are fit with a continuous monotone function in order to express damage cost as a function of debris-flow volume in each basin. These curves are used as input to the optimization model.

### 3.1.6 Economic Risk

The discussion provided in this subsection was previously published in McCoy et al. (2014).

Lee and Jones (2004) state that if the probabilities of a specific magnitude landslide event occurring in a given time are known, specific risk can be calculated as follows:

$$R_s = P(H_k) * \sum_k(E * U * E_x) \quad (\text{Eq. 1})$$

Where:  $R_s$  is the specific risk associated with a slide of magnitude  $H$ ,  $P(H_k)$  is the probability of the slide of magnitude  $H$  occurring in a given time period,  $E$  is the total value of all threatened items (elements at-risk),  $U$  is the vulnerability (proportion of  $E$  reduced by event), and  $E_x$  is the exposure (proportion of total value likely to be present at the time of the event),  $k$  indicates summation of all elements affected by the event.

If the vulnerability ( $U$ ) is integrated into the damage estimate and exposure is assumed to be complete ( $E_x = 1$ ), Eq. 1 can be re-written for a given basin and estimated volume as:

$$R_v = (P_A * D) \quad (\text{Eq. 2})$$

$$P_A = (P * P_{storm}) \quad (\text{Eq. 3})$$

Where:  $R_v$  is the specific risk associated the basin for the modeled volume scenario expressed in units of cost,  $P_A$  is the total annual probability of a debris-flow occurring,  $D$  is the total modeled damage (cost),  $P$  is the probability of a debris-flow occurring given the occurrence of the modeled storm, and  $P_{storm}$  is the annual probability of the storm occurring (e.g., 0.5 for a 2-year recurrence storm).

### 3.1.7 Estimating Cost and Effectiveness of Post-Fire Debris-Flow Mitigation Methods

The following sections briefly describe design and cost assumptions for the selected debris-flow mitigation methods and erosion-control best-management-practices used for the optimization modeling. This list is not a comprehensive review of post-fire debris-flow mitigation techniques, but is instead a list of representative techniques supplied as inputs for proof-of-concept modeling. Key assumptions are summarized in Table 2. In practice, all dollar figures mentioned in this study should be inflation adjusted to a common year so that their marginal costs and benefits may be equated during optimization.

**Table 2.** Cost and Effectiveness Assumptions for Mitigation Strategies  
(McCoy et al. in preparation)

Parameter	Assumed value	Reference
Straw wattle cost per km <sup>2</sup> of application at full density (USD 2012)	1,261,452	(Napper 2006)
Mulching cost per km <sup>2</sup> of application at full intensity (USD 2012)	293,289	(Napper 2006)
Check dam cost (each) (USD (2012))	478.59	(Napper 2006)
Debris basin cost per m <sup>3</sup> of capacity (USD 2012)	21.14	(Standard-Examiner 2011) (LA Times 2009)
Probability reduction from straw wattles across full basin at full density	85%	-
Probability reduction from mulching full basin at full intensity	90%	-
Backfill angle for straw wattles (degrees)	5	-
Backfill angle for check dams (degrees)	0	-

### Straw Wattles

Straw wattles and contour felled log erosion barriers (LEBs) are hillslope treatment options aimed at reducing erosion, slowing overland flow of water, and supporting recovery of vegetation. Straw wattles are used in areas where LEBs are not practical (e.g., chaparral environments, Napper 2006); however, both treatments have similar functionality.

Straw wattles range in size from 10 - 30 feet (3.048 - 9.144 m) long, and are 9 - 12 inches (0.229 – 0.305 m) in diameter (Napper 2006). It is commonly recommended that wattles be installed in a staggered overlapping pattern, with 12 to 18 inches of overlap (Napper 2006). Napper (2006) suggests spacing successive rows of wattles between 20- to 50-feet (6.096 m to 15.24 m) apart. Based on this spacing, a single acre can accommodate between 4 and 11 rows of 11 wattles each, or 44 – 110 wattles per acre. This range of application density is consistent with the range of LEB application density utilized by the United States Forest Service, and at the Lemon Dam site (deWolfe et al. 2008).

The cost of straw wattle application ranged from \$1,100 to \$4,000 per acre of application in year 2000 – 2003 USD (Napper 2006). Assuming that cost can be related to application density, we assign the higher end of the cost range (\$4,000 per acre) to the higher end of the density scale (110/wattles per acre) and allow cost to decrease linearly with respect to density, and therefore effectiveness.

It is expected that installation of straw wattles will retard rainfall-runoff response, therefore reducing the likelihood of channel scour and debris-flow generation. Wattles also trap some sediment, potentially reducing the erosive power of the runoff as it enters channels. Numerous studies (e.g., Robichaud et al. 2010; Robichaud et al. 2008) have been performed to quantitatively evaluate the effectiveness of these methods at reducing hillslope erosion; however, quantitative effects with respect to reducing probability of debris-flow occurrence at the basin scale are as-yet unclear. For this study, it was assumed that installing straw wattles or LEBs would result in an 85% reduction in probability of debris-flow occurrence relative to the

untreated condition. This estimate is not based on any quantitative studies of basin-wide debris-flow-specific hazard reduction. Volume of sediment retained per wattle can be calculated using Eq. 4.

$$V = L * \frac{d^2}{2(\tan\beta - \tan\alpha)} \quad (\text{Eq. 4})$$

Where:

V = volume of sediment retained per wattle (m<sup>3</sup>)

L = length of wattle (m)

d = diameter of wattle (m)

α = angle of soil backfilled behind wattle (°)

β = slope angle (°)

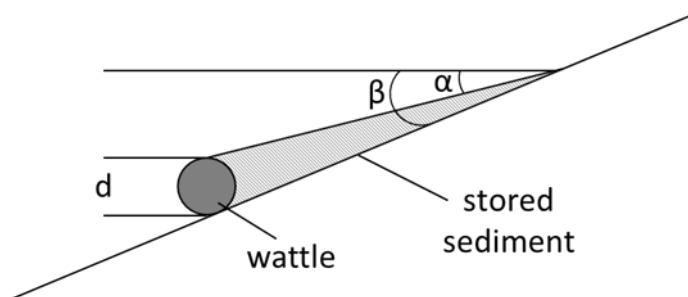


**Figure 3.** Key parameters for calculating volume of sediment trapped per unit width behind a straw wattle, log erosion barrier, or check dam (McCoy et al. in preparation).

Straw wattles are most commonly applied on slopes ranging in steepness from 20 – 50% (Napper 2006). For volume estimation purposes, a 20-foot (6.096 m) long by 9 inch diameter (0.229 m) “design wattle” was selected. Using Eq. 4 with a presumed backfill angle (α) of 5°, and slope angles of 20% – 50% (11° – 27°) yields unit volumes ranging from 0.38 to 1.5 m<sup>3</sup>/wattle. Total area available for wattle application in each basin is determined in ArcGIS by identifying areas with moderate to high burn severity and slope angles between 20% and 50%. The slope angle used in calculating volume reduction is the average slope angle in the straw wattle application area of that basin. It is assumed that the entire application area would be covered with wattles at some density up to 110 wattles per acre when straw wattles are used.

### Straw Mulch

Straw mulch has mixed effectiveness at reducing likelihood of debris-flow occurrence, and the treatment is most effective when applied evenly with care (deWolfe and Santi 2009; deWolfe et al. 2008). Cost of hand-application of straw mulch ranged from \$500 -\$1,200/acre between the years 2000 and 2003. Straw mulch can be applied aerially (dropped from helicopters) more cheaply than hand-applied mulch, but also less effectively (deWolfe and Santi 2009; Napper 2006). Cost of aerial straw mulch application ranged from \$250 -\$930/acre between the years 2000 and 2003. Probability reduction was presumed to be related to application density/quality and therefore cost. The quantitative effects of straw mulch with respect to reducing probability of debris-flow occurrence are as-yet unclear. For this study, it was assumed that complete mulch coverage in applicable zones would result in a 90% reduction in probability of debris-flow occurrence relative to the untreated condition. This estimate is not based on any quantitative

studies of basin-wide debris-flow-specific hazard reduction. Straw mulch is effective on slopes up to 65% (Napper 2006). Maximum area for application was determined in ArcGIS by selecting areas burned at moderate and high severity, with slopes up to 65%.

### Check Dams

Check dams are placed in series within channels to intercept eroded sediment (deWolfe and Santi 2009; deWolfe et al. 2008; Napper 2006). Volume of intercepted sediment can be estimated using Eq. 4, with  $d$  = check dam height instead of wattle diameter. Estimates of check dam cost from 2000 – 2003 ranged from \$150 – \$600 each depending on construction material (logs, rock, or straw-bales). The middle of this range was used in this study.

Check dams are commonly more effective near the upper reaches of a channel, where the material can be captured before generating larger debris flows (deWolfe and Santi 2009). However, check dams may be placed in series along many accessible reaches of channel as needed. The maximum number of check dams can be calculated by dividing the minimum spacing between check dams by the total available length of channel. deWolfe (2006) suggests that check dams should be installed in channels with gradients  $< 47\%$  ( $25^\circ$ ). This criterion was used to evaluate the maximum length of channel available for installation of check dams in ArcGIS. The minimum check dam spacing can be estimated using Eq. 5 (deWolfe 2006).

$$S = \frac{d}{(\tan\beta - \tan\alpha)} \quad (\text{Eq. 5})$$

Where:

$S$  = minimum spacing between check dams (m)

$d$  = height of check dam (m)

$\alpha$  = angle of soil backfilled behind check dam ( $^\circ$ )

$\beta$  = slope angle ( $^\circ$ )

A design check dam was assumed to be constructed approximately 12 m long and 2.5 m high. These measurements are consistent with log crib check dams (deWolfe 2006) and are within the range of commonly used off-the-shelf VX series flexible-ring-net debris-flow barriers (Geobrugg 2013). As an example, using Eq. 5 with the assumptions of  $\alpha = 0^\circ$  and  $\beta = 25^\circ$  (steepest slope), length of 12 m, and height of 2.5m results in an estimated  $80 \text{ m}^3$  of captured sediment per check dam.

### Debris Basins

Debris basins are emergency retention basins for controlling debris volume when a threat to human life and property is present (Napper 2006). Debris basins are placed at canyon mouths or upstream of critical structures to capture the debris flow. Ideally, a debris basin would be designed to capture the entire expected debris-flow volume; however, available space and alluvial fan geometry may limit available storage volume. Design, construction, and maintenance of in-channel treatments (e.g., debris basins, check dams, debris racks) are site- and condition-specific processes. Extrapolation of a design-cost scenario from one design volume or project location to other locations and/or debris volumes could lead to significant errors in estimated costs but is necessary when local data are unavailable. The following cost values have

been provided for generalized cost estimation and comparison purposes with the caveat that that actual designs may vary significantly.

The cost associated with debris basins includes two major factors: 1 – design and construction, and 2 – maintenance and cleanout. Cost estimates provided below are for design and construction of a debris basin near Salt Lake City, Utah, and cleanout of debris basins in Los Angeles, California. Design and construction of a debris basin near Salt Lake City, Utah was estimated (prior to completion) as \$2,250,000 (year 2011 dollars) with a design capacity of 220,000 cubic yards (yd<sup>3</sup>) of debris (Standard-Examiner 2011). This gives a cost per volume of approximately \$10.23/yd<sup>3</sup> in 2011 dollars. Los Angeles debris basins estimated \$10/yd<sup>3</sup> (year 2009 dollars) for cleanout (LA Times 2009). The cost is assumed to be \$21.14/yd<sup>3</sup>, or \$27.65/m<sup>3</sup> (2012 USD) for combined design, construction, and cleanout.

The ideal utilization of these values would be base cost of debris basin construction and cleanout of design basin volume, followed by cleanout of subsequent debris-flow volumes. Since this level of detail is beyond the scope of the project, the estimates can be combined to provide a single cost per volume of debris basins. The combined value will lead to an overestimate of cost for repeated debris-flow events in the same basin.

### **No Mitigation**

The no mitigation option has been included for analysis of the economic impact assuming that a given basin is left as-is after a fire. As suggested, this option results in no change to damages, and does not require any cost for implementation. Some cost could be allocated in future studies to account for measures such as community hazard education and early-warning-system design and installation. The no mitigation option is only valid where loss of human life is unlikely.

## **3.2 Optimization Modeling**

This section summarizes methods for estimating optimal decisions for managing post-fire debris flows. The method descriptions in Section 3.2 and associated sub-sections were previously published in McCoy et al. (in preparation).

The results of the analysis of previous sections can be used as inputs to a model that optimally selects mitigation strategies and minimizes potential damages from post-wildfire debris flows for an entire burned area comprising multiple basins. We begin with a simple management model where the objective is to minimize expected debris-flow damages from a single-basin event that occurs with probability  $p$ . If such an event occurs, it generates a debris flow of volume  $v$ , resulting in economic damages (including market and non-market values) of  $d$ . Values of  $d$  for a specific debris-flow volume in a specific basin can be derived from the damage curves.

The land-use manager's choice of mitigation strategies (which may include dozens of specific activities) has been categorized into three main sets of actions. *Prevention effort*, denoted,  $x^p$ , is any kind of slope treatment, including mulching, that counteracts the flow initiation effects of the fire and effectively reduces the probability of a debris-flow event. *Reduction effort*,  $x^r$ , is any channel mitigation treatment, including check dams, that intercepts debris in the event of a debris-flow occurrence and effectively reduces volume conditional on occurrence. *Protection*

effort,  $x^t$ , including building walls and putting up sandbag barricades, protects specific structures and effectively reduces the value of elements-at-risk. Because managers have finite resources available, the total cost of activities must satisfy budget  $B$ , such that  $c^p x^p + c^r x^r + c^t x^t = B$ , where  $c$  is the cost of a particular action.

Thus the land-use manager solves the following optimization problem to minimize expected damages:

$$\min_{x^p, x^r, x^t} p(x^p; \alpha) * d(v(x^r; \alpha), x^t; \beta) \quad (\text{Eq. 6})$$

$$\text{s. t. } c^p x^p + c^r x^r + c^t x^t = B \quad (\text{Eq. 7})$$

where  $\alpha$  represents the set of physical basin characteristics that influence the probability and volume of a debris flow, and  $\beta$  represents the values and locations of elements-at-risk from the debris flow. These parameters are outside the control of the manager.

A solution in which multiple mitigation strategies are used is one in which the ratio of marginal expected benefits to marginal costs for each activity is equated. Alternatively, for an activity that is sufficiently beneficial or sufficiently inexpensive, solutions may be obtained where the entire budget is devoted to a single activity. The optimal budget for mitigating a single basin for a single storm event can be found by moving the cost of mitigation to the objective function:

$$\min_{x^p, x^r, x^t} p(x^p; \alpha) * d(v(x^r; \alpha), x^t; \beta) - c^p x^p - c^r x^r - c^t x^t \quad (\text{Eq. 8})$$

While the representation above is appropriate for a single basin and a single storm event, managers may face challenges related to minimizing expected damages over multiple basins or multiple storm scenarios of varying magnitudes and probabilities (e.g., frequent but small 2-year storms or infrequent but large 100-year storms). Multiple basins can be considered using Eq. 9 and Eq. 10, where  $i$  indexes the drainage basins within the fire perimeter:

$$\min_{x_i^p, x_i^r, x_i^t} \sum_i (p_i(x_i^p; \alpha_i) * d_i(v_i(x_i^r; \alpha_i), x_i^t; \beta_i)) \quad (\text{Eq. 9})$$

$$\text{s. t. } \sum_i (c_i^p x_i^p + c_i^r x_i^r + c_i^t x_i^t) = B \quad (\text{Eq. 10})$$

The intuition underlying the solution to this problem is similar to the above, but accounts for the fact that resources need to be allocated across multiple basins.

### 3.3 Description of Three Sites for Case Study

This section describes the three case study sites used to demonstrate the optimization model. The discussions in Section 3.3 and associated sub-sections were previously published in McCoy et al. (in preparation).

As an example of the optimization process, the methods and models described in previous sections were implemented for studies of three diverse areas prone to post-fire debris flows:

Site 1 – Santa Barbara after the 2009 Jesusita fire (Cannon et al. 2010a), Site 2 – Great Sand Dunes National Park after the 2010 Medano fire (Friedman and Santi 2014), and Site 3 – Colfax and Las Animas Counties after the 2011 Track fire (Tillery et al. 2011). Figure 5 shows the location of these sites.

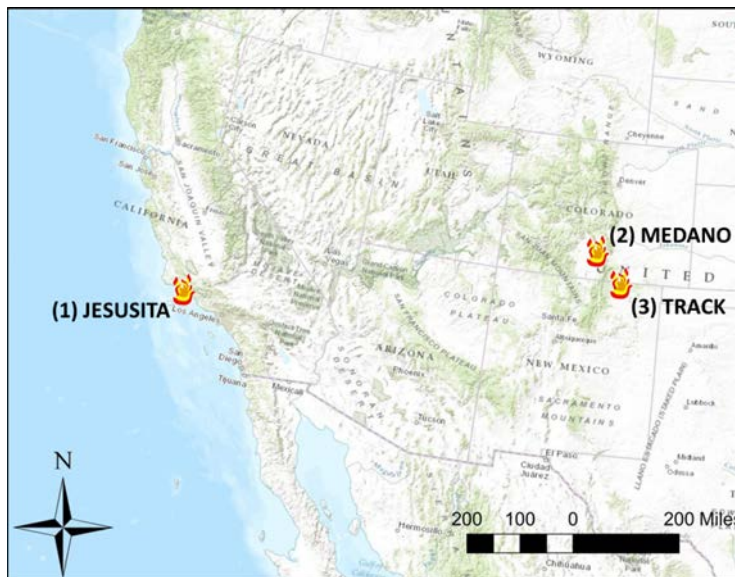


**Figure 4.** Location of modeling study sites in the western United States – Topographic base map layer from ArcGIS Online, accessed in ArcMap 10.0 (ESRI 2010) from (McCoy et al. in preparation).

Santa Barbara, California (Site 1) is a populated urban area with drainage basins prone to post-fire debris flows located just north of the city. Seventeen basins were delineated for study. With human settlement encroaching on the wildland-urban interface, this area has the most elements-at-risk and provides the greatest motivation for mitigation. Great Sand Dunes National Park (Site 2) in western Colorado provides an interesting study of mitigating to protect non-market values. Fifty-five basins were delineated for study. While the park is free of residences and other structures, it contains recreation value, which can be measured by enthusiasts' willingness to pay for access such as hiking, camping, and 4x4 trails. The area in Colfax County, New Mexico and Las Animas County, Colorado burned by the 2011 Track fire (Site 3) is by far the largest of the three selected areas in terms of size and demonstrates diversity in terms of elements-at-risk. While there are some residences the area also contains reservoirs, streams, roads, and railroad tracks sparsely distributed across a large area. Forty-nine basins were delineated for study.

For each of these sites, digital terrain data (10-m horizontal resolution) was downloaded from National Elevation Dataset (NED) (Gesch et al. 2002). All GIS datasets were projected to North American Datum of 1983 (NAD 1983) Universal Transverse Mercator system (Zone 11N for California, Zone 13N for Colorado and New Mexico). Soil characteristics were downloaded from the Natural Resource Conservation Service (NRCS) web soil survey and analyzed in ArcGIS using the soil data viewer extension (Soil Survey Staff 2014). The burn severity map for Site 1 and Site 2 was downloaded from the BAER imagery support catalog (Forest Service 2013). Burn severity data for Site 3 was provided by the USGS (E. Locke, personal

communication). Precipitation data were downloaded from NOAA (2013). A more detailed discussion of data sources for modeling post-fire debris-flow hazards is provided by (McCoy et al. 2014). Hydrologic basin characteristics and rainfall scenarios are presented in Appendix A.

The following probability and volume models are provided as background for the methods used in this study. New models (e.g., USGS 2014) are continually being developed as additional data is collected and modeling techniques evolve. The methods described in this paper are flexible enough that they will be applicable using newer models as they are developed. For this study, optimal mitigation strategies were found using specific equations for the probability of debris-flow occurrence and the expected debris-flow volume conditional on occurrence taken from (Cannon et al. 2010b). The probability for the Intermountain western United States is defined as

$$p(\alpha) = \frac{\exp(-0.7+0.03\alpha_1-1.6\alpha_2+0.06\alpha_3+0.2\alpha_4-0.4\alpha_5+0.07\alpha_6)}{1+\exp(-0.7+0.03\alpha_1-1.6\alpha_2+0.06\alpha_3+0.2\alpha_4-0.4\alpha_5+0.07\alpha_6)} \quad (\text{Eq. 11})$$

and the volume for all study sites is defined as

$$v(\alpha) = \alpha_7^{(0.6)} * \exp(7.5 + 0.7\sqrt{\alpha_8} + 0.2\sqrt{\alpha_9}) \quad (\text{Eq. 12})$$

where  $\alpha_1$  is the percent of basin area with slope over 30%,  $\alpha_2$  is the ruggedness (change in basin elevation divided by the square root of basin area),  $\alpha_3$  is the percent of basin area burned at moderate or high severity,  $\alpha_4$  is the percent soil clay content,  $\alpha_5$  is the percent liquid limit of the soil,  $\alpha_6$  is the average storm intensity in millimeters per hour,  $\alpha_7$  is the size of the basin area with slope over 30% in square kilometers,  $\alpha_8$  is the size of the basin area burned at moderate or high severity in square kilometers, and  $\alpha_9$  is the total 1-hour storm rainfall in millimeters.

For southern California (e.g., Jesusita fire Site 1), the probability model (S. Cannon, Personal Communication) is defined as

$$p(\alpha) = \frac{\exp(-3.82+0.002\alpha_{10}+0.022\alpha_{11}+0.026\alpha_{12}-0.022\alpha_{13}-0.020\alpha_{14}+0.016\alpha_{15})}{1+\exp(-3.82+0.002\alpha_{10}+0.022\alpha_{11}+0.026\alpha_{12}-0.022\alpha_{13}-0.020\alpha_{14}+0.016\alpha_{15})} \quad (\text{Eq. 13})$$

where  $\alpha_{10}$  is the elevation range in meters,  $\alpha_{11}$  is the percent of basin area burned with slopes over 50%,  $\alpha_{12}$  is the percent of basin burned at high severity,  $\alpha_{13}$  is the standard deviation of slope,  $\alpha_{14}$  is the storm duration in hours, and  $\alpha_{15}$  is the total 15 minute storm rainfall in millimeters. Note that parameters  $\alpha_6$  and  $\alpha_9$ , and are determined by the storm scenario, while all of the other parameters are related to physical parameters unique to each basin.

The damage function,  $d(v(\alpha), \beta)$ , was defined for each basin using the methods outlined in Section 3.1 and 3.2 with the values and locations of elements-at-risk,  $\beta$ , being included implicitly. The effects of selected mitigation strategies were included based on the assumptions stated in section 3.1. Protection efforts,  $x^t$ , were not included in this study due to the difficulty of incorporating different damage functions based on protected elements. Optimal mitigation strategies for the three study sites were found for a 2-year storm and a 10-year storm.

## **3.4 Evaluating Increases in Debris-Flow Occurrence with Climate Change**

This section explains the data acquisition and analysis for the understanding of the relationship of post-wildfire debris flows and fire area. The method descriptions and discussions from this section and associated sub-sections were previously published in Brunkal and Santi (in review).

### **3.4.1 Data acquisition, post-wildfire debris flows**

Records of wildfires that produced debris flows in western North America, specifically including Washington, Oregon, Idaho, Montana, Utah, Arizona, New Mexico, California and Colorado as well as data from British Columbia, Canada were compiled into a database using published reports, other wildfire studies, and information that was available online and in news reports. The main sources for data in the final catalog of post-wildfire debris-flow events included a USGS open file report that compiles post-wildfire run off data (<http://pubs.usgs.gov/of/2004/1085/Database.htm>, Gartner et al. 2004), the Interagency Fire Center ([http://www.nifc.gov/fireInfo/fireInfo\\_statistics.html](http://www.nifc.gov/fireInfo/fireInfo_statistics.html)), and (Riley et al. 2013), who compiled debris-flow data for a worldwide comparison of frequency-magnitude distribution. Other events were found through various news reports of ‘mudslides’ that had occurred after a fire; in these cases the event was only recorded as a debris flow if the report mentioned mud, debris, and boulders. In cases where a report mentioned post-wildfire debris flows but was non-specific regarding the number of debris flows generated, it was recorded in the database as one single debris-flow event, to provide a conservative data point. Attributes that were collected for analysis include: fire size in acres burned and number of debris flows produced from that burned area. In most cases the record of the intensity of the initiating rainfall was not available or was generalized as a ‘strong’ storm, or intense ‘cloud burst storm’. The resulting data set (DS1) is small and likely incomplete, containing 50 fires and 355 individual debris-flow events, and only spanning a time frame of 40 years (Table B-1). Nevertheless, it provides a reliable starting point to judge the potential change in debris-flow occurrence.

### **3.4.2 Database analysis**

Statistical analysis was performed to establish if the total compiled dataset, DS1, could demonstrate a significant relationship between wildfire burned area and number of debris flows generated. The first statistical test was to establish if acres burned explains the number of debris flows within this dataset. Other statistical tests involved examining the log-log relationship, regression analysis, non-parametric correlation, and time-dependent analysis for both fire area, and numbers of debris flows independently.

### **3.4.3 Analysis of better-documented post-wildfire debris flows**

After a thorough literature review and consideration of the biases in reporting and recording of post-wildfire debris flows it was concluded that a subset of the total collected data may better represent the actual number of debris flows that are generated per fire area. This subset, DS2, includes 16 cases considered to be better-documented fire areas (Table 3). These specific cases were chosen to represent a more accurate data set because in each case researchers have gone

into the field to map, monitor, and document the erosional responses of the total fire area. These better-documented areas record a higher accuracy for the total number of debris-flow events or basins producing debris flows, and not just those that had an impact on infrastructure or property. Although considered better-documented overall, in some cases multiple debris flows from a single basin may be considered a single debris-flow record, therefore this data set records minimum numbers for individual debris flows from a burned area, and thus a conservative record of number of debris flows overall. This subset includes fires that span a time frame from 1994 to 2010. Statistical analysis of this data included a linear mixed effect model that takes into account the random effects for intercept by state. The log-log fit was done by REML with an Akaike Information Criterion (AIC). This analysis provides a method to account for variability by location.

#### **3.4.4 Analysis of post-wildfire debris-flow probabilities**

To assess the potential changes in debris-flow occurrence with climate change and the change in debris flow volumes expected, a hypothetical basin was created as an average from data collected for 16 basins burned by the Hat Creek Fire in Idaho, in 2003 (Cannon et al. 2010b). These average basin values were used in three predictive model equations from Cannon et al. (2010b) to establish the baseline numbers from which to measure the percent increase in debris-flow probability and debris-flow volume with climate change. This strategy was employed because using the model coefficients with a 1 in the variables place did not produce usable values for comparison; a baseline value was created from the ‘average’ basin data. The variables averaged from the Hat Creek Fire basins were basin area with gradient greater than 30%, basin ruggedness, percentage clay content and liquid limit of the soil, percent area burned at moderate and high severity, and rainfall intensity. The latter two variables were the two values changed based on the percentage increase with predicted climate change values. These baseline average values were also used to calculate the percent increase in predicted debris-flow volumes from a hypothetical basin with the increased burn area and rainfall intensity values.

**Table 3.** DS2, A subset of data focusing on well-documented post-wildfire debris flow areas. These specific areas were measured and monitored, post-wildfire, to assess the drainage basin response. This data set was deemed more reliable, although it has a limited number of regions and authors represented, because the reports record all debris-flow events and not just those that had impacted humans (Brunkal and Santi in review).

<b>Well-studied post-wildfire debris flow areas</b>					
<b>State</b>	<b>Year of debris flows</b>	<b>Name of Fire/Complex</b>	<b>Acres burned</b>	<b>Minimum basins known to have produced debris flows</b>	<b>Number of debris flows/acres burned</b>
CO	1994	South Canyon/Glenwood <sup>1</sup>	2115	6	2.84E-03
NM	1996	Dome Fire <sup>1</sup>	16516	1	6.06E-05
CA	1997	Baker Fire <sup>1</sup>	6150	1	1.63E-04
MT	2000	Bear/Bitterroot Complex <sup>2</sup>	300000	35	1.17E-04
NM	2000	Cerro Grande Fire <sup>3</sup>	47650	5	1.05E-04
CO	2002	Coal Seam Fire <sup>4</sup>	12200	15	1.23E-03
UT	2002	Mollie (2001) <sup>5</sup>	8000	10	1.25E-03
CO	2002	Missionary Ridge Fire <sup>4</sup>	73000	13	1.78E-04
CA	2003	Grand Prix/Old Fire <sup>6</sup>	150729	47	3.12E-04
BC	2003	Okanagan Mountain Park <sup>7</sup>	64030	2	3.12E-05
BC	2004	Cedar Hills Fire (2003) <sup>7</sup>	4003	1	2.50E-04
BC	2004	Kuskonook (2003) <sup>7</sup>	11940	2	1.68E-04
BC	2004	Lamb Creek (2003) <sup>7</sup>	29361	1	3.41E-05
BC	2005	Ingersoll (2003) <sup>7</sup>	18063	12	6.64E-04
ID	2009	Castle Rock Fire (2007) <sup>2</sup>	48520	20	4.12E-04
CA	2010	Station Fire (2009) <sup>8</sup>	160577	57	3.55E-04
references					
<sup>1</sup> Cannon, 2001					
<sup>2</sup> Riley et al., 2013					
<sup>3</sup> Gartner et al., 2005					
<sup>4</sup> Cannon et al., 2003					
<sup>5</sup> McDonald and Giraud, 2007					
<sup>6</sup> Cannon et al., 2008					
<sup>7</sup> Jordan and Covert, 2009					
<sup>8</sup> Ahlstrom, 2013					

## 4.0

# Results

The following subsections briefly summarize results of the three primary tasks. Section 4.1 describes methods for evaluating post-fire debris-flow hazard risk, Section 4.2 describes methods for optimization modeling, and Section 4.3 describes methods for evaluating increases in debris-flow occurrence with climate change. Results and discussion presented in Sections 4.1 and 4.2 and associated sub-sections will be published in (McCoy et al. in preparation). Results and discussion presented in Section 4.3 and associated sub-sections will be published in (Brunkal and Santi in review).

### 4.1 Results of Debris-Flow Damage and Optimization Modeling at 3 Case Study Sites

Appendix C presents results of probability and volume calculations for each of the hydrologic basins at each of the three sites. Appendix D presents tabulated results of extracted damages for a range of debris-flow volumes for each of the hydrologic basins at each of the three sites. The following sub-sections present results and discussion of post-fire debris-flow damage estimates and optimal natural-hazard response modeling.

#### 4.1.1 Damage Estimates

The results and discussion presented in this section and associated subsections will be published in (McCoy et al. in preparation).

The methods discussed in section 2.3 can be used to estimate the expected damages caused by a post-wildfire debris flow of a particular volume in a particular basin. In order to find the marginal benefit of reducing debris-flow volume for use in the optimization model, it is necessary to express economic damage as a function of debris-flow volume. In other words, we need to know how decreasing the expected debris-flow volume affects the expected damages. This is done for each basin by using a set of discrete volumes in the runout model and then fitting or interpolating a function on the resulting data points. One possible technique for doing this is described by Rebennack and Kallrath (2014). Several examples from Site 1 are presented below in Figure 6. As can be seen in Figure 6, there can be a significant difference in volume magnitudes, damage magnitudes, and shapes of the functions across different basins.

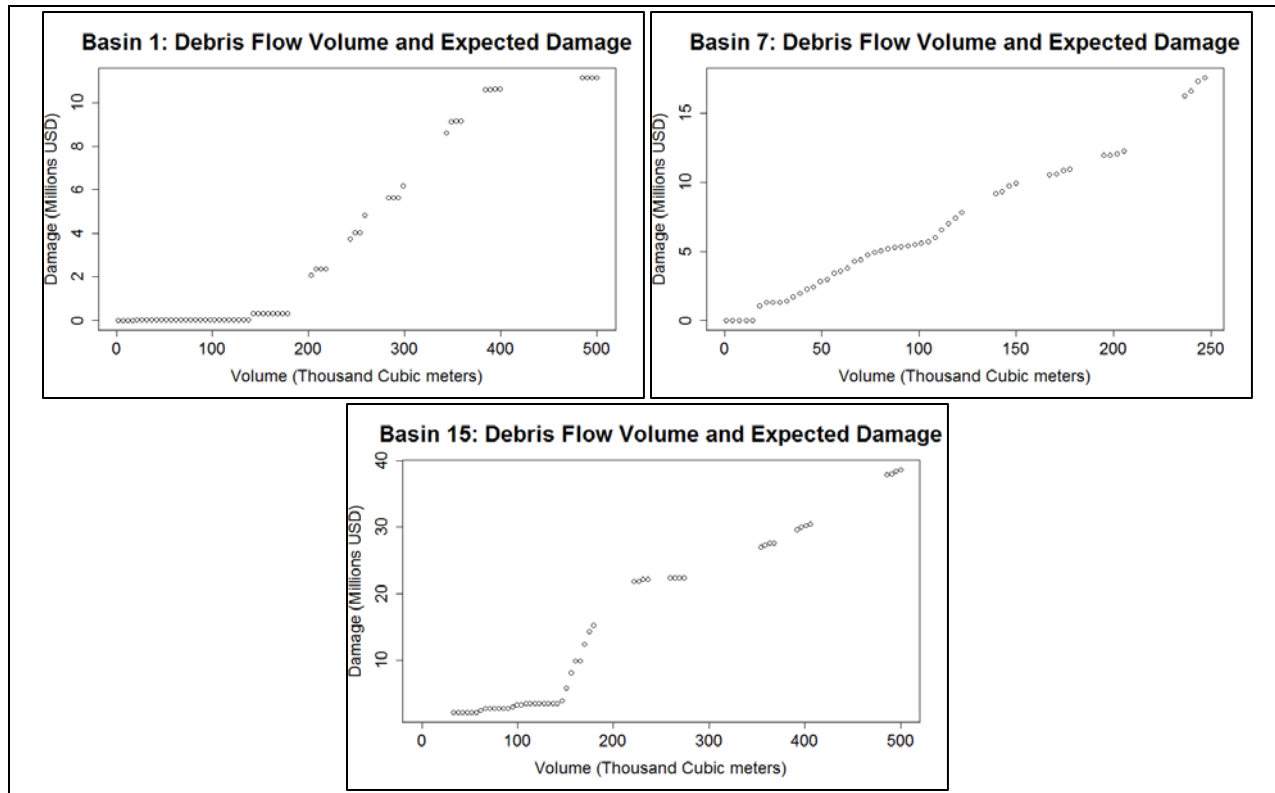


**Figure 5.** Damage as function of volume in three basins from Site 1. Note that the scale of the vertical axis (damage) is different for each chart (McCoy et al. in preparation).

The expected damages in each of the case study sites given certain storms are illustrated in Figures 7-10. Table 4 summarizes damages across all basins, divided out by each element-at-risk for the 2-year and 10-year rainfall scenarios. These numbers are calculated by multiplying the probability of debris-flow occurrence in each basin by the damage associated with its debris-flow volume. These figures are conditional on the occurrence of the specified storm scenario, meaning they do not take into account the probability of that storm occurring, and assume no mitigation. Note that although less frequent storms cause more damage once they occur, their expected damages independent of storm occurrence are generally lower. For example, post-fire debris flows following a 10-year storm in the Jesusita fire site cause approximately \$24 million in damages; since this storm has a 10% chance of occurring any given year, its expected damage without mitigation is \$2.4 million per applicable year. On the other hand the 100-year storm that causes about \$30 million in damages conditional on occurrence has a 1% chance of occurring in a given year; the expected cost independent of storm occurrence is only \$300,000 per year. For this reason, smaller but more probable storms generally have higher expected damage overall but lower damage conditional on storm occurrence. The increase in damages from more severe storms is gradual in Santa Barbara compared to the other two sites.

In the Santa Barbara site four out of the 15 basins are responsible for almost all of the damage. In the Track fire site, two of the 53 basins make up more than two thirds of damages, with the others each having only a small share of the total. In the Medano site, the five out of 55 basins that are responsible for more than half of the damage during more frequent storms are relatively less important with less frequent storms.

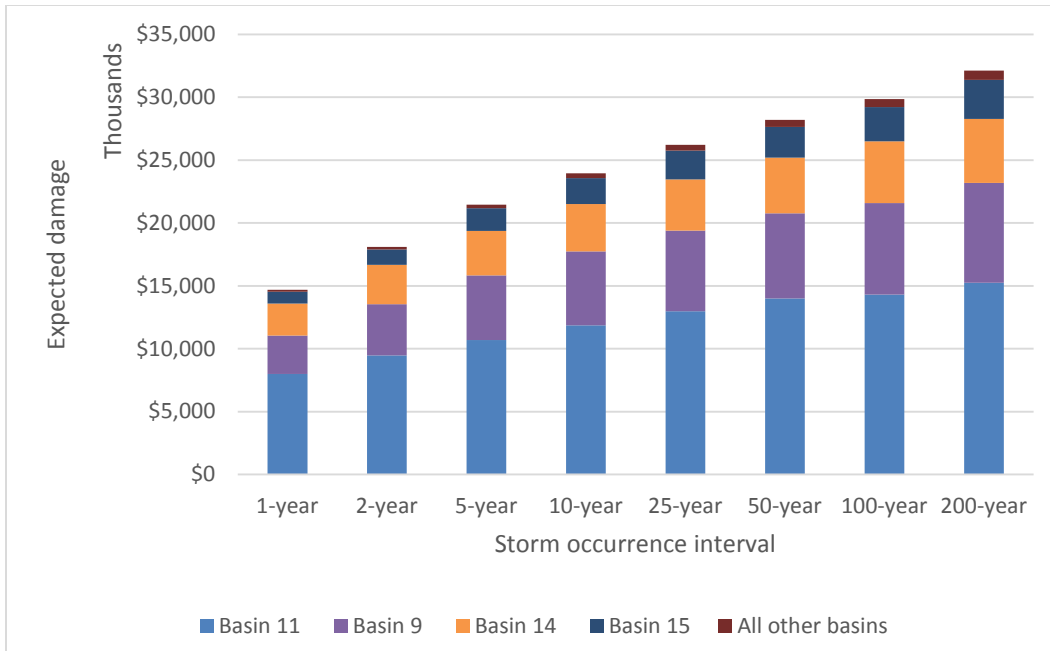


**Figure 6.** Expected debris flow damage in Jesusita fire case study without mitigation (McCoy et al. in preparation).

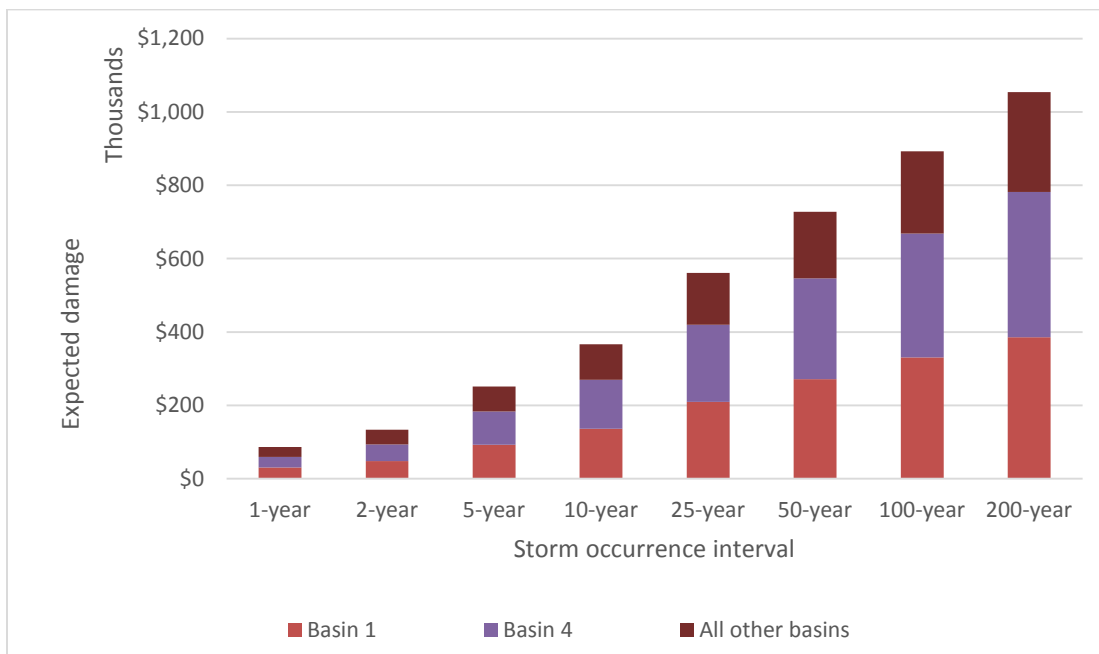


**Figure 7.** Expected debris-flow damage in Track fire case study without mitigation (McCoy et al. in preparation).

Hiking and 4x4 trails in the Medano case study are evaluated using two different methods for comparison purposes. Direct trail damage, illustrated in figure 9, considers the direct cost of sediment removal from hiking and 4x4 trails. Lost access, illustrated in figure 10, considers the value of lost recreation in the event that trails are not cleared following the debris flow. Figures 9 and 10 show the five basins with the highest expected damages for more frequent storms and

group the other basins together. We observe that only two of the five basins appear in both figures. Their relative importance compared to all other basins diminishes for less frequent storms in both figures. The damages are significantly higher in the case with lost access values suggesting that the recreational value of hiking and 4x4 trails outweighs the cost of trail cleanup. The lost damage functions also have very distinct breakpoints because when the debris flow crosses a trail it can eliminate access to a large portion of “upstream” trail; because a small amount of a large debris flow can cause large lost-access damages, it is also generally more cost-effective to clean up the affected trails after a debris flow than to implement any specific debris-flow mitigations for this site.

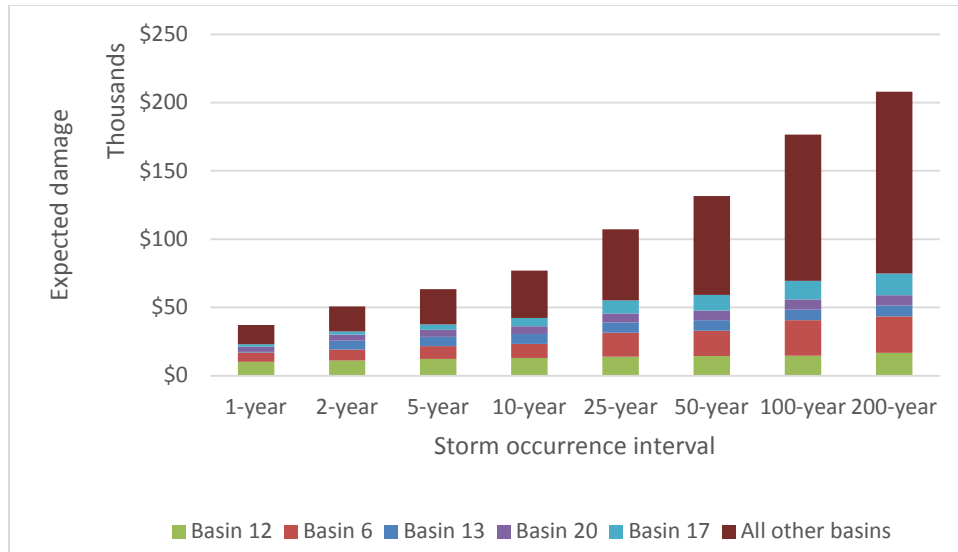


**Figure 8.** Expected debris-flow damage in Medano fire case study without mitigation, direct trail damage (McCoy et al. in preparation).

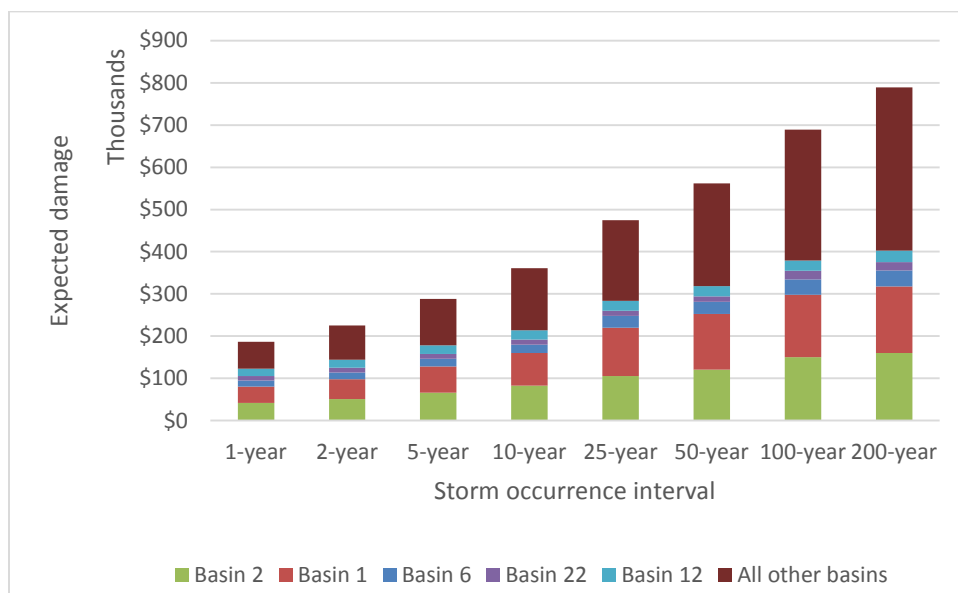


**Figure 9.** Expected debris flow damage in Medano fire case study without mitigation, lost trail access (McCoy et al. in preparation).

**Table 4.** Site features and estimated damages (2012 USD)  
from 2-yr and 10-yr recurrence storm scenarios (McCoy et al. in preparation).

Feature	Site 1 (Jesusita Fire)		Site 2 (Medano Fire)		Site 3 (Track Fire)	
	2-yr storm	10-yr storm	2-yr storm	10-yr storm	2-yr storm	10-yr storm
Residences	\$29,011,432	\$31,311,626	--	--	\$0	\$0
Roads (streets and highways)	\$116,016	\$132,758	--	--	\$125,374	\$151,834
4x4 Trails Direct Damage	--	--	\$25,931	\$37,872	--	--
4x4 Trails Lost Access	--	--	\$166,876	\$210,050	--	--
Railroads	\$0	\$0	--	--	\$43,039	\$60,639
Hiking Trails Direct Damage	--	--	\$1,586	\$1,732	--	--
Hiking Trails Lost Access	--	--	\$767,581	\$767,604	--	--
Camp Sites	--	--	\$126,126	\$133,133	--	--
Small Lakes/ Reservoirs	\$27,625	\$34,850	--	--	\$14,875	\$22,950
Large Lakes/ Reservoirs	--	--	--	--	\$500,550	\$661,578
Streams	\$23,800	\$27,396	\$27,935	\$32,293	\$20,860	\$26,020
<b>Total Damage (no lost access)</b>	<b>\$29,178,873</b>	<b>\$31,506,630</b>	<b>\$181,578</b>	<b>\$205,030</b>	<b>\$704,698</b>	<b>\$923,021</b>
<b>Total Damage (w/lost access)</b>	--	--	<b>\$1,116,035</b>	<b>\$1,182,684</b>	--	--

#### 4.1.2 Optimization Modeling

The effects of hazard mitigation with an optimally allocated budget are illustrated in Figures 11-13. These results are based on the assumptions listed in Tables 1-2 and the expected damages are conditional on storm occurrence.

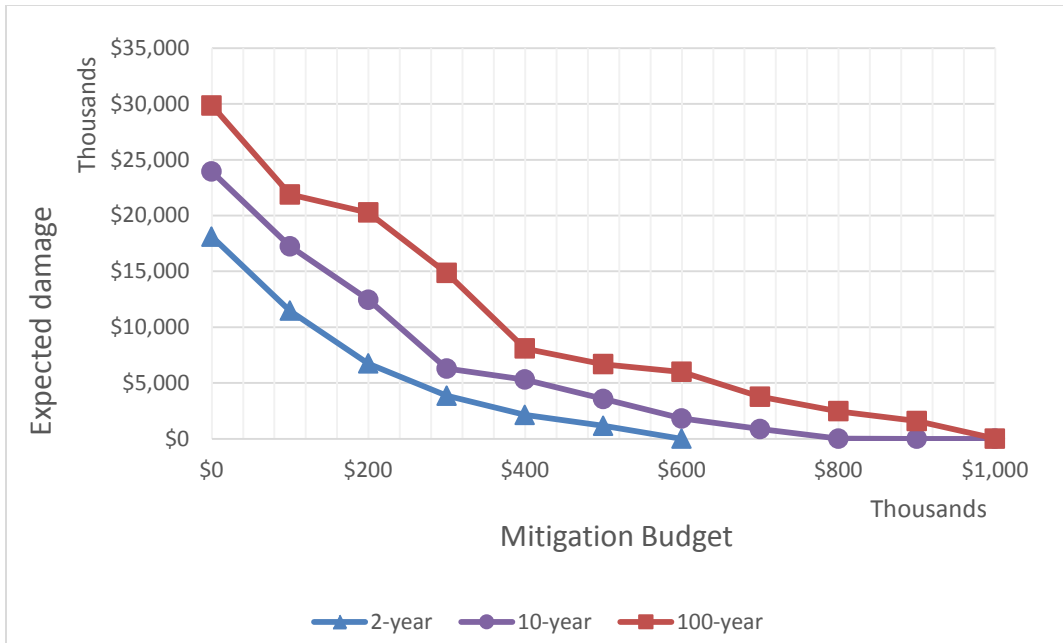


**Figure 10.** Expected debris-flow damage in Jesusita fire case study with mitigation (McCoy et al. in preparation).

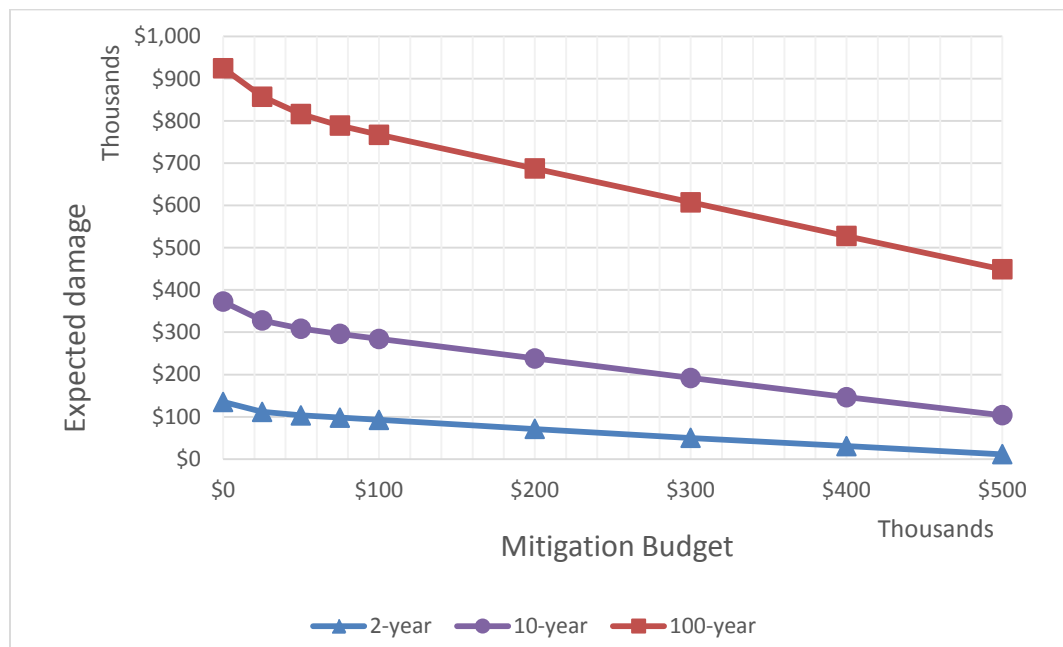


**Figure 11.** Expected debris-flow damage in Track fire case study with mitigation (McCoy et al. in preparation).

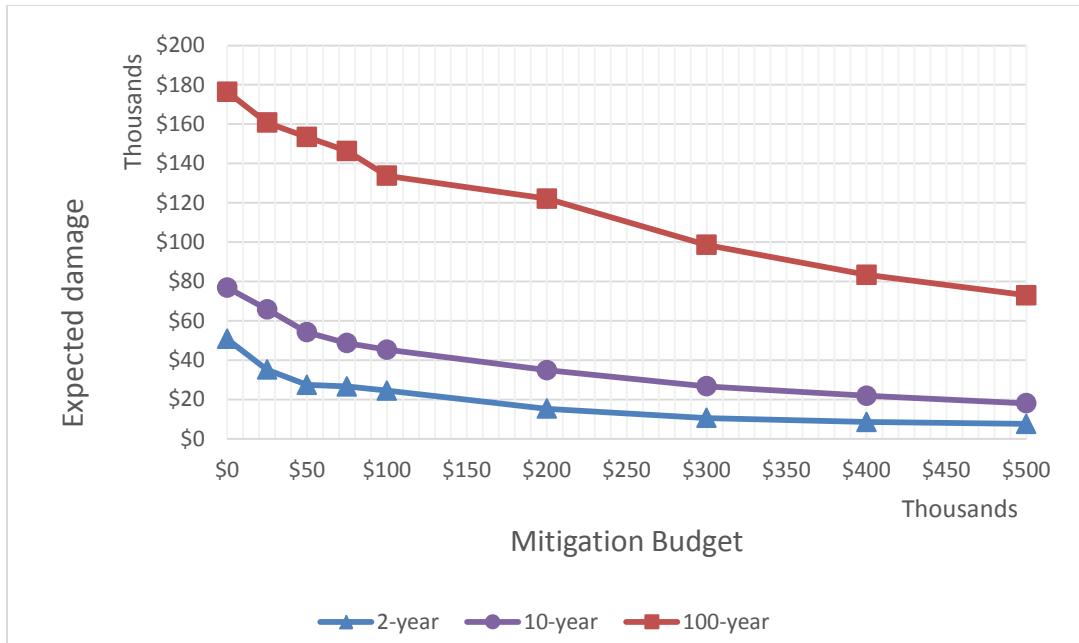


**Figure 12.** Expected debris-flow damage in Medano fire case study with mitigation, trail clean up (McCoy et al. in preparation).

Optimal mitigation budgets are summarized in Table 5. These budgets describe the point where the marginal benefit of mitigation is equal to the marginal cost. For the results in Table 5 we also assume that the marginal benefit is equal to the reduction in expected damage conditional on occurrence of the specified storm scenario. This is an important assumption because we do not know which storm(s), if any, will occur during the two year time window after the fire. More advanced risk management strategies are needed to fully balance the cost of mitigation with the uncertain risk of post-fire debris flows.

**Table 5. Budget where marginal reduction in damage is equal to marginal cost of mitigation.** (McCoy et al. in preparation)

	2-year storm	10-year storm	100-year storm
Jesusita Fire	\$ 597,639	\$ 752,259	\$ 977,352
Track Fire	\$ 3,879	\$ 18,260	\$ 71,947
Medano Fire – trail clean up	\$ 1,969	\$ 417	\$ 0

Results in Table 5 suggest that the benefit of mitigation for post-fire debris flows can easily outweigh the costs of implementation. This is especially true in the Jesusita fire case study where the density of housing development leads to steep damage curves. We observe that the optimal budget increases for less frequent storms in Jesusita and Track but decreases in Medano. This is due to the fact that Medano damage curves tend to flatten out as the volume increases.

The dominant mitigation strategy out of the options described in section 3.1 is installation of check dams across all sites and storm scenarios. This result is dependent on the assumptions in Tables 1-2. Figure 14 compares the effects of using a single mitigation strategy for Jesusita fire with a 1-hour-duration, 10-year-recurrence storm scenario. Check dams are clearly the most effective mitigation option given our assumptions, followed by mulching. While debris basins

are commonly designed and constructed for long-term community protection from randomly generated debris-flow events, they remain unaffordable as a post-fire response for the major basins analyzed.

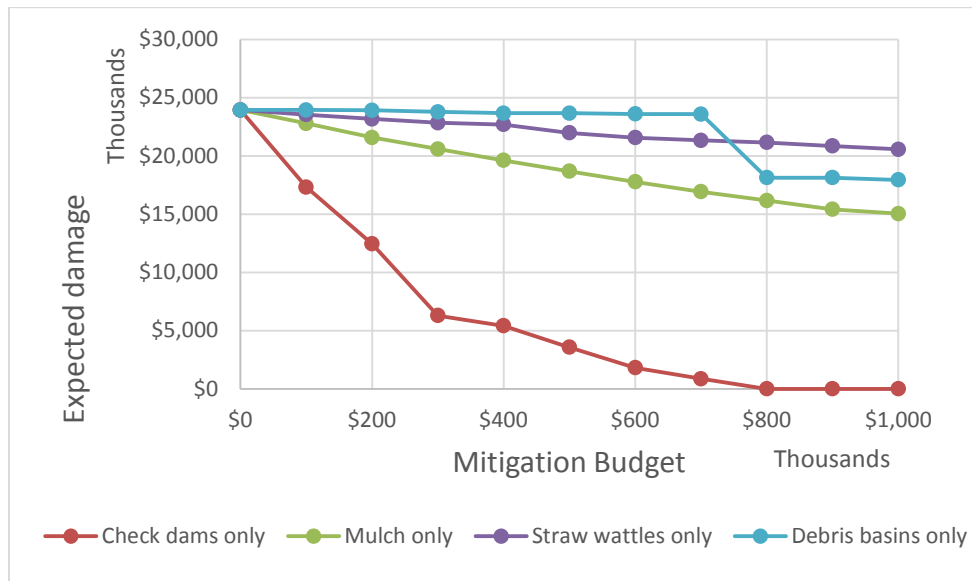


**Figure 13.** Expected damages with one mitigation strategy, Jesusita fire, 10-year storm (McCoy et al. in preparation).

### 4.1.3 Limitations

The following discussion will be published in McCoy et al. (in preparation).

Several important considerations should be made when using the methods presented in this paper. The methods described here are intended as a proof-of-concept rather than a strict prescription. Debris-flow volumes predicted using model described by Cannon et al. (2010b) and Gartner et al. (2008) are generally valid to within an order of magnitude. Cannon et al. (2010a) and Tillery et al. (2011) show how the models are commonly used in current practice. More detailed and accurate parameter data can easily be incorporated as the models evolve.

The results indicate that check dams are the most cost-effective treatment in the study sites considered; however, this may be largely driven by the assumptions of Table 2. The parameter assumptions described in Tables 1 and 2 have a wide reported range and are derived from limited sources.

In the case of debris-flow mitigation effectiveness, the uncertainty in parameter assumptions is driven by the lack of such data in literature. For instance, many site-specific physical studies (e.g., Robichaud et al. 2010; Robichaud et al. 2013a; Robichaud et al. 2008; Robichaud et al. 2013b) have been performed to evaluate the effectiveness of post-fire erosion control treatments. However, most of these studies were performed to evaluate erosion control on the hillslope-plot or small catchment scale, and not directly to evaluate debris flows. While sediment eroded from

hillslopes contributes to debris-flow volume, and likely contributes to debris-flow initiation, it cannot be assumed that a given effectiveness of hillslope-erosion reduction directly translates to effectiveness at debris-flow prevention. As Santi et al. (2008) discuss, less than 10% of volume of post-fire debris flows in their dataset was derived from hillslope erosion and rill formation. The remaining more than 90% of the volume was derived from in-channel erosion, a process that is potentially affected by application of erosion-control best-management-practices, but is not directly evaluated by plot and hillslope scale studies. Additional studies focused specifically on the relationship between application of erosion-control best-management-practices on hillslopes and generation of debris flows at the basin-scale may significantly improve confidence in the analysis. The process of fitting the damage function to the discrete data points may produce error as well. Additional studies to evaluate the influence of these uncertainties on the optimization results may help guide further research.

Another important limitation of this study is that it does not consider the possibility for loss of life or injury. This aspect is not considered here because the methods used to account for spatially static structures cannot be as easily applied to people, who move around in the city. For a completely random debris-flow occurrence, assumptions can be made about the likelihood of people being present in residences or other structures when the debris flow hits, and the statistical value of a life could be applied. However, the occurrence of the fire sets up a condition where debris flows may be expected under a predictable set of rainfall intensity and duration conditions (Staley et al. 2013a). Public notifications and evacuation orders can be issued when storms are expected that could exceed threshold values for debris-flow generation (Santi et al. 2011). This activity significantly decreases the likelihood that people will be present when a debris flow occurs, relative to a completely random event. With additional study, it may be possible to account for the human-life-risk aspect of post-fire debris flows in this framework; this would essentially result in an increase to damages associated with certain structures. Further research is needed to incorporate this important aspect.

## **4.2 Evaluating Increases in Debris-Flow Occurrence with Climate Change**

The results and discussion presented in this section and associated subsections will be published in (Brunkal and Santi in review).

A review of the literature that sought to pinpoint the changes in wildfire occurrence, length, and severity with climate change resulted in a wide variety of future scenarios over a range of spatial and temporal scales. The overall consensus in the literature is that wildfire season will get longer, and more severe wildfires will occur with increasing frequency in the future decades, both worldwide and in the western U.S. It is difficult to obtain one definitive predictive equation for the increase in fire danger, length of season, or fire area because researchers use different models and criteria for assessment of future fire hazard; such as the ERC or the SSR systems. Researchers do note that vegetation types, amount and structure influence the fire regime characteristics; therefore any changes in vegetation due to climate or fire would have a feedback on the fire regime. Human activities such as fire management policies and effectiveness will continue to change. Other human influences such as forest conversion and fragmentation will also influence the fire regime. For the examination below on post-wildfire debris flow numbers the fire regime will be considered to follow the current trend and the predicted models, to 2050,

without the potential feedback mechanisms of longer-term vegetative changes due to climate and fire changes.

Because of the established relationship of wildfire area, burn severity, and debris flow generation, a few different model results were chosen to represent the future changes to wildfire area and severity in the coming decades. The two models presented by Flannigan et al. (2000), both GCM, use coarse resolution (400km) and give a basis for general expected increases for burned area in the western U.S. with 2 x CO<sub>2</sub> by mid-century, 2050. Holding other factors constant, the predicted higher Seasonal Severity Rating will increase burned areas by 10% in the western U.S. These predictions of future fire regime are more conservative than the results from the National Research Council (NRC) as summarized by Climate Central, which state that for every 1 degree Celsius of temperature rise in the West, the wildfire burn area could quadruple. The IPCC 5th assessment report predicts a range of warming of 1.5 – 5.8° C by mid-century for North America, which would translate to a 400 - 2000% increase in wildfire burn area by 2050, using the NRC estimate. The regional forecast for California as presented by Fried et al. (2004) uses a finer resolution model that focuses on California's landscape and predicts fire behavior based on weather, fuels and slope. The results of this study show an increase, on average, of 50% in area burned per fire in California with climate change. Fried et al. (2004) warn that these estimates are a minimum expected change or the 'best-case' forecast. For this study we use the end members of 10% and 400% fire area increase as low end, and conservative high end value for analysis of the potential change in probability of post-wildfire debris flows.

Precipitation models almost universally show that with a warming atmosphere the hydrologic cycle will have increased heavy precipitation events, mostly at the expense of other forms of precipitation. The trend toward increased rainfall has been documented and is expected to continue in most areas of the western U.S. Climate change is expected to affect the delivery of moisture seasonally, resulting in wetter falls and springs and drier summers and winters. The IPCC 5th assessment report (Christensen, et al 2013) includes a chapter on regional climate phenomena and the conclusion presented is that there will be precipitation increases across the West by mid-century in both July and August (+ 0.1 mm/day °C-1) and December, January, and February (+0.1 to +0.4 mm/day °C-1). Based on the report's predicted range of warming, +1.5° – +5.8°C, the rainfall amounts would increase in the summer months by a range of 0.15 - 0.58 mm/day, and a range in the winter months of 0.15 - 2.32 mm/day.

It is difficult to apply GCMs and even most regional scale models to precipitation patterns for the West because the general coarse resolution of the models does not accurately reflect the diversity of topography and orographic influences across mountain ranges. For the analysis presented in this paper, a range of percentage increase in extreme events will be applied to debris-flow predictive models to calculate the percentage increase in debris flow probability. Increases in heavy and extreme highest 1-day precipitation events in areas of the West will be in the range of 3.5% (Karl and Knight 1998) to 50% (Kim 2005), in keeping with the recorded trend. These heavy and extreme 1-day events have defined thresholds of 50.8 mm/day and 101.6 mm/day, respectively (Kim 2005). These thresholds are well above debris-flow triggering thresholds defined by (Cannon et al. 2010b; Cannon et al. 2008) for parts of the Western U.S., who showed that many debris flows from burned areas are triggered by events as small as the 2 year

recurrence storm, which is a common summer convective thunderstorm with a high-intensity short-duration burst of rainfall.

In summary, using a dataset of 50 fires and 355 individual debris-flow events, conservative model interpretations show increased probabilities for a flow in an individual drainage basin by an average of 21%, with different climate scenarios ranging from 2% to 39%, by the year 2050. As fires increase in size due to climate change, a positive trend is also shown between the area burned and the number of debris flows generated. A predictive debris-flow volume equation for the Intermountain West is also influenced by factors that will be affected by climate change, and debris-flow volumes are calculated to increase with changing conditions by 4% to 52% over the next 35 years. The variability of both climate models and debris-flow predictive models prevent accurate prediction of number, probability, and volume of future debris-flow events, but the trends demonstrated by this data will help agencies and communities better anticipate and manage both hazards and risks.

The following discussion was previously (or will be) published in McCoy et al. (2014), McCoy et al. (in preparation), and/or Brunkal and Santi (in review).

A method was developed that utilizes previously existing post-fire hazard assessment calculations and debris-flow runout models combined with easily obtainable feature data in a GIS to model expected damages and economic risk from individual burned basins following a fire. Preliminary case study results suggest that this process can identify the drainage basins posing the greatest economic risk. The process is modular; a variety of probability, volume, and runout models can be used depending on data availability, project needs, and skills of the analyst. The output of this model can guide allocation of emergency management funds and selection of cost-optimized debris-flow management strategies for entire burned areas. This is a unique method of evaluating post-fire debris-flow mitigation options using risk-analysis techniques based on new applications of existing hazard models. These methods can be employed rapidly following a fire and have the potential to transform the way hazard managers approach debris-flow mitigation decisions following wildfires. Some limitations should be kept in mind when performing post-fire debris-flow risk assessment using the process described in this paper. The process was specifically developed to address economic risk associated with post-fire debris-flows; it has not been designed to address other concerns (e.g. fatalities, flooding, encroachment by invasive species, or long-term erosion and sedimentation). The quality of the estimates is tied to the methods used to calculate probability and volume, the methods used to model runout, and the assumptions used to identify and value the elements at-risk. Additional research aimed at reducing uncertainties in some key parameters may lead to improvement of the model over time.

A quantification of the future impact of climate change on the number of post-wildfire debris flows shows a positive correlation between wildfire size and number of debris flows generated. Climate change is expected to increase the probability of a debris flow occurring in an individual burned basin by 20.6%, on average, and to increase the debris-flow volume expected to be generated from a burned watershed by 3% to 52.5%, conservatively.

## 6.0

## References

- Allan RP, Soden BJ (2008) Atmospheric warming and the amplification of precipitation extremes. *Science* 321:1481-1484
- Amendola A, Ermoliev Y, Ermolieva TY, Gitis V, Koff G, Linnerooth-Bayer J (2000) A systems approach to modeling catastrophic risk and insurability. *Natural Hazards* 21:381-393
- Archetti R, Lamberti A (2003) Assessment of Risk due to Debris Flow Events. *Natural Hazards Review, American Society of Civil Engineers* 4:115-125
- Balling RC, Jr., Meyer GA, Wells SG (1992) Climate change in Yellowstone National Park: is the drought-related risk of wildfires increasing? *Climatic Change* 22:35-45
- Bernard DR (2007) Estimation of Inundation Areas of Post-Wildfire Debris Flows. Colorado School of Mines
- Berti M, Simoni A (2007) Prediction of debris flow inundation areas using empirical mobility relationships. *Geomorphology* 90:144-161  
doi:<http://dx.doi.org/10.1016/j.geomorph.2007.01.014>
- BLS (2013) Consumer Price Index. <http://www.bls.gov/cpi/>. Accessed June 13 2013
- Bovis MJ, Jakob M (1999) The role of debris supply conditions in predicting debris flow activity. *Earth surface processes and landforms* 24:1039-1054
- Bowker JM, Bergstrom JC, Gill J (2007) Estimating the economic value and impacts of recreational trails: a case study of the Virginia Creeper Rail Trail. *Tourism Economics* 13:241-260 doi:10.5367/000000007780823203
- Brock RJ (2007) Controlling factors for the onset of deposition of wildfire-related debris flows. Colorado School of Mines
- Brown T, Hall B, Westerling A (2004) The impact of twenty-first century climate change on wildland fire danger in the western United States: an applications perspective. *Climatic Change* 62:365-388
- Brunkal H, Santi P (in review) Expected Increase in Post-wildfire Debris Flows with Climate Change. *Environmental and Engineering Geoscience*
- Burns S, Cannon SH, Keaton J (2011) Landslide Hazards: A stealth threat to the nation. Presentation in cooperation with the Congressional Hazards Caucus
- Calkin DE, Hyde KD, Robichaud PR, Jones JG, Ashmun LE, Loeffler D (2007) Assessing post-fire values-at-risk with a new calculation tool. Gen. Tech. Rep. RMRS-GTR-205. U.S.

Department of Agriculture, Forest Service, Rocky Mountain Research Station, Fort Collins, CO

- Cannon SH (2001) Debris-flow generation from recently burned watersheds. *Environmental and Engineering Geoscience* VII:321-341
- Cannon SH, De Graff J (2009) The Increasing Wildfire and Post-Fire Debris-Flow Threat in Western USA, and Implications for Consequences of Climate Change. In: Sassa K, Canuti P (eds) *Landslides – Disaster Risk Reduction*. Springer Berlin Heidelberg, pp 177-190 doi:10.1007/978-3-540-69970-5\_9
- Cannon SH, Gartner JE (2005) Wildfire-related debris flow from a hazards perspective. In: Jakob M, Hungr O (eds) *Debris-flow Hazards and Related Phenomena*. Springer Praxis Books. Springer Berlin Heidelberg, pp 363-385 doi:10.1007/3-540-27129-5\_15
- Cannon SH, Gartner JE, Holland-Sears A, Thurston BM, Gleason JA (2003) Debris flow response of basins burned by the 2002 Coal Seam and Missionary Ridge fires, Colorado. In: Boyer DD, Santi PM, Rogers WP (eds) *Engineering Geology in Colorado-Contributions, Trends, and Case Histories: Association of Engineering Geologists Special Publication 14, Colorado Geological Survey Special Publication 55*.
- Cannon SH, Gartner JE, Rupert MG, Michael JA (2010a) Emergency Assessments of Postfire Debris-Flow Hazards for the 2009 La Brea, Jesusita, Guiberson, Morris, Sheep, Oak Glen, Pendleton, and Cottonwood Fires in Southern California. U.S. Department of the Interior, U.S. Geological Survey, Reston, Virginia
- Cannon SH, Gartner JE, Rupert MG, Michael JA, Rea AH, Parrett C (2010b) Predicting the probability and volume of postwildfire debris flows in the intermountain western United States. *Geological Society of America Bulletin* 122:127-144 doi:10.1130/b26459.1
- Cannon SH, Gartner JE, Wilson RC, Bowers JC, Laber JL (2008) Storm rainfall conditions for floods and debris flows from recently burned areas in southwestern Colorado and southern California. *Geomorphology* 96:250-269 doi:http://dx.doi.org/10.1016/j.geomorph.2007.03.019
- Census (2012) Topologically Integrated Geographic Encoding and Referencing (TIGER®). <http://www.census.gov/geo/maps-data/data/tiger.html>. Accessed February 18 2013
- Chen CT, Knutson T (2008) On the verification and comparison of extreme rainfall indices from climate models. *Journal of Climate* 21:1605-1621
- Chen K, Blong R, Jacobson C (2003) Towards an integrated approach to natural hazards risk assessment using GIS: With reference to bushfires. *Environmental Management* 31:546-560
- Clark C (1990) *Mathematical Bioeconomics: The Optimal Management of Renewable Resources*. 2nd ed. edn. Wiley Interscience, New York

- Costello C, Kaffine D (2010) Marine Protected Areas in spatial property rights fisheries. *Australian Journal of Agricultural and Resource Economics* 54:321-341
- Crowder BM (1987) Economic costs of reservoir sedimentation: A regional approach to estimating cropland erosion and damages. *Journal of Soil and Water Conservation* May-June 1987
- Dai FC, Lee CF, Ngai YY (2002) Landslide risk assessment and management: an overview. *Engineering Geology* 64:65-87
- DeGraff JV, Cannon SH, Gallegos AJ (2007) Reducing post-wildfire debris flow risk through the Burned Area Emergency Response (BAER) process. In Conference Presentations, 1st North American Landslide Conference, Vail, CO, AEG Special Publication, No 23, pp 1440-1447
- Deisenroth D, Loomis J, Bond C (2009) Non-market valuation of off-highway vehicle recreation in Larimer County, Colorado: Implications for Trail Closures. *Journal of Environmental Management* 90
- deWolfe V (2006) An Evaluation of the Effectiveness of Erosion Control Treatments After Wildfire in Debris-Flow Prone Areas. Colorado School of Mines
- deWolfe V, Santi P (2009) Debris-Flow Erosion Control Treatments After Wildfire: An Evaluation of Erosion Control Effectiveness. VDM Verlag Dr. Müller Aktiengesellschaft & Co. KG, Saarbrücken, Germany
- deWolfe VG, Santi PM, Ey J, Gartner JE (2008) Effective mitigation of debris flows at Lemon Dam, La Plata County, Colorado. *Geomorphology* 96:366-377
- Donovan IP (2014) A Probabilistic Approach to Post-Wildfire Debris-Flow Volume Modeling. Colorado School of Mines
- Ebel BA, Moody JA (2013) Rethinking infiltration in wildfire-affected soils. *Hydrological Processes* 27:1510-1514
- ESRI (2010) ArcGIS, 10.0 edn. ESRI, Redlands, California
- Finnoff D, Tschirhart J (2008) Linking dynamic economic and ecological general equilibrium models. *Resource and Energy Economics* 30:91-114
- Flannigan MD, Stocks BJ, Wotton BM (2000) Climate Change and forest fires. *The Science of the Total Environment* 262:221-229
- Forest Service (2013) BAER Imagery Support Data Download. USDA Forest Service: Burned Area Emergency Response. <http://activefiremaps.fs.fed.us/baer/download.php>. Accessed June 6 2013

- Fowler HJ, Blenkinsop S, Tebaldi C (2007) Linking climate change modelling to impacts studies: recent advances in downscaling techniques for hydrological modelling. *International Journal of Climatology* 27:1547-1578
- Fried JS, Torn MS, Mills E (2004) The impact of climate change on wildfire severity: A regional forecast for Northern California. *Climatic Change* 64:169-191
- Friedman EQ, Santi PM (2014) Debris-flow hazard assessment and validation following the Medano Fire, Great Sand Dunes National Park and Preserve, Colorado. *Landslides* 11
- Fuchs S, Kaitna R, Scheidl C, Hubl J (2008) The application of the risk concept to debris flow hazards. <http://www.dsireusa.org/> (in English):120-129
- Gartner JE, Bigio ER, Cannon SH (2004) Compilation of post wildfire runoff-events data from the Western United States. US Geological Survey Open-file report 2004-1085
- Gartner JE, Cannon SH, Santi PM, Dewolfe VG (2008) Empirical models to predict the volumes of debris flows generated by recently burned basins in the western U.S. *Geomorphology* 96:339-354 doi:<http://dx.doi.org/10.1016/j.geomorph.2007.02.033>
- Geobruigg (2013) Flexible ring net barriers for debris flow protection: The economic solution.
- Gesch D, Oimoen M, Greenlee S, Nelson C, Steuck M, Tyler D (2002) The National Elevation Dataset. *Photogrammetric Engineering and Remote Sensing* 68:5-11
- Giraud RE, McDonald GN (2007) The 2000–2004 fire-related debris flows in Northern Utah. *AEG Special Publication* 23:1522-1531
- Grissino-Mayer HD, Romme WH, Floyd ML, Hanna DD (2004) Climatic and human influences on fire regimes of the southern San Juan Mountains, Colorado, USA. *Ecology* 85:1708-1724
- Griswold JP, Iverson RM (2008) Mobility Statistics and Automated Hazard Mapping for Debris Flows and Rock Avalanches. U.S. Department of the Interior, U.S. Geological Survey, Reston, Virginia
- Hamlet AF, Lettenmaier DP (2007) Effects of 20th century warming and climate variability on flood risk in the western U.S. *Water Resources Research* 43
- Hidalgo HG et al. (2009) Detection and attribution of streamflow timing and changes to climate change in the Western United States. *Journal of Climate* 22:3838-3855
- Holmes TP, Bergstrom JC, Huszar E, Kask SB, Orr Iii F (2004) Contingent valuation, net marginal benefits, and the scale of riparian ecosystem restoration. *Ecological Economics* 49:19-30 doi:<http://dx.doi.org/10.1016/j.ecolecon.2003.10.015>

- Horton P, Jaboyedoff M, Rudaz B, Zimmermann M (2013) Flow-R, a model for susceptibility mapping of debris flows and other gravitational hazards at a regional scale. *Nat Hazards Earth Syst Sci* 13:869-885 doi:10.5194/nhess-13-869-2013
- Iverson RM, Schilling SP, Vallance JW (1998) Objective delineation of lahar-inundation hazard zones. *Geological Society of America Bulletin* 110:972-984 doi:10.1130/0016-7606(1998)110<0972:odolih>2.3.co;2
- Jakob M, Holm K, Weatherly H, Liu S, Ripley N (2013) Debris flood risk assessment for Mosquito Creek, British Columbia, Canada. *Natural Hazards* 65:1653 - 1681 doi:10.1007/s11069-012-0436-6
- Karl TR, Knight RW (1998) Secular trends of precipitation amount, frequency, and intensity in the United States. *Bulletin of the American Meteorological Society*:231-241
- Kharin VV, Zwiers FW, Zhang X, Hegerl GC (2007) Changes in temperature and precipitation extremes in the IPCC ensemble of global coupled model simulations. *Journal of Climate* 20:1419-1444
- Kim J (2005) A projection of the effects of the climate change induced by increased CO<sub>2</sub> on the extreme hydrologic events in the Western U.S. *Climatic Change* 68:153-168
- LA Times (2009) Storm to test Southern California debris basins. *Los Angeles Times*, Los Angeles, California
- Lee EM, Jones DKC (2004) *Landslide Risk Assessment*. 1st edn. Thomas Telford Publishing, London
- Leung LR, Qian Y, Bian X, Washington WM, Han J, Roads JO (2004) Mid-Century ensemble regional climate change scenarios for the western United States. *Climatic Change* 62:75-113
- Lin G, Chen L, Lai J (2006) Assessment of risk due to debris flow events: a case study in Central Taiwan. *Natural Hazards* 39:1-14
- Littell JS, McKenzie D, Peterson DL, Westerling AL (2009) Climate and wildfire area burned in western U.S. ecoprovinces, 1916-2003. *Ecological Applications* 19:1003-1021
- Magirl CS, Griffiths PG, Webb RH (2010) Analyzing debris flows with the statistically calibrated empirical model LAHARZ in southeastern Arizona, USA. *Geomorphology* 119:111-124 doi:http://dx.doi.org/10.1016/j.geomorph.2010.02.022
- Maraun D et al. (2010) Precipitation Downscaling Under Climate Change: Recent developments to bridge the gap between dynamical models and end user. *Reviews in Geophysics* 48
- McCoy K, Krasko V, Santi P, Kaffine D, Rebennack S (in preparation) Minimizing economic impacts from post-fire debris flows in the western United States. *Natural Hazards*

- McCoy K, Santi P, Kaffine D, Krasko V GIS Modeling to Assess Economic Risk from Post-Fire Debris-Flows. In: Strickland JA, P.E., Wiltshire RL, P.E., Goss CM, Ph.D., P.E. (eds) Rocky Mountain Geo-Conference 2014, Lakewood, Colorado, November 7 2014. ASCE Publications Geotechnical Practice Publication No. 9, pp 9-30
- Means RS (1999a) Heavy Construction Cost Data. 13th Annual edn. R.S. Means Company, Inc., Kingston, MA
- Means RS (1999b) Site Work & Landscape Cost Data. 18th Annual edn. R.S. Means Company, Inc., Kingston, MA
- Mearns LO, Giorgi F, Whetton P, Pabon D, Hulme M, Lal M (2003) Guidelines for Use of Climate Scenarios Developed from Regional Climate Model Experiments. [http://www.ipcc-data.org/guidelines/pages/gcm\\_guidehtml](http://www.ipcc-data.org/guidelines/pages/gcm_guidehtml), DDC of IPCC TG CIA Final Version - 10/30/03
- Meehl GA, Zwiers F, Evans J, Knutson T, Mearns L, Whetton P (2000) Trends in extreme weather and climate events: Issues related to modeling extremes in projections of future climate change. *Bulletin of the American Meteorological Society* 81:427-436
- Meyer GA, Pierce JL, Wood SH, Jull AJT (2001) Fire, storms, and erosional events in the Idaho Batholith. *Hydrological Processes* 15:3025-3038
- Meyer GA, Wells SG, Balling RC, Jr., Jull AJT (1992) Response of alluvial systems to fire and climate change in Yellowstone National Park. *Nature* 357:147-150
- Millsbaugh SH, Whitlock C, Bartlein PJ (2000) Variations in fire frequency and climate over the past 17 000 yr in central Yellowstone National Park. *Geology* 28:211-214
- Moody JA, Martin DA, Cannon SH (2008) Post-wildfire erosion response in two geologic terrains in the western USA. *Geomorphology* 95:103-118
- Morgan P, Heyerdahl, E. K., and Gibson, C. E. (2008) Multi-season climate synchronized forest fires throughout the 20th century, northern Rockies, USA. *Ecology* 89:717-728
- MTBS (2014) Monitoring Trends in Burn Severity (MTBS). <http://www.mtbs.gov/index.html>. Accessed April 30 2014
- Napper C (2006) Burned Area Emergency Response Treatments Catalog (BAERCAT) vol 625. USDA Forest Service, National Technology and Development Program, Watershed, Soil, Air Management, San Dimas Technology & Development Center, San Dimas, California
- National Park Service (1995) Economic Impacts of Protecting Rivers, Trails, and Greenway Corridors. A Resource Book., Fourth edn.,
- Nearing MA (2001) Potential changes in rainfall erosivity in the U.S. with climate change during the 21st century. *Journal of Soil and Water Conservation* 56:229-232

- NOAA (2013) Precipitation Frequency Data Server. <http://dipper.nws.noaa.gov/hdsc/pfds/>. Accessed June 4 2013
- Nordhaus W (1992) An optimal transition path for controlling greenhouse gases. *Science* 258:1315-1319
- Parsons A, Robichaud PR, Lewis SA, Napper C, Clark JT (2010) Field Guide for Mapping Post-Fire Soil Burn Severity. General Technical Report RMRS-GTR-243. U.S. Department of Agriculture, Forest Service, Rocky Mountain Research Station, Fort Collins, CO
- Price C, Rind D (1994) The impact of a  $2\times$  CO<sub>2</sub> climate on lightning-caused fires. *Journal of Climate* 7:1484-1494
- Prochaska AB, Santi PM, Higgins JD (2008) Debris Basin and Deflection Berm Design for Fire-Related Debris-Flow Mitigation. *Environmental & Engineering Geoscience* 14:297-313 doi:10.2113/gsegeosci.14.4.297
- Rebennack S, Kallrath J (2014) Continuous piecewise linear delta-approximations for univariate functions: computing minimal breakpoint systems. *Journal of Optimization Theory and Applications*:1-27
- Rickenmann D (2005) Runout prediction methods. In: Jakob M, Hungr O (eds) *Debris-flow Hazards and Related Phenomena*. Springer Praxis Books. Springer Berlin Heidelberg, pp 305-324 doi:10.1007/3-540-27129-5\_15
- Riley KL, Bendick R, Hyde KD, Gabet EJ (2013) Frequency–magnitude distribution of debris flows compiled from global data, and comparison with post-fire debris flows in the western US. *Geomorphology* 191:118-128
- Robichaud PR, Ashmin LE, Simms BD (2010) Post-Fire Treatment Effectiveness for Hillslope Stabilization. Gen. Tech. Rep. RMRS-GTR-240. U.S. Department of Agriculture, Forest Service, Rocky Mountain Research Station, Fort Collins, CO
- Robichaud PR, Elliot WJ, Pierson FB, Hall DE, Moffet CA, Ashmun LE (2007) Erosion Risk Management Tool (ERMiT) User Manual (version 2006.01.18). General Technical Report RMRS-GTR-188. U.S. Department of Agriculture, Forest Service, Rocky Mountain Research Station, Fort Collins, CO
- Robichaud PR, Lewis SA, Wagenbrenner JW, Ashmun LE, Brown RE (2013a) Post-fire mulching for runoff and erosion mitigation Part I: Effectiveness at reducing hillslope erosion rates. *Catena* 105:75-92
- Robichaud PR, Pierson FB, Brown RE, Wagenbrenner JW (2008) Measuring effectiveness of three postfire hillslope erosion barrier treatments, western Montana, USA. *Hydrological Processes* 22:159-170

- Robichaud PR, Wagenbrenner JW, Lewis SA, Ashmun LE, Brown RE, Wohlgemuth PM (2013b) Post-fire mulching for runoff and erosion mitigation Part II: Effectiveness in reducing runoff and sediment yields from small catchments. *Catena* 105:93-111
- Rupert MG, Cannon SH, Gartner JE, Michael JA, Helsel DR (2008) Using Logistic Regression to Predict the Probability of Debris Flows in Areas Burned by Wildfires, Southern California, 2003-2006. U.S. Department of the Interior, U.S. Geological Survey, Reston, Virginia
- Santi PM, deWolfe VG, Higgins JD, Cannon SH, Gartner JE (2008) Sources of debris flow material in burned areas. *Geomorphology* 96:310-321
- Santi PM, Hewitt K, VanDine DF, Cruz EB (2011) Debris-flow impact, vulnerability, and response. *Natural Hazards* 56:371-402
- Santi PM, Morandi L (2013) Comparison of debris-flow volumes from burned and unburned areas. *Landslides* 10:757-769
- Schilling SP (1998) LAHARZ: GIS programs for automated mapping of lahar-inundation hazard zones. U.S. Department of the Interior, U.S. Geological Survey, Vancouver, Washington
- Scott KM (1971) Origin and sedimentology of 1969 debris flows near Glendora, CA. US Geological Survey Prof Paper 750-C:C242-C247
- Settle C, Crocker TD, Shogren JF (2002) On the joint determination of biological and ecological systems. *Ecological Economics* 42:301-311
- Shakesby RA, Doerr SH (2006) Wildfire as a hydrological and geomorphological agent. *Earth-Science Reviews* 74:269-307
- Skinner KD (2013) Post-Fire Debris-Flow Hazard Assessment of the Area Burned by the 2013 Beaver Creek Fire near Hailey, Central Idaho. U.S. Department of the Interior, U.S. Geological Survey, Reston, Virginia
- Soil Survey Staff (2014) Soil Data Viewer. [http://www.nrcs.usda.gov/wps/portal/nrcs/detailfull/soils/home/?cid=nrcs142p2\\_053620](http://www.nrcs.usda.gov/wps/portal/nrcs/detailfull/soils/home/?cid=nrcs142p2_053620). Accessed April 30 2014
- Spittler TE (1995) Fire and the debris flow potential of winter storms. *Brushfires in California: Ecology and Resource Management*:113-120
- Staley DM (2013) Emergency assessment of post-fire debris-flow hazards for the 2013 Rim Fire, Stanislaus National Forest and Yosemite National Park, California. US Geological Survey Open-File Report 2013-1260
- Staley DM (2014) Emergency assessment of post-fire debris-flow hazards for the 2013 Springs Fire, Ventura County, California. US Geological Survey Open-File Report 2014-1001

- Staley DM, Kean JW, Cannon SH, Schmidt KM, Laber JL (2013a) Objective definition of rainfall intensity-duration thresholds for the initiation of post-fire debris flows in southern California. *Landslides* 10:547-562
- Staley DM, Smoczyk GM, Reeves RR (2013b) Emergency assessment of post-fire debris-flow hazards for the 2013 Powerhouse fire, southern California. US Geological Survey Open-File Report 2013-1248
- Standard-Examiner (2011) Debris basin will safeguard homes. Standard-Examiner, Ogden, UT
- Tillery AC, Darr MJ, Cannon SH, Michael JA (2011) Postwildfire debris flow hazard assessment for the area burned by the 2011 Track Fire, northeastern New Mexico and southeastern Colorado vol Open-File Report 2011-1257. United States Geological Survey,
- Trenberth KE, Dai A, Rasmussen RM, Parsons DB (2003) The changing character of precipitation. *Bulletin of the American Meteorological Society* 84:1205-1217
- USGS (2005) Southern California - Wildfires and Debris flows. Fact sheet 2005-3106
- USGS (2014) Scientific Background. [http://landslides.usgs.gov/current/postfire\\_debrisflow/background.php](http://landslides.usgs.gov/current/postfire_debrisflow/background.php). Accessed April 30 2014
- Wells HG (1987) The effects of fire on the generation of debris flows in southern California. In: Costa JE, Wieczorek GF (eds) *Debris flows/avalanches - process, recognition, and mitigation: Geological Society of America, Reviews in Engineering Geology VII*.
- Westerling AL, Hidalgo HG, Cayan DR, Swetnam TW (2006) Warming and earlier spring increase western U.S. forest wildfire activity. *Science* 313:940-943
- Wilbanks TJ, Kafine SM, Leiby PN, Perlack RD, Shogren JF, Smith JB (2003) Possible responses to Global Climate Change: Integrating Mitigation and Adaptation. *Environment* 45
- Witt AC, Gillon KA, Wooten RM, Douglas TJ, Bauer JB, Fuemmeler SJ (2012) Determining potential debris flow inundation zones for an emergency response using LAHARZ: The Ghost Town debris flow, Maggie Valley, N.C., USA. In: Eberhardt E, Froese C, Turner AK, Leroueil S (eds) *Landslides and Engineered Slopes: Protecting Society through Improved Understanding*, vol 1. CRC Press/Balkema,
- Wohl EE, Pearthree PP (1991) Debris flows as geomorphic agents in the Huachuca Mountains of southeastern Arizona. *Geomorphology* 4:273-292
- Wondzell SM, King JG (2003) Postfire erosional processes in the Pacific Northwest and Rocky Mountain regions. *Forest Ecology and Management* 178:75-87

**Appendix A**  
**Basin Characteristics for 3 Case Study Sites**

**Table A - 1 – Site 1 Basin Characteristics**

<b>BASIN ID</b>	<b>Shape Length (m)</b>	<b>Shape Area (m)</b>	<b>Area Slope <math>\geq 30\%</math> (m<sup>2</sup>)</b>	<b>Area Slope <math>\geq 30\%</math> (km<sup>2</sup>)</b>	<b>Area Burned Slope <math>\geq 50\%</math> (m<sup>2</sup>)</b>	<b>Area Moderate Burn Severity (m<sup>2</sup>)</b>	<b>Area High Burn Severity (m<sup>2</sup>)</b>
1	2,955	303,469	267,400	0.27	42,200	107,500	51,500
2	4,240	446,600	343,800	0.34	89,200	297,000	111,100
3	5,140	844,900	710,400	0.71	122,900	635,700	13,500
4	3,920	542,400	432,200	0.43	102,700	187,600	0
5	18,700	4,866,919	4,029,800	4.0	2,271,400	2,959,100	965,800
6	3,020	224,500	21,500	0.02	0	0	0
7	5,360	857,400	400,300	0.40	79,300	391,300	0
8	7,660	1,576,300	556,200	0.56	115,200	652,300	8,100
9	11,260	2,668,300	1,992,600	2.0	940,400	1,412,700	941,100
10	4,840	750,100	442,800	0.44	156,400	345,600	30,600
11	16,601	7,239,857	5,950,600	6.0	3,715,300	3,798,000	2,225,500
12	4,120	664,500	481,500	0.48	149,600	443,100	96,300
13	3,500	406,200	201,700	0.20	23,200	90,900	0
14	16,865	6,132,650	5,132,100	5.1	3,619,800	2,966,800	2,306,200
15	17,129	6,288,541	4,829,600	4.8	2,569,900	2,354,300	2,259,500
16	7,420	1,555,600	1,457,900	1.5	1,120,800	742,100	688,900
17	1,980	107,400	65,500	0.07	10,400	33,900	0

**Table A – 1 Continued**

<b>BASIN ID</b>	<b>Area Moderate and High Burn Severity (km<sup>2</sup>)</b>	<b>Area Moderate and High Burn Severity and Slopes ≥50% (km<sup>2</sup>)</b>	<b>% Slopes ≥ 30% (%)</b>	<b>% Moderate Burn Severity (%)</b>	<b>% High Burn Severity (%)</b>	<b>% Burned Slope ≥50% (%)</b>	<b>Clay Content (%)</b>
1	0.16	0.04	88	35	17	14	17.5
2	0.41	0.08	77	67	25	20	17.5
3	0.65	0.11	84	75	1.6	15	22.6
4	0.19	0.04	80	35	0	19	26.5
5	3.92	2.11	83	61	20	47	20.7
6	0.00	0.00	9.6	0	0	0	15.0
7	0.39	0.06	47	46	0	9.2	17.0
8	0.66	0.11	35	41	0.5	7.3	21.3
9	2.35	0.93	75	53	35	35	29.5
10	0.38	0.15	59	46	4.1	21	35.6
11	6.02	3.45	82	52	31	51	23.3
12	0.54	0.14	72	67	14	23	28.4
13	0.09	0.01	50	22	0	5.7	43.5
14	5.27	3.42	84	48	38	59	19.3
15	4.61	2.39	77	37	36	41	21.7
16	1.43	1.09	94	48	44	72	17.5
17	0.03	0.00	61	32	0	9.7	43.3

**Table A – 1 Continued**

<b>BASIN ID</b>	<b>Liquid Limit</b>	<b>K factor</b>	<b>Max. El. (m)</b>	<b>Min. El. (m)</b>	<b>Ruggedness</b>	<b>El. Range (m)</b>	<b>StDev. Slope</b>
1	27.5	0.20	816.5	421.2	0.72	395.3	14
2	27.5	0.20	788.8	356.9	0.65	431.9	14
3	26.1	0.20	701.6	166.6	0.58	535.0	13
4	25.0	0.20	428.1	144.8	0.38	283.4	16
5	26.2	0.22	1,026.6	122.1	0.41	904.4	21
6	25.0	0.32	246.0	130.2	0.24	115.8	9.3
7	25.0	0.30	316.8	88.6	0.25	228.2	14
8	26.2	0.27	353.5	69.5	0.23	284.0	15
9	33.5	0.23	719.0	99.3	0.38	619.7	19
10	45.5	0.29	309.1	95.2	0.25	213.9	19
11	29.5	0.21	1,032.9	86.7	0.35	946.3	23
12	28.2	0.21	385.9	164.1	0.27	221.8	16
13	52.6	0.27	310.0	134.0	0.28	176.0	13
14	27.6	0.20	1,212.2	187.6	0.41	1,025	26
15	28.5	0.21	1,134.3	152.5	0.39	981.8	21
16	27.5	0.20	1,009.3	360.9	0.52	648.4	21
17	52.3	0.27	300.2	166.2	0.41	134.0	14

**Table A - 2 – Site 2 Basin Characteristics**

<b>BASIN ID</b>	<b>Area Slope &gt;30% (km<sup>2</sup>)</b>	<b>% Basin w/Slope &gt;30% (%)</b>	<b>Area Mod. &amp; Hi. Sev. (km<sup>2</sup>)</b>	<b>% Basin Burn Mod. &amp; Hi. Sev. (%)</b>	<b>Clay Content (%)</b>	<b>Liquid Limit (%)</b>	<b>Basin Ruggedness</b>
1	2.12	87	1.24	51	14.6	22.5	0.69
2	1.30	86	0.86	57	13.9	22.5	0.73
3	0.45	75	0.02	2.9	11.2	22.5	0.72
4	3.83	90	0.26	6.0	14.6	22.5	0.53
5	0.18	86	0.004	2.0	13.0	22.5	0.84
6	1.35	88	1.24	80	15.1	22.5	0.81
7	0.24	82	0.29	99	15.0	22.5	0.94
8	0.33	95	0.005	1.4	15.0	22.5	0.90
9	0.54	94	0.07	12	15.0	22.5	1.00
10	0.28	85	0.14	44	15.0	22.5	1.33
11	0.49	95	0.16	31	15.1	22.5	1.10
12	0.33	98	0.29	88	15.0	22.5	1.12
13	0.35	93	0.38	100	15.0	22.5	1.01
14	3.94	88	0.45	10	15.2	22.5	0.42
15	0.31	96	0.32	98	15.2	22.5	1.34
16	0.50	97	0.35	66	15.1	22.5	1.07
17	3.21	91	1.35	38	15.2	22.5	0.59
18	0.77	85	0.18	20	15.2	22.5	0.39
19	0.79	85	0.49	53	15.0	22.5	0.55
20	0.40	77	0.36	68	15.0	22.5	0.50
21	0.12	85	0.12	83	15.0	22.5	1.31
22	0.73	93	0.78	98	15.1	22.5	0.96
23	0.11	99	0.10	89	15.0	22.5	1.10
24	0.14	97	0.13	95	15.0	22.5	1.14
25	0.12	89	0.14	100	15.0	22.5	1.39
26	0.14	92	0.09	61	15.0	22.5	0.81
27	0.08	98	0.05	68	15.0	22.5	1.07
28	0.03	70	0.05	100	15.0	22.5	0.99
29	0.26	88	0.17	58	15.0	22.5	1.05
30	0.04	83	0.04	80	15.0	22.5	1.00
31	0.11	97	0.11	97	15.0	22.5	0.80
32	0.09	95	0.10	100	15.0	22.5	0.80
33	0.14	75	0	0	15.0	22.5	0.63
34	0.05	47	0.001	0.9	15.0	22.5	0.40
35	0.03	94	0.001	1.7	15.0	22.5	1.50

**Table A – 2 Continued**

<b>BASIN ID</b>	<b>Area Slope &gt;30% (km<sup>2</sup>)</b>	<b>% Basin w/Slope &gt;30% (%)</b>	<b>Area Mod. &amp; Hi. Sev. (km<sup>2</sup>)</b>	<b>% Basin Burn Mod. &amp; Hi. Sev. (%)</b>	<b>Clay Content (%)</b>	<b>Liquid Limit (%)</b>	<b>Basin Ruggedness</b>
36	0.04	73	0.03	58	15.0	22.5	1.29
37	0.04	94	0.002	4.8	15.0	22.5	1.36
38	0.03	95	0.01	41	15.0	22.5	1.88
39	0.02	94	0.02	98	15.0	22.5	2.29
40	0.03	85	0.01	14	15.0	22.5	1.18
41	0.01	42	0.03	92	15.0	22.5	1.13
42	0.02	99	0.02	100	15.0	22.5	1.31
43	0.03	97	0.03	100	15.0	22.5	1.28
44	0.05	98	0.05	96	15.0	22.5	1.21
45	0.03	0	0.03	91	15.0	22.5	1.03
46	0.03	96	0.01	33	15.0	22.5	1.11
47	0.03	90	0.003	7.3	15.0	22.5	1.20
48	0.04	76	0.002	2.8	15.0	22.5	1.24
49	0.05	86	0.04	67	15.0	22.5	0.79
50	0.02	60	0.01	56	15.0	22.5	0.67
51	0.02	41	0.04	81	15.0	22.5	0.55
52	0.09	60	0.03	17	15.0	22.5	0.43
53	3.59	74	0.10	2.0	15.4	22.5	0.44
54	1.81	90	0.04	1.9	15.2	22.5	0.68
55	6.08	83	0.74	10	15.2	22.5	0.40

**Table A - 3 – Site 3 Basin Characteristics**

<b>BASIN ID</b>	<b>Area Slope ≥ 30% (km<sup>2</sup>)</b>	<b>% Basin w/Slope ≥ 30% (%)</b>	<b>Area Mod. &amp; Hi. Sev. (km<sup>2</sup>)</b>	<b>% Basin Burn Mod. &amp; Hi. Sev. (%)</b>	<b>Clay Content (%)</b>	<b>Liquid Limit (%)</b>	<b>Basin Ruggedness</b>
1	5.52	43	10.7	83	33.8	38.4	0.14
2	0.49	35	1.43	100	25.7	32.0	0.32
3	2.02	30	3.98	60	35.4	40.4	0.17
4	5.33	40	11.2	84	36.8	40.1	0.13
5	0.68	33	1.60	77	31.1	37.3	0.26
6	0.04	20	0.20	95	28.6	34.9	0.68
7	0.09	33	0.24	88	29.5	35.7	0.60
8	0.10	41	0.24	96	29.5	35.7	0.63
9	1.84	14	4.83	37	34.9	40.6	0.14
10	0.80	49	1.50	93	37.7	38.6	0.17
12	0.67	20	3.02	92	34.0	39.8	0.25
13	0.31	46	0.60	89	34.3	40.5	0.41
14	0.44	11	2.14	51	34.9	41.0	0.23
15	0.46	5.5	2.32	28	35.7	41.8	0.19
16	0.22	33	0.43	66	29.6	35.8	0.42
17	0.03	8.8	0.31	96	27.5	33.7	0.54
18	0.03	15	0.18	87	34.3	40.4	0.65
19	0.05	9.1	0.23	41	34.8	41.0	0.48
20	0.05	13	0.31	74	34.4	40.5	0.58
21	0.14	8.8	0.45	27	34.6	40.5	0.20
22	0.41	17	0.80	34	33.2	39.4	0.28
23	0.14	35	0.19	50	31.1	37.3	0.55
24	0.26	34	0.70	94	30.1	35.4	0.43
25	0.19	15	0.86	67	32.2	37.8	0.37
26	0.68	18	2.10	55	33.0	38.6	0.25
27	0.08	21	0.32	82	31.7	37.9	0.59
28	0.14	28	0.47	97	30.9	37.1	0.51
31	0.48	25	0.60	32	31.8	38.0	0.23
32	0.11	46	0.22	92	25.7	32.0	0.57
33	0.03	7.8	0.31	78	27.8	33.2	0.19
34	0.21	30	0.35	50	27.0	33.3	0.42
35	0.13	20	0.52	79	27.3	32.9	0.20
36	0.09	30	0.27	96	26.0	32.2	0.27

**Table A – 3 Continued**

<b>BASIN ID</b>	<b>Area Slope ≥ 30% (km<sup>2</sup>)</b>	<b>% Basin w/Slope ≥ 30% (%)</b>	<b>Area Mod. &amp; Hi. Sev. (km<sup>2</sup>)</b>	<b>% Basin Burn Mod. &amp; Hi. Sev. (%)</b>	<b>Clay Content (%)</b>	<b>Liquid Limit (%)</b>	<b>Basin Ruggedness</b>
37	0.15	18	0.73	84	32.9	36.0	0.19
38	0.04	34	0.12	94	25.7	32.0	0.86
39	0.25	25	0.57	58	27.2	33.4	0.37
40	0.03	20	0.14	93	26.1	32.4	0.91
41	0.19	25	0.70	90	26.0	32.3	0.41
42	0.04	17	0.13	61	28.6	34.9	0.77
43	0.08	10	0.68	93	26.4	32.7	0.40
44	0.59	30	1.95	98	37.1	38.3	0.11
45	0.02	15	0.13	94	26.8	33.1	0.89
47	0.12	21	0.49	88	27.8	33.8	0.45
48	0.14	18	0.74	98	28.2	34.3	0.39
49	0.04	26	0.10	69	35.9	37.6	0.55
50	0.04	24	0.16	98	37.7	38.6	0.29
51	0.17	27	0.63	99	37.2	39.0	0.45
52	0.01	4.9	0.16	61	32.1	37.7	0.53
53	0.01	5.9	0.08	35	35.4	41.6	0.72

## Appendix B

### Climate Change Study - Debris-Flow Dataset DS1

Table B-1 presents a database of collected occurrences of post-wildfire debris flows. This dataset will be published in Brunkal and Santi (in review).

Data was collected from published journal articles, USGS Open File Reports, and news articles and reports found on-line. The overall database is skewed toward those events that impacted humans and/or infrastructure, as that is what is typically reported in the news. The table is sectioned by fire size: small fires <10,000 acres, large fires 11-25,000 acres, and very large fires >25,000 acres. These designations are from results of data analysis from the USFS regarding the increase in fire size and fire numbers each year. In the past decade fires > 1,000 acres have doubled, there are 7 times more fires > 10,000 acres, and nearly 5 times more > 25,000 acres (Climate Central, 2012 - <http://www.climatecentral.org/>).

**Table B - 1 – Climate Change Study Dataset DS1**

STATE	YEAR OF DEBRIS FLOW(S)	FIRE/COMPLEX	ACRES BURNED (km <sup>2</sup> )	Number of debris flows	Number of debris flows/acres burned	REFERENCES
CA	2005	Harvard	1094 (4.43)	4	3.66E-03	Gartner, 2005
UT	2003	Farmington Fire	1935 (7.83)	3	1.55E-03	Gartner, 2005
UT	2013	Quail Hollow fire (2012)	1993 (8.07)	2	1.00E-03	<a href="http://www.heraldextra.com/news/local/north/alpine/popular-trail-closed-after-mudslide-damage/article_34910122-5d73-5a67-a8a3-d51345734501.html">http://www.heraldextra.com/news/local/north/alpine/popular-trail-closed-after-mudslide-damage/article_34910122-5d73-5a67-a8a3-d51345734501.html</a>
CO	1994	South Canyon/Glenwood	2115 (8.56)	6	2.84E-03	Cannon, 2001
CO	2003	Overland fire	3439 (13.91)	3	8.72E-04	Gartner, 2005
BC	2004	Cedar Hills Fire (2003)	4003 (16.12)	1	2.50E-04	Jordan and Covert, 2009 <a href="http://bcwildfire.ca/History/SummaryArchive.htm#2005">http://bcwildfire.ca/History/SummaryArchive.htm#2005</a>
CA	1972	Molera	4300 (17.4)	1	2.33E-04	<a href="http://pubs.usgs.gov/of/2004/1085/Database.htm">http://pubs.usgs.gov/of/2004/1085/Database.htm</a>
OR	1989	Tanner Gulch Fire	4413 (17.86)	3	6.80E-04	<a href="http://www.hcn.org/issues/30/846">http://www.hcn.org/issues/30/846</a>
WA	2013	Milepost 10 fire	5760 (23.31)	3	5.21E-04	<a href="http://www.king5.com/news/local/Wildfire-threatens-homes-near-Malaga-in-Chelan-County-219307591.html">http://www.king5.com/news/local/Wildfire-threatens-homes-near-Malaga-in-Chelan-County-219307591.html</a>
CA	1997	Baker Fire	6150 (24.89)	1	1.63E-04	Cannon, 2001
CO	2013	Fourmile Canyon Fire (2010)	6181 (25.01)	2	3.24E-04	<a href="http://www.denverpost.com/ci_21021863/flash-flood-warning-issued-central-larimer-county">http://www.denverpost.com/ci_21021863/flash-flood-warning-issued-central-larimer-county</a>
OR	1996	Sloans Ridge Fire	7300 (29.54)	1	1.37E-04	<a href="http://www.fs.usda.gov/detail/wallowa-whitman/specialplaces/?cid=stelprdb5213448">http://www.fs.usda.gov/detail/wallowa-whitman/specialplaces/?cid=stelprdb5213448</a>
CA	2004	Gaviota Fire	7440 (30.11)	2	2.69E-04	Gartner, 2005
UT	2002	Mollie (2001)	8000 (32.37)	5	6.25E-04	McDonald and Giraud, 2007
MT	1984	North Hills	8000 (32.37)	25	3.13E-03	<a href="http://pubs.usgs.gov/of/2004/1085/Database.htm">http://pubs.usgs.gov/of/2004/1085/Database.htm</a>

**Table B-1 continued**

STATE	YEAR OF DEBRIS FLOW(S)	FIRE/COMPLEX	ACRES BURNED (km <sup>2</sup> )	Number of debris flows	Number of debris flows/ acres burned	REFERENCES
NM	2013	Tres Lagunas Fire	10219 (41.35)	1	9.79E-05	<a href="http://www.abqjournal.com/219796/news/mudslide-burries-pecos-ranch.html">http://www.abqjournal.com/219796/news/mudslide-burries-pecos-ranch.html</a>
CA	2008	Sayre	11262 (45.57)	12	1.07E-03	Cannon, 2009
CO	2002	Coal Seam	12200 (49.37)	15	1.23E-03	Cannon et al, 2003
BC	2004	Kuskonook (2003)	11940 (48.32)	2	1.68E-04	Jordan and Covert, 2009 <a href="http://bcwildfire.ca/History/SummaryArchive.htm#2005">http://bcwildfire.ca/History/SummaryArchive.htm#2005</a>
CA	1993	Laguna Beach	14337 (58.02)	1	6.97E-05	<a href="http://pubs.usgs.gov/of/2004/1085/Database.htm">http://pubs.usgs.gov/of/2004/1085/Database.htm</a>
CA	1996	Dome fire	16516 (66.84)	1	6.05E-05	Cannon, 2001
BC	2005	Ingersoll (2003)	18063 (73.1)	12	6.64E-04	Jordan and Covert, 2009 <a href="http://bcwildfire.ca/History/SummaryArchive.htm#2005">http://bcwildfire.ca/History/SummaryArchive.htm#2005</a>
CO	2013	Waldo Canyon Fire (2012)	18247 (73.84)	3	1.64E-04	<a href="http://denver.cbslocal.com/2013/07/11/mud-slide-washes-away-cars-near-waldo-canyon-burn-area/">http://denver.cbslocal.com/2013/07/11/mud-slide-washes-away-cars-near-waldo-canyon-burn-area/</a>
CA	1994	Old Topanga/ North Malibu (1993)	18949 (76.68)	3	1.58E-04	<a href="http://pubs.usgs.gov/of/2004/1085/Database.htm">http://pubs.usgs.gov/of/2004/1085/Database.htm</a>
CA	1969	Canyon Fire, Glendora (1968)	20200 (81.75)	8	3.96E-04	<a href="http://pubs.usgs.gov/of/2004/1085/Database.htm">http://pubs.usgs.gov/of/2004/1085/Database.htm</a>
CA	1980	San Bernardino	23600 (95.51)	2	8.47E-05	<a href="http://pubs.usgs.gov/of/2004/1085/Database.htm">http://pubs.usgs.gov/of/2004/1085/Database.htm</a>
CA	1978	Kanan	25000 (101.17)	1	4.00E-05	Gartner, 2005
OR	2012	Pole Creek Fire	26795 (108.44)	1	3.73E-05	<a href="http://www.bendbulletin.com/home/1823023-151/oregon-gauges-health-impact-of-pole-creek-fire">http://www.bendbulletin.com/home/1823023-151/oregon-gauges-health-impact-of-pole-creek-fire</a>
CA	2013	Mountain Fire	27332 (110.61)	2	7.32E-05	<a href="http://news.yahoo.com/blogs/the-sideshow/video--rainstorms-lead-to-mudslides-near-palm-springs-161811708.html">http://news.yahoo.com/blogs/the-sideshow/video--rainstorms-lead-to-mudslides-near-palm-springs-161811708.html</a>
BC	2004	Lamb Creek (2003)	29361 (118.82)	1	3.41E-05	Jordan and Covert, 2009 <a href="http://bcwildfire.ca/History/SummaryArchive.htm#2005">http://bcwildfire.ca/History/SummaryArchive.htm#2005</a>
AZ	2011	Monument fire	30526 (123.53)	6	1.97E-04	Wohl and Pearthree, 1991 <a href="http://azgeology.azgs.az.gov/article/environmental-geology/2011/09/post-monument-fire-floods-and-debris-flows-huachuca-mountains">http://azgeology.azgs.az.gov/article/environmental-geology/2011/09/post-monument-fire-floods-and-debris-flows-huachuca-mountains</a>
UT	2012	Wood hollow fire	46190 (186.92)	7	1.52E-04	<a href="http://www.sltrib.com/sltrib/news/54591900-78/weather-burn-national-reported.html.csp">http://www.sltrib.com/sltrib/news/54591900-78/weather-burn-national-reported.html.csp</a>
ID	1989	Lowman Fire	47000 (190.20)	20	4.26E-04	<a href="http://pubs.usgs.gov/of/2004/1085/Database.htm">http://pubs.usgs.gov/of/2004/1085/Database.htm</a>
NM	2000	Cerro Grande Fire	47650 (192.83)	5	1.05E-04	Cannon and Reneau, 2000
ID	2009	Castle rock fire (2007)	48520 (196.35)	20	4.12E-04	Riley et al, 2013
WA	1970	Entiat Valley	49200 (199.11)	3	6.10E-05	<a href="http://pubs.usgs.gov/of/2004/1085/Database.htm">http://pubs.usgs.gov/of/2004/1085/Database.htm</a>
BC	2003	Okanagan mountain park	64030 (259.12)	2	3.12E-05	Jordan and Covert, 2009 <a href="http://bcwildfire.ca/History/SummaryArchive.htm#2005">http://bcwildfire.ca/History/SummaryArchive.htm#2005</a>
CO	2002	Missionary Ridge	73000 (295.42)	13	1.78E-04	Cannon et al, 2003
CO	2012	High Park Fire (2012)	87284 (353.23)	2	2.29E-05	<a href="http://www.krdo.com/news/Mudslide-closes-highway-near-High-Park-Fire-burn-area/15447256">http://www.krdo.com/news/Mudslide-closes-highway-near-High-Park-Fire-burn-area/15447256</a>

**Table B-1 continued**

STATE	YEAR OF DEBRIS FLOW(S)	FIRE/COMPLEX	ACRES BURNED (km <sup>2</sup> )	Number of debris flows	Number of debris flows/acres burned	REFERENCES
OR	1998	Tower Fire(1996)	104599 (423.3)	3	2.87E-05	Howell, P. 2006
CA	2003	Simi	108204 (437.89)	2	1.85E-05	Gartner, 2005
ID	2013	Beaver creek fire	111000 (449.2)	3	2.70E-05	<a href="http://www.mtexpress.com/index2.php?ID=2007151950#.U9lfUuNdV8E">http://www.mtexpress.com/index2.php?ID=2007151950#.U9lfUuNdV8E</a>
ID	2013	Elk Complex	131258 (531.18)	5	3.81E-05	<a href="http://www.idahostatesman.com/2013/09/19/2768152/fires-mudslides-transform-the.html">http://www.idahostatesman.com/2013/09/19/2768152/fires-mudslides-transform-the.html</a>
NM	2011	Las Conchas Fire	150000 (607.03)	2	1.33E-05	<a href="http://criticalzone.org/national/publications/pub/orempelletier-using-airborne-and-terrestrial-lidar-to-quantify-and-monitor/">http://criticalzone.org/national/publications/pub/orempelletier-using-airborne-and-terrestrial-lidar-to-quantify-and-monitor/</a>
CA	2003	Grand prix/Old Fire	150729 (609.98)	47	3.12E-04	Cannon et al, 2008
CA	2010	Station Fire (2009)	160577 (649.83)	57	3.55E-04	Ahlstrom, 2013
CA	2009	Basin-Complex Fire (2008)	162818 (658.9)	1	6.14E-06	<a href="http://www.ktvu.com/news/news/mudslides-shut-down-highway-1/nKsqf/">www.ktvu.com/news/news/mudslides-shut-down-highway-1/nKsqf/</a>
CA	1978	Marble Cone Fire (1977)	178000 (720.34)	1	5.62E-06	<a href="http://himlyn.tripod.com/pico.blanco/id30.html">http://himlyn.tripod.com/pico.blanco/id30.html</a>
ID	1994	Foothills Fire (1992)	250000 (1011.7)	1	4.00E-06	<a href="http://www.hcn.org/issues/30/846">http://www.hcn.org/issues/30/846</a>
CA	2003	Paradise/Cedar	280278 (1134.24)	2	7.14E-06	<a href="http://www.utsandiego.com/news/2005/Apr/10/new-growth-protects-fire-areas-from-major/3/?#article-copy">http://www.utsandiego.com/news/2005/Apr/10/new-growth-protects-fire-areas-from-major/3/?#article-copy</a>
MT	2000	Bear/Bitterroot fires	300000 (1214.06)	35	1.17E-04	Riley et al, 2013

**Appendix C**  
**Calculated Debris-Flow Probability and Volume for 2-year and 10-year**  
**Rainfall Scenarios at 3 Case Study Sites**

**Table C - 1 – Site 1 Calculated probability and volume for 1-hr, 2-yr recurrence storm**

<b>BASIN ID</b>	<b>Rainfall Total (mm)</b>	<b>P<sub>storm</sub></b>	<b>P<sub>DF Given Storm</sub></b>	<b>P<sub>DF Tot.</sub></b>	<b>V<sub>DF</sub> (m<sup>3</sup>)</b>
1	26	0.5	0.10	0.05	3,000
2	26	0.5	0.14	0.07	4,100
3	26	0.5	0.09	0.05	7,200
4	26	0.5	0.06	0.03	4,100
5	26	0.5	0.37	0.18	46,300
6	26	0.5	0.03	0.02	500
7	26	0.5	0.04	0.02	4,500
8	26	0.5	0.05	0.02	6,200
9	26	0.5	0.28	0.14	22,200
10	26	0.5	0.06	0.03	4,700
11	26	0.5	0.47	0.24	81,500
12	26	0.5	0.08	0.04	5,400
13	26	0.5	0.04	0.02	2,400
14	26	0.5	0.58	0.29	66,700
15	26	0.5	0.48	0.24	58,000
16	26	0.5	0.54	0.27	14,500
17	26	0.5	0.04	0.02	1,100

**Table C - 2 – Site 1 Calculated probability and volume for 1-hr, 10-yr recurrence storm**

<b>BASIN ID</b>	<b>Rainfall Total (mm)</b>	<b>P<sub>storm</sub></b>	<b>P<sub>DF Given Storm</sub></b>	<b>P<sub>DF Tot.</sub></b>	<b>V<sub>DebrisFlow</sub> (m<sup>3</sup>)</b>
1	39	0.1	0.12	0.012	3,800
2	39	0.1	0.17	0.017	5,200
3	39	0.1	0.11	0.011	9,000
4	39	0.1	0.07	0.007	5,200
5	39	0.1	0.42	0.042	58,200
6	39	0.1	0.04	0.004	600
7	39	0.1	0.05	0.005	5,600
8	39	0.1	0.06	0.006	7,800
9	39	0.1	0.33	0.033	27,900
10	39	0.1	0.07	0.007	5,900
11	39	0.1	0.52	0.052	102,400
12	39	0.1	0.10	0.010	6,800
13	39	0.1	0.05	0.005	3,000
14	39	0.1	0.63	0.063	83,900
15	39	0.1	0.53	0.053	72,900
16	39	0.1	0.59	0.059	18,300
17	39	0.1	0.05	0.005	1,400

**Table C - 3 – Site 2 Calculated probability and volume for 1-hr, 2-yr recurrence storm**

<b>BASIN ID</b>	<b>Rainfall Total (mm)</b>	<b>P<sub>storm</sub></b>	<b>P<sub>DF</sub> Given Storm</b>	<b>P<sub>DF</sub> Tot.</b>	<b>V<sub>DebrisFlow</sub> (m<sup>3</sup>)</b>
1	20	0.5	0.30	0.152	15,100
2	20	0.5	0.33	0.166	9,900
3	20	0.5	0.01	0.004	3,000
4	20	0.5	0.04	0.020	14,100
5	20	0.5	0.01	0.006	1,700
6	20	0.5	0.71	0.354	11,600
7	20	0.5	0.83	0.417	2,800
8	20	0.5	0.02	0.011	2,400
9	20	0.5	0.03	0.017	3,700
10	20	0.5	0.10	0.049	2,700
11	20	0.5	0.09	0.045	3,800
12	20	0.5	0.75	0.376	3,300
13	20	0.5	0.87	0.433	3,600
14	20	0.5	0.06	0.031	16,100
15	20	0.5	0.79	0.396	3,200
16	20	0.5	0.47	0.233	4,400
17	20	0.5	0.23	0.116	20,100
18	20	0.5	0.10	0.052	5,100
19	20	0.5	0.39	0.194	6,300
20	20	0.5	0.58	0.288	3,900
21	20	0.5	0.53	0.266	1,600
22	20	0.5	0.87	0.434	6,800
23	20	0.5	0.78	0.392	1,500
24	20	0.5	0.82	0.409	1,700
25	20	0.5	0.76	0.380	1,600
26	20	0.5	0.45	0.226	1,700
27	20	0.5	0.49	0.247	1,100
28	20	0.5	0.77	0.387	600
29	20	0.5	0.30	0.150	2,600
30	20	0.5	0.60	0.301	800
31	20	0.5	0.90	0.449	1,500
32	20	0.5	0.90	0.452	1,300
33	20	0.5	0.02	0.009	1,400
34	20	0.5	0.01	0.006	700
35	20	0.5	0.01	0.004	600
36	20	0.5	0.16	0.080	800

**Table C – 3 Continued**

<b>BASIN ID</b>	<b>Rainfall Total (mm)</b>	<b>P<sub>storm</sub></b>	<b>P<sub>DF</sub> Given Storm</b>	<b>P<sub>DF</sub> Tot.</b>	<b>V<sub>DebrisFlow</sub> (m<sup>3</sup>)</b>
37	20	0.5	0.01	0.006	600
38	20	0.5	0.05	0.024	600
39	20	0.5	0.45	0.223	400
40	20	0.5	0.02	0.011	600
41	20	0.5	0.42	0.208	400
42	20	0.5	0.83	0.413	400
43	20	0.5	0.83	0.414	600
44	20	0.5	0.82	0.409	800
45	20	0.5	0.19	0.093	600
46	20	0.5	0.10	0.049	600
47	20	0.5	0.02	0.008	600
48	20	0.5	0.01	0.004	700
49	20	0.5	0.50	0.252	800
50	20	0.5	0.23	0.115	400
51	20	0.5	0.48	0.242	500
52	20	0.5	0.04	0.020	1,200
53	20	0.5	0.03	0.013	11,800
54	20	0.5	0.03	0.014	7,300
55	20	0.5	0.06	0.029	23,900

**Table C - 4 – Site 2 Calculated probability and volume for 1-hr, 10-yr recurrence storm**

<b>BASIN ID</b>	<b>Rainfall Total (mm)</b>	<b>P<sub>storm</sub></b>	<b>P<sub>DF</sub> Given Storm</b>	<b>P<sub>DF</sub> Tot.</b>	<b>V<sub>DF</sub> (m<sup>3</sup>)</b>
1	32	0.1	0.50	0.050	19,200
2	32	0.1	0.53	0.053	12,600
3	32	0.1	0.02	0.002	3,800
4	32	0.1	0.09	0.009	17,900
5	32	0.1	0.03	0.003	2,100
6	32	0.1	0.85	0.085	14,700
7	32	0.1	0.92	0.092	3,500
8	32	0.1	0.05	0.005	3,000
9	32	0.1	0.08	0.008	4,700
10	32	0.1	0.20	0.020	3,400
11	32	0.1	0.19	0.019	4,800
12	32	0.1	0.88	0.088	4,200
13	32	0.1	0.94	0.094	4,600
14	32	0.1	0.13	0.013	20,400
15	32	0.1	0.90	0.090	4,100
16	32	0.1	0.67	0.067	5,600
17	32	0.1	0.41	0.041	25,400
18	32	0.1	0.21	0.021	6,500
19	32	0.1	0.59	0.059	7,900
20	32	0.1	0.76	0.076	4,900
21	32	0.1	0.73	0.073	2,000
22	32	0.1	0.94	0.094	8,600
23	32	0.1	0.89	0.089	1,900
24	32	0.1	0.91	0.091	2,200
25	32	0.1	0.88	0.088	2,000
26	32	0.1	0.66	0.066	2,200
27	32	0.1	0.69	0.069	1,400
28	32	0.1	0.89	0.089	800
29	32	0.1	0.50	0.050	3,300
30	32	0.1	0.78	0.078	1,000
31	32	0.1	0.95	0.095	1,900
32	32	0.1	0.96	0.096	1,700
33	32	0.1	0.04	0.004	1,700
34	32	0.1	0.03	0.003	900
35	32	0.1	0.02	0.002	700
36	32	0.1	0.30	0.030	1,000

**Table C – 4 Continued**

<b>BASIN ID</b>	<b>Rainfall Total (mm)</b>	<b>P<sub>storm</sub></b>	<b>P<sub>DF</sub> Given Storm</b>	<b>P<sub>DF</sub> Tot.</b>	<b>V<sub>DebrisFlow</sub> (m<sup>3</sup>)</b>
37	32	0.1	0.03	0.003	800
38	32	0.1	0.10	0.010	800
39	32	0.1	0.65	0.065	600
40	32	0.1	0.05	0.005	700
41	32	0.1	0.62	0.062	500
42	32	0.1	0.92	0.092	600
43	32	0.1	0.92	0.092	700
44	32	0.1	0.91	0.091	1,100
45	32	0.1	0.35	0.035	700
46	32	0.1	0.20	0.020	800
47	32	0.1	0.04	0.004	700
48	32	0.1	0.02	0.002	800
49	32	0.1	0.70	0.070	1,100
50	32	0.1	0.41	0.041	500
51	32	0.1	0.68	0.068	600
52	32	0.1	0.09	0.009	1,500
53	32	0.1	0.06	0.006	15,000
54	32	0.1	0.06	0.006	9,200
55	32	0.1	0.12	0.012	30,300

**Table C - 5 – Site 3 Calculated probability and volume for 1-hr, 2-yr recurrence storm**

<b>BASIN ID</b>	<b>Rainfall Total (mm)</b>	<b>P<sub>storm</sub></b>	<b>P<sub>DF Given Storm</sub></b>	<b>P<sub>DF Tot.</sub></b>	<b>V<sub>DF</sub> (m<sup>3</sup>)</b>
1	29	0.5	0.23	0.115	145,900
2	29	0.5	0.55	0.274	8,000
3	29	0.5	0.03	0.015	32,700
4	29	0.5	0.21	0.105	150,900
5	29	0.5	0.10	0.051	10,200
6	29	0.5	0.16	0.078	1,100
7	29	0.5	0.15	0.075	1,800
8	29	0.5	0.25	0.127	1,900
9	29	0.5	0.00	0.002	35,600
10	29	0.5	0.55	0.277	11,000
12	29	0.5	0.11	0.057	14,100
13	29	0.5	0.13	0.063	4,500
14	29	0.5	0.01	0.003	9,100
15	29	0.5	0.00	0.001	9,600
16	29	0.5	0.06	0.029	3,300
17	29	0.5	0.18	0.090	900
18	29	0.5	0.03	0.017	900
19	29	0.5	0.00	0.001	1,200
20	29	0.5	0.02	0.008	1,300
21	29	0.5	0.00	0.001	2,600
22	29	0.5	0.00	0.002	5,800
23	29	0.5	0.01	0.007	2,200
24	29	0.5	0.30	0.152	4,200
25	29	0.5	0.03	0.015	3,800
26	29	0.5	0.02	0.008	11,600
27	29	0.5	0.05	0.026	1,800
28	29	0.5	0.19	0.093	2,600
31	29	0.5	0.01	0.003	5,900
32	29	0.5	0.41	0.205	2,000
33	29	0.5	0.15	0.073	1,000
34	29	0.5	0.03	0.017	3,100
35	29	0.5	0.21	0.105	2,600
36	29	0.5	0.48	0.238	1,700
37	29	0.5	0.23	0.115	3,100

**Table C – 5 Continued**

<b>BASIN ID</b>	<b>Rainfall Total (mm)</b>	<b>P<sub>storm</sub></b>	<b>P<sub>DF Given Storm</sub></b>	<b>P<sub>DF Tot.</sub></b>	<b>V<sub>DF</sub> (m<sup>3</sup>)</b>
38	29	0.5	0.26	0.128	1,000
39	29	0.5	0.05	0.025	3,900
40	29	0.5	0.16	0.080	900
41	29	0.5	0.29	0.145	3,600
42	29	0.5	0.02	0.009	900
43	29	0.5	0.23	0.114	2,000
44	29	0.5	0.51	0.254	10,300
45	29	0.5	0.13	0.066	700
47	29	0.5	0.19	0.095	2,400
48	29	0.5	0.28	0.139	3,000
49	29	0.5	0.08	0.038	900
50	29	0.5	0.39	0.195	1,000
51	29	0.5	0.31	0.156	3,200
52	29	0.5	0.01	0.006	500
53	29	0.5	0.00	0.000	500

**Table C - 6 – Site 3 Calculated probability and volume for 1-hr, 10-yr recurrence storm**

<b>BASIN ID</b>	<b>Rainfall Total (mm)</b>	<b>P<sub>storm</sub></b>	<b>P<sub>DF Given Storm</sub></b>	<b>P<sub>DF Total</sub></b>	<b>V<sub>DF</sub> (m<sup>3</sup>)</b>
1	46	0.1	0.50	0.050	192,900
2	46	0.1	0.80	0.080	10,600
3	46	0.1	0.09	0.009	43,200
4	46	0.1	0.47	0.047	199,500
5	46	0.1	0.27	0.027	13,500
6	46	0.1	0.38	0.038	1,400
7	46	0.1	0.37	0.037	2,300
8	46	0.1	0.53	0.053	2,500
9	46	0.1	0.01	0.001	47,100
10	46	0.1	0.80	0.080	14,500
12	46	0.1	0.30	0.030	18,600
13	46	0.1	0.32	0.032	6,000
14	46	0.1	0.02	0.002	12,000
15	46	0.1	0.004	0.0004	12,700
16	46	0.1	0.17	0.017	4,400
17	46	0.1	0.42	0.042	1,200
18	46	0.1	0.10	0.010	1,200
19	46	0.1	0.01	0.001	1,600
20	46	0.1	0.05	0.005	1,800
21	46	0.1	0.01	0.001	3,500
22	46	0.1	0.01	0.001	7,700
23	46	0.1	0.05	0.005	2,900
24	46	0.1	0.59	0.059	5,600
25	46	0.1	0.09	0.009	5,000
26	46	0.1	0.05	0.005	15,400
27	46	0.1	0.15	0.015	2,300
28	46	0.1	0.43	0.043	3,400
31	46	0.1	0.02	0.002	7,800
32	46	0.1	0.70	0.070	2,600
33	46	0.1	0.36	0.036	1,300
34	46	0.1	0.10	0.010	4,100
35	46	0.1	0.47	0.047	3,500
36	46	0.1	0.75	0.075	2,300
37	46	0.1	0.50	0.050	4,100

**Table C – 6 Continued**

<b>BASIN ID</b>	<b>Rainfall Total (mm)</b>	<b>P<sub>storm</sub></b>	<b>P<sub>DF</sub> Given Storm</b>	<b>P<sub>DF</sub> Total</b>	<b>V<sub>DF</sub> (m<sup>3</sup>)</b>
38	46	0.1	0.53	0.053	1,400
39	46	0.1	0.14	0.014	5,100
40	46	0.1	0.38	0.038	1,100
41	46	0.1	0.57	0.057	4,700
42	46	0.1	0.06	0.006	1,300
43	46	0.1	0.49	0.049	2,700
44	46	0.1	0.77	0.077	13,600
45	46	0.1	0.34	0.034	900
47	46	0.1	0.44	0.044	3,200
48	46	0.1	0.56	0.056	3,900
49	46	0.1	0.21	0.021	1,200
50	46	0.1	0.68	0.068	1,300
51	46	0.1	0.60	0.060	4,300
52	46	0.1	0.04	0.004	700
53	46	0.1	0.003	0.0003	600

## Appendix D Publications and Presentations

### Presentations

Vitaliy Krasko, Steffen Rebennack, Kevin McCoy, Paul Santi, Daniel Kaffine (2013) Debris flow hazard management via global optimization. Institute for Operations Research and the Management Sciences (INFORMS) Annual Meeting, Minneapolis, Minnesota.

Kevin McCoy and Paul Santi (2013) Quantifying Potential Economic Impacts from Post-Wildfire Debris Flows. Association of Environmental and Engineering Geologists (AEG) 56th Annual Meeting, Seattle, Washington.

Kevin McCoy, Paul Santi, Daniel Kaffine, Steffen Rebennack, Vitaliy Krasko, and Timo Lohmann (2013) Analysis of Economic Risk from Post-Wildfire Debris Flows, Geological Society of America 125th Annual Meeting, Denver, Colorado.

Vitaliy Krasko, Steffen Rebennack, Kevin McCoy, Paul Santi, Daniel Kaffine (2014) Natural Hazard Management for post-wildfire debris flows. Institute for Operations Research and the Management Sciences (INFORMS) Annual Meeting, San Francisco, California.

Kevin McCoy, Paul Santi, Daniel Kaffine, Vitaliy Krasko V. (2014) GIS Modeling to Assess Economic Risk from Post-Fire Debris-Flows. Rocky Mountain Geo-Conference 2014, Lakewood, Colorado.

Kevin McCoy, Paul Santi, Daniel Kaffine, Steffen Rebennack, Vitaliy Krasko, Timo Lohmann (2014) Comparison of Economic Risk from Post-Wildfire Debris Flows at Three Sites in the Western United States. AEG 57th Annual Meeting, Scottsdale, Arizona.

Santi, P.M. and Donovan, I. (2014) A Probabilistic Approach to Post-Wildfire Debris-Flow Volume Modeling, Association of Environmental and Engineering Geologists 57th Annual Meeting Program with Abstracts, Scottsdale, AZ.

Donovan, I.P., and Santi, P.M. (2013) A Probabilistic Approach to Post-Wildfire Debris-Flow Volume Modeling, Geological Society of America Annual Meeting Abstracts with Programs.

### List of Publications with Abstracts

**Brunkal H, Santi P, (in review) Expected Increase in Post-wildfire Debris Flows with Climate Change. Environmental and Engineering Geoscience.**

Increasing area burned by wildfire and increasing intense precipitation events with predicted climate change will produce a significant increase in the number of post-wildfire debris flows in the western United States. A positive correlation is shown between an increase in wildfire area

and numbers of debris flows. The probability of a debris flow being generated from a burned watershed is influenced by climate change and with conservative model interpretation post-wildfire debris-flow probabilities increase on average by 20.6%, with different climate scenarios increasing the probability of post-wildfire debris flows by 1.6% to 38.9%. A predictive debris-flow volume equation for the Intermountain West is also influenced by factors that will be affected by climate change in the coming decades, and debris-flow volumes are calculated to increase with changing conditions by 3% to 52.5%. Understanding the future implications of increased incidence of wildfire-related debris flows will help agencies and communities better manage the associated risk.

**Donovan, I, Santi P, (in review) A Probabilistic Approach to Post-Wildfire Debris-Flow Modeling . Landslides.**

As populations continue to move into more mountainous terrain, a greater understanding of the processes controlling debris flows has become important for the protection of human life and property. The potential volume of an expected debris flow must be known to effectively mitigate any hazard it may pose, yet an accurate estimate of this parameter has to this point been difficult to model. To this end, a probabilistic method for the prediction of debris-flow volumes using a database of 33 debris flows in the Western United States is presented herein. A number of geomorphological, climatic, and geotechnical basin characteristics were considered for inclusion in the model, and correlation analysis was conducted to identify those with the greatest influence on debris-flow yield rates. Groupings within the database were then clustered based on their similarity levels; a total of six clusters were identified with similar slope angle and burn intensity characteristics. For each of these six clusters, a probability density function detailing the distribution of yield rates within the cluster was developed. The model uses a Monte Carlo simulation to combine each of these distributions into a single probabilistic model for any basin in which a debris flow is expected to occur. This approach was validated by applying the model to ten basins that experienced debris flows of known volumes throughout the western United States. The model predicted nine of the ten debris flow volumes to within the 95% confidence interval of the final distribution; a regression analysis for the ten volumes resulted in an  $R^2$  of 0.816. These results compared favorably with those generated by an existing volume model. This approach provides accurate results based on easily obtainable data, encouraging widespread use in land planning and development.

**McCoy K, Santi P, Kaffine D, Krasko V GIS Modeling to Assess Economic Risk from Post-Fire Debris-Flows. In: Strickland JA, P.E., Wiltshire RL, P.E., Goss CM, Ph.D., P.E. (eds) Rocky Mountain Geo-Conference 2014, Lakewood, Colorado, November 7 2014. ASCE Publications Geotechnical Practice Publication No. 9.**

Post-fire debris-flows are a serious hazard in the western United States. Potential impacts of these events include loss of human life, destruction of structures, and degradation of habitat and water quality. While loss of human life is the most important concern in a geohazard assessment, potential loss of life is extremely difficult to quantify and is beyond the scope of this paper. This paper focuses instead on the analysis of economic risk from post-fire debris-flows in

support of cost-optimized post-fire debris flow hazard management strategies. Common approaches to evaluating post-fire debris-flow hazards provide either qualitative estimates of inundation zones, or no inundation estimates at all. Quantitative estimates of debris-flow damage and economic risk support the selection of natural hazard management strategies following a fire via optimization approaches. The first step in this process is an analysis of damage cost estimates and related probabilities. Debris-flow hazards and associated damage costs for individual drainages can be analyzed in ArcGIS utilizing existing models and readily available GIS data. Preliminary case study results suggest that this process can be used to identify the most economically concerning drainages. These results can guide allocation of emergency management funds and optimization of debris-flow management strategies following a wildfire. This paper discusses where to acquire geologic and social input data, and how to operate the GIS models in support of the post-fire debris-flow economic risk assessment. A case study from southern California is provided to illustrate the methods.

**McCoy K, Krasko V, Santi P, Kaffine D, Rebennack S, (In Preparation) Minimizing economic impacts from post-fire debris flows in the western United States. Natural Hazards.**

Debris flows can be triggered when relatively common rainstorms fall on recently burned drainage basins, creating new hazards to communities downstream from the burn scar. This paper describes methods to identify and value elements-at-risk from a range of possible post-fire debris-flow scenarios, methods to integrate these results with common debris-flow mitigation techniques and best management practices, and methods to optimize the mitigation decisions for burned areas. For individual burned drainage basins, existing hazard models and readily available data can be combined in a geographic information system to rapidly estimate debris-flow damage costs following a wildfire. The results can then be integrated into an optimization model, whose output can guide allocation of emergency management funds and selection of cost-optimized debris-flow management strategies for entire burned areas consisting of multiple drainage basins. As far as the authors are aware, natural hazard and social science management models have not previously been linked for post-fire debris flows. These methods have the potential to transform the way hazard managers approach debris-flow mitigation decisions following wildfires. Results from Santa Barbara (CA), Great Sand Dunes National Park (CO), and Colfax/Las Animas Counties (CO, NM) study sites are provided. Results indicate that optimization modeling can be used to select natural hazard management methods whose benefit for mitigation of post-fire debris flows can easily outweigh the cost of implementation.

**Krasko V, Rebennack S (In Preparation) Optimal Hazard Management for Post-Wildfire Debris Flows using Global Optimization and Reformulation**

Previous work has shown that the economic risk of post-wildfire debris flows varies greatly for different storm scenarios. It has also been mentioned in literature that public notification and evacuation of potentially threatened areas is a common practice when potential debris-flow triggering storms are expected. This paper extends the general framework of optimal hazard management for post-fire debris flows (McCoy et al In Preparation) to consider a stochastic

storm uncertainty and incorporate elements of the emergency supply pre-positioning problem. This structure allows the land manager to hedge the mitigation response on storm scenario uncertainty and to optimally allocate emergency evacuation resources across different population nodes. Thus it addresses two shortcomings of the previous model: uncertainty about the magnitude of the future storm event, and consideration of preventing loss of life through notification and evacuation. Our formulation is a two-stage stochastic mixed integer nonlinear program. The first stage of the model decides on which mitigation treatments to utilize in various drainage basins, identifies population nodes in which to build emergency search and rescue resource stations, and decides on how many resources to stock in those stations while minimizing total expenditures on these actions. The realization of the storm scenario determines the probability of debris flow occurrence in each basin and the expected volume of debris in each basin. The volume also determines the demand for emergency search and rescue resources at each population node, and the intact arc capacity between nodes. In the second stage, the model decides on flows of resources between the various nodes while minimizing the cost of transport plus the holding cost for any unused resources and the penalty for unmet demand.

#### **Kaffine D, Krasko V (In Preparation) Endogenous Natural Hazard Risk at the Wildland-Urban Interface**

This paper considers the response of human agents to changes in endogenous natural hazard risk using a monocentric open city model. The unique spatial aspects of the wildland-urban interface are modeled by considering two general hazard management strategies: hazard prevention that effectively reduces expected damages at all locations, and hazard mitigation which effectively moves the border of the risky area further from the city center. Preliminary results suggest that prevention efforts increase structural density in the risky area while mitigation only increases structural density at the border. If development already exists in the risky area then prevention efforts push the city boundary further from the center while mitigation leaves the boundary unchanged. In a city where the development ends at the border between safe and risky areas, mitigation efforts strictly increase the city boundary while prevention efforts weakly increase it. Future research seeks to analyze what effects these efforts have on value of land across space, total value of land in the city, welfare across space, the number of people affected by the management efforts, and the magnitude of risk reduction for those affected.